THE FLEXURAL DESIGN OF PRETENSIONED BENT CAPS

A Thesis

by

USHA RANI BAROOAH

Submitted to the Office of Graduate and Professional Studies of
Texas A&M University
in partial fulfillment of the requirements for the degree of

MASTER OF SCIENCE

Chair of Committee,	Anna Birely
Co-Chair of Committee,	John Mander
Committee Member,	Mohammed Haque
Head of Department,	Robin Autenrieth

December 2016

Major Subject: Civil Engineering

ABSTRACT

The use of pretensioned bent caps has brought the opportunity to utilize the advantages of accelerated construction and increased worker safety. At the same time they offer the benefits of enhanced performance. To facilitate a widespread implementation of pretensioned bent caps, this research seeks to develop flexural design procedures and recommendations on design and detailing that can benefit design engineers with readily available guidelines.

A design procedure for pretensioned bent caps is proposed in this work. In this procedure, the bent caps will be primarily designed to achieve zero tension under dead load, to provide adequate strength under design load combinations and to satisfy the stress limits specified in the American Association of State Highway and Transportation Officials (AASHTO) LRFD Bridge Design specifications. To evaluate the design procedure, a bridge inventory comprising standard Texas Department of Transportation (TxDOT) bridges with I-girders, box beams and X-beams, as well as non-standard bridges have been considered. Design results indicate no cracking expected under service loads and limited cracking expected under ultimate loads.

End region detailing of the pretensioned bent caps, for resistance against tensile stresses during prestress transfer, have been reviewed from previous investigations. The pocket connections, used between pretensioned bent caps and columns, offer benefits in the use of concrete instead of grout and in the availability of large construction tolerance. A medium pocket size formed by corrugated pipe is preferable for accommodating

accidental misalignment of column. The connection provides resistance to vehicle collision loads.

Optimization of bridges with pretensioned bent caps has been assessed with modifications to the prestressing layout and the reconfiguration of the arrangement of columns. Change in strand design and geometry contributed in reduction of flexural cracking and increasing performance. Elimination of the column is expected to result in economic benefits.

DEDICATION

I dedicate this to my family Ajit Barooah, Lily Barooah, Asha Bordoloi and Nisa Sharma.

ACKNOWLEDGEMENTS

I would like to thank my committee chair, Dr. Birely and co-chair, Dr. Mander for their invaluable guidance and encouragement throughout the course of this research. I could do this only because of their immense support.

I would like to thank Dr. Haque for serving on my advisory committee. I also take this opportunity to thank the department faculty and staff for making my time at Texas A&M University a great experience.

Thanks to my research partners Kevin Yole and Judong Lee for their assistance and for making an enjoyable work experience. I would also like to thank my friends at Texas A&M University and elsewhere for their love and support.

Finally, special thanks to my mother, father and sisters for their unconditional love, encouragement and prayers.

TABLE OF CONTENTS

Page

LIST OF FIGURES

Page

LIST OF TABLES

Page

1. INTRODUCTION

Pretensioned bent caps have been recently introduced in bridge design as a step toward improving the durability and speed of substructure construction. Similar to other prestressed bridge members, pretensioned bent caps offer the advantages of accelerated construction and increased worker safety. At the same time, they offer the benefits of enhanced performance.

Prestressed concrete bent caps have the potential to introduce the benefits of reduced cracking. They also have the advantage of significant cost reduction when constructed in high numbers. However, the use of pretensioned bent caps is not widespread. Flexural design procedures and recommendations on pretensioned bent cap design and detailing can provide design engineers with readily available guidelines for the implementation of this economical and efficient alternative for bent caps.

To address this need, this research develops recommendations for the flexural design of pretensioned bent caps. The bent caps are primarily designed to achieve zero tension under dead load, to provide adequate strength under design load combinations and to satisfy the stress limits specified in the American Association of State Highway and Transportation Officials (AASHTO) LRFD Bridge Design specifications.

1.1. Research objective and scope

The primary objective of this research is to develop details for the design of pretensioned bent caps. Additional objectives are to determine effective detailing for the pretensioned bent cap and bent cap-to-column connection and to evaluate opportunities for optimization in bridges with pretensioned bent caps. Thus to design and implement

pretensioned bent caps in bridges, the following scope of work will be conducted in this research,

(a) Review of previous research and state-of-the-art practice which will contribute to the development of pretensioned bent caps.

(b) Establish design characteristics of bent caps in TxDOT standard bridges and in non-standard bridges.

(c) Develop design procedures for concentrically prestressed bent caps conforming to the design goals of achieving superior performance.

(d) Facilitate the understanding of the behavior of pretensioned bent caps by applying the procedure to a wide variety of bridges.

(e) Provide recommendations for issues anticipated in the performance of precast prestressed bent caps, precast connections in non-seismic regions and the resistance of bridges to vehicle collision loads.

(f) Provide recommendations for optimization of bridges with pretensioned bent caps for lower cost and increased safety.

(g) Provide design examples.

1.2. Organization of thesis

The thesis has been organized in eight chapters discussing the characteristics, analysis, design, detailing and optimization of pretensioned bent caps. Chapter 2 presents a review of previous work on precast bent caps and discusses recommendations that will enhance the design and detailing of pretensioned bent caps. Chapter 3 presents the proposed flexural design procedure based on the philosophy of zero tension under dead loads. In

addition, an alternate design procedure, eccentric prestressed design and effect of strand configuration in the bent cap are discussed. Chapter 4 presents a bridge inventory of standard TxDOT bridges and other nonstandard bridges for evaluation of the proposed flexural design procedure. Chapter 5 presents the results of pretensioned design of bent caps in the bridge inventory. Chapter 6 discusses the detailing required at the end zones and at the connection region of pretensioned bent caps. Chapter 7 presents the potential for optimization in bridges with pretensioned bent caps. Finally, Chapter 8 presents salient results and implications from the research and provides recommendations on future research needs.

2. LITERATURE REVIEW

This chapter discusses previous research on the development of reinforced concrete (RC) bent caps and studies which would aid the design and detailing of a pretensioned bent cap. Section 2.1 discusses history of precast highway bridge substructure construction in the United States. Section 2.2 presents research on improving the design and detailing of RC bent caps. Section 2.3 describes the feasible prestressing design space using the Magnel diagram approach. Section 2.4 discusses methods to reduce the weight of bent caps to enable more extensive application. Section 2.5 presents the issue of end zone cracking in prestressed members and previous recommendations on detailing to impede such cracking. Section 2.6 discusses earlier work on the connections types between precast bent caps and columns.

2.1. History of precast highway bridge substructure construction in the United States

Historically, reinforced concrete bridge piers have been constructed in-situ. Only since the 1970's have parts of a bridge pier, specifically either pile or pier caps, been precast to speed up construction. It has been quite common for on line renewals of railway bridges to be constructed from precast/prefabricated structural elements over a very short period of time.

Only recently, around the turn of the millennium, this practice has been investigated for widespread application to highway bridges (Matsumoto et al., 2001, 2008). One of the major changes in cast-in-situ and precast construction is dealing with connections between members. The use of precast bent caps started in Texas in the mid-

1990s, generally at the request of contractors wishing to facilitate unique construction projects. One of the earliest documented uses of precast bent caps by the Texas Department of Transportation (TxDOT) was the Pierce Street Elevated Project in 1996, which needed replacement of 113 superstructure spans and bent caps. Connections between precast bent cap and columns were made with post-tensioned bars embedded in the column and projected from the column top to corrugated ducts built in the precast bent cap. The ducts were grouted and the bars were anchored at the cap top. The Red Fish Bay and Morrings & Cummings Cut Bridges built in 1994 involved use of rectangular precast bent caps to minimize casting over water. The connection between precast bent cap and precast trestle piles consisted of two U-shaped reinforcing bars epoxy grouted into ducts at the top of precast piles and projected into two voids built along the full depth of the bent cap. Concrete was cast within the voids following placement of the cap (Freeby et al. 2003).

2.2. RC bent cap performance

Prior research efforts have been made to improve the design and detailing of bent caps. Ferguson (1964) conducted 36 tests on the overhang region of 36 inch square bent caps to determine design procedures for flexural and shear strengths. The test parameters included shear span, reinforcement size and end anchorage length, column support, web reinforcement and steel grade. Ferguson made recommendations on the end anchorage requirements for longitudinal reinforcement in the overhang and on development of a flexural design procedure. Test results indicated vertical stirrups had limited effects on shear strength for small shear span ratios.

An investigation has been conducted to minimize the side face cracking observed in large RC beam; the results can be directly implemented in deep beams such as bent caps. Frentz and Breen (1978) experimentally tested 44 scaled specimens of an inverted T-bent cap prototype, to determine the cause of cracking at mid-depth of side faces of RC members. Test parameters were the factors believed to affect the side face cracking, which included the amount and distribution of side face reinforcement, cover, web width and beam depth. The beneficial effect of so-called "skin reinforcement" in controlling side face cracking was evident from the test results. Based on the results, a detailed design procedure was established that was effective in side face crack control. The authors noted that the contribution of the side face reinforcement in the flexural capacity would offset the additional cost due to skin reinforcement.

Bracci et al. (2000) performed 16 full scale experimental tests to mitigate unexpected flexural and flexure-shear/shear cracking in the negative moment regions of cantilever bent caps. The test parameters were controlled by design and detailing requirements of longitudinal, transverse and skin reinforcement. Important test results included that tension stress in longitudinal reinforcement significantly affected flexural cracking in bent caps, reinforcement strains were higher at the column center than at column face, and higher shear strength reduced flexural-shear cracking and induced a favorable ductile failure. Recommendations were presented on the critical location for flexural design, required amount of shear strength and distribution of skin reinforcement in the web tensile region.

Fonseca et al. (2003) performed experimental tests to determine the effects of deterioration on bent cap strength. Four cantilever bent cap specimens were tested; two were obtained from a bridge demolition in Utah and the other two were newly constructed. Testing was conducted up to yield and failure on an old and a new specimen. Test results indicated deterioration has no effects on the strength of bent caps if reinforcing bars are not significantly corroded.

2.3. Prestressing design aids using Magnel diagram

Magnel (1948) developed a graphical solution as a feasible solution space for the number and location of prestressing strands. Equations are written for the governing stresses at critical locations in terms of eccentricity (e) and reciprocal of prestressing force ($1/F$). Each equation is plotted in the form of e vs. 1/F to form the Magnel diagram. A choice of acceptable combinations for F and e are available in the region of the plot satisfied by all the conditions. The range of eccentricities for a given prestressing force can be determined from the Magnel diagram. Likewise, for a particular eccentricity the range of permissible prestressing force is easily available from the Magnel diagram.

Subsequently, improvements have been suggested by researchers to increase plotting efficiency. Krishnamurthy (1983) established that a precise safe zone could be determined and its location directly compared with the beam cross section by swapping the axes of the Magnel diagram, i.e., plotting $1/F$ in the x-axis and e in the y-axis. Ehssani and Blewitt (1986) reported on the limitations of the Magnel diagram that a different plot needs to be constructed for each critical location along the member length.

This constraint was resolved with the development of design charts for determining acceptable values of eccentricity for the entire length of a simply-supported uniformly-distributed beam.

2.4. Methods to reduce bent cap weight

Bridge projects that require longer bent caps may be limited by the restrictions in weight for shipping and erecting. This section provides information regarding potential methods for avoiding the problem of weight exceedance. Methods providing permanent and temporary voids (U-shaped shell beams, box beams, and concrete block outs) in the bent cap are discussed in Section 2.4.1. A method to reduce shipping and erection weight by connecting individual bent caps is also described in Section 2.4.2.

2.4.1. *Permanent and temporary voids*

U-shaped shell beams

Park et al. (1995) presented general details of the widespread application in New Zealand of precast pretensioned shell beams as structural elements. The paper gives an overview of the construction of floors, moment resisting frames, and structural walls of buildings using prestressed concrete. Figure 2.1 shows one such application in the use of precast concrete shell beams. The shell beams are precast pretensioned U-shaped beams. After placing the beams in position, an additional reinforcing cage is placed within the hollow portion of the beam and then is filled with cast-in-place concrete. The beam is designed for its low self-weight and imposed construction loads. All external loads are carried by both the beam and the core concrete compositely. Reinforcement is not projected from either the beam or core concrete; composite action is dependent on the

bond developed at the roughened interface. Park et al. also reported that tests on moment resisting frames incorporating this system and subjected to seismic loading have been performed. Results from the tests demonstrated that during severe seismic loading plastic hinging in the beams is not concentrated only at the column faces but also spreads along the reinforced concrete core due to bond failure.

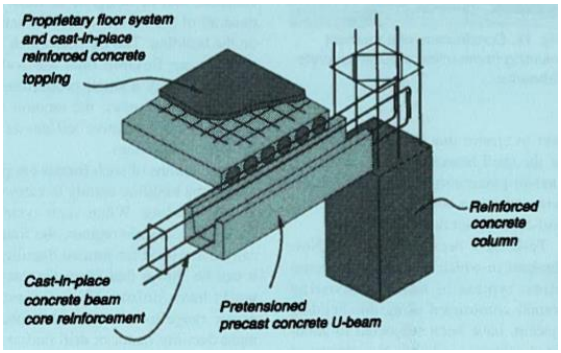

Figure 2.1. Pretensioned precast concrete U-beam (Park et al. 1995).

Box beam bent caps

Zhenqiang et al. (2010) discussed the use of precast concrete structures incorporated both in the superstructure and substructure of an interchange bridge project in Honduras. The bridge had four spans with a total length of 213 ft. Each pier cap was composed of a precast concrete box beam and served as a 'stay-in-place formwork' for the cast-in-place concrete filled in the center of the box beams. The box units were 3 ft wide, 2.3 ft deep, and 26 ft long, and were assembled using precast, prestressed concrete panels and reinforcing-steel cages. Figure 2.2 shows the design details of the cap box beam (Figure 2.2(a)) and the underside of the bridge (Figure 2.2(b)).

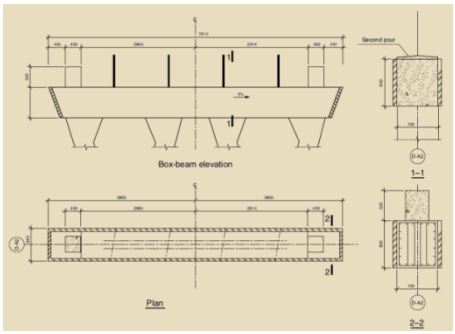

(a) Design Details of the Cap Box

(b) Underside of the Completed Bridge

Figure 2.2. Cap box beam used in bridge in Honduras (Zhenqiang et al., 2010).

Concrete blockouts in bent caps

Figure 2.3 presents standard drawings reported in SHRP 2 Report S2-R04-RR-2 (2013). The figures show a straddle bent that has hollow sections on two sides from middle of the cap along its length by placing polystyrene block outs. The report also mentions the use of light weight concrete in place of polystyrene block outs for pier cap weight reduction.

Billington et al. (1998) proposed full precast substructure systems for both faster construction and improvement in bridge aesthetics. One of the initial proposals was the use of segmentally constructed inverted T-bent caps supported on single columns. Wide bent caps up to 88 ft could be used with this system by joining two cap segments with longitudinal post-tensioning. A method to reduce bent cap weight was examined by introducing voids in the web and outer corners of the ledge. The precast bent cap had options for pretensioning, post-tensioning or both.

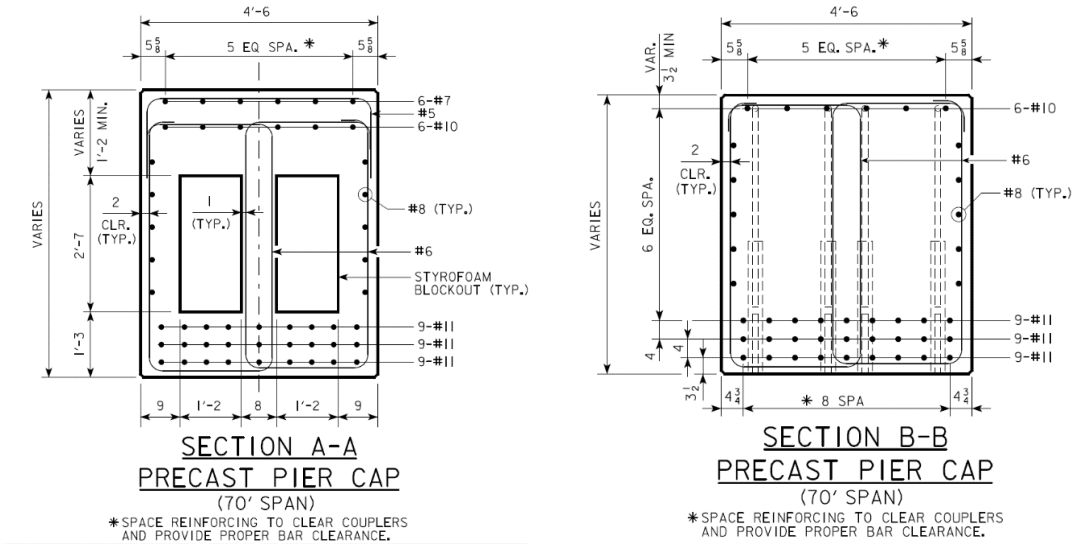

Figure 2.3. Straddle bents with styroform in the cap (SHRP 2).

A variation in this method of weight reduction is an inverted U-shaped beam. Culmo (2009) reported an inverted U-shaped bent cap used by Florida DOT for weight reduction in the design of the Edison Bridge.

2.4.2. *Other methods of weight reduction*

SHRP 2 Report S2-R04-RR-2 (2013) proposed that limitations in the length of pier caps due to weight or shipping could be avoided by combining a number of shorter caps to form a straight pier cap.

Similar solutions using multiple pier cap segments have also been addressed in the optional standard bent cap drawings prepared by WisDOT and available online. Figure 2.4 shows the use of non-shrink grout to connect the individual segments. The WisDOT manual has set as standard that if two or more segments compose a pier cap, each segment may be supported by two columns.

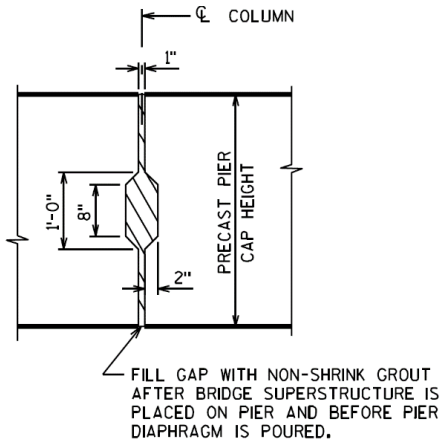

Figure 2.4. Connection between multiple pier cap segments (WisDOT standard drawing).

Khaleghi et al. (2012) reported the development of a precast concrete bridge bent system to achieve accelerated bridge construction in seismic regions. The system included a cast-in-place spread footing, precast column and a bent cap built in two stages. In the first stage, the bent cap was built of two segments and then joined with a closure pour at mid width of the bridge. In the second stage, the bent cap was cast-in-place. The bridge bent system was then implemented in a bridge replacement project over Interstate-5.

The PCI Northeast Bridge Tech Committee conceptualized a detail for connecting adjacent precast cap beams (Culmo, 2009). The Committee commented that this detail has already been in use in the building industry. Figure 2.5 shows the bars projecting from adjacent precast bent caps connected by grouted sleeve couplers and then poured with cast-in-place concrete.

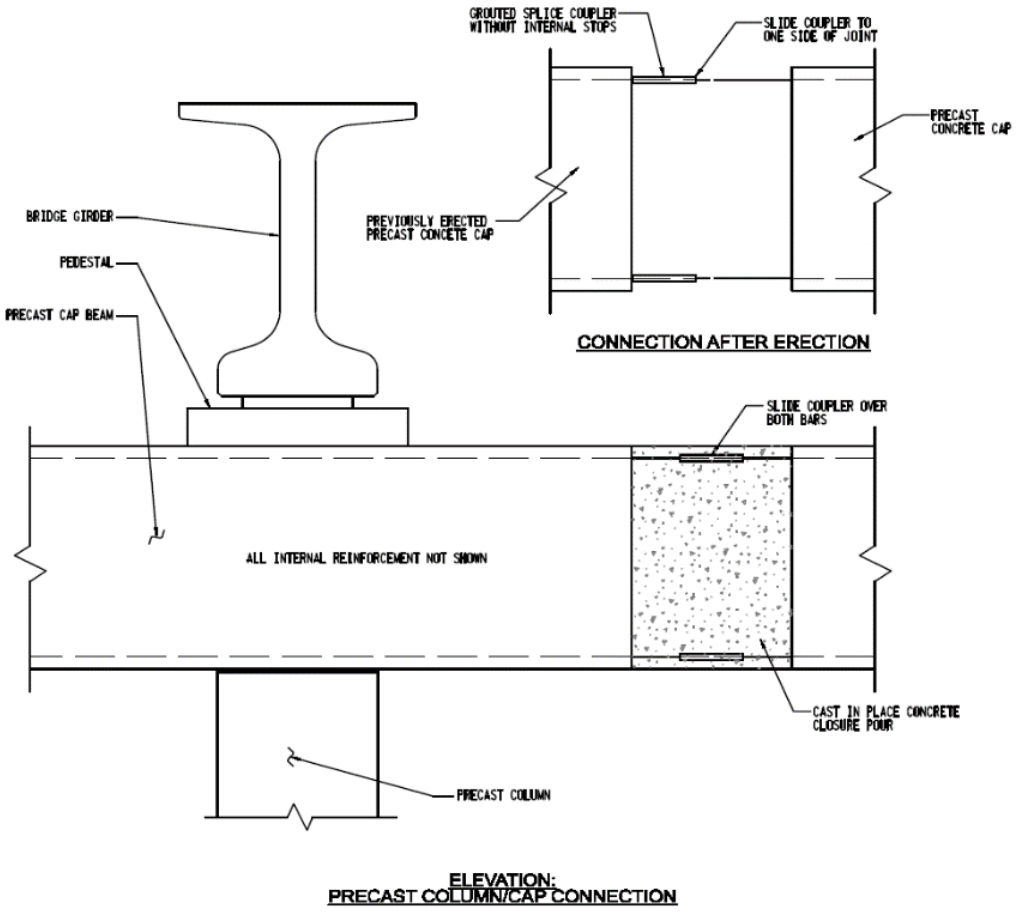

Figure 2.5. PCI Northeast bridge tech committee (Culmo, 2009).

2.5. Recommendations for end regions of pretensioned concrete members

Pretensioned concrete members have been observed to have high tensile stresses in the end regions during prestress transfer actions. These bursting stresses may lead to tensile splitting cracks and thereby affect the serviceability of the bent cap. This subsection discusses the background to the phenomenon of splitting, spalling and bursting stresses, the provisions in AASHTO LRFD Bridge Design Specifications for handling these issues, and other recommendations arising from recent research.

2.5.1. *Stresses in end regions of prestressed concrete beams*

On release of a strand, the full prestressing force develops through bond over a transfer length. At this transfer length, where the steel stress reduces from a high tensile force to zero at transfer, the strand dilates and a high localized circumferential hoop tension stress forms in the concrete around each strand. Radial cracks form transversely to these circumferential tensions (see Figure 2.6(a)). Figure 2.6(b) shows how these radial cracks propagate when the strand is close to the edge or another strand, resulting in spalling of the concrete. One method of mitigating this end splitting effect and the potential for spalling is to provide transverse hoop steel to bridge cracks as shown in Figure 2.6(c).

In addition to the local effects of prestressing discussed above, global effects of applied prestress occur. When prestress is applied the high end-stress concentrations eventually disperse, in accordance with St. Venant's principle, over about one-member depth to provide a uniform distribution of prestress. Figure 2.7 show this effect for two cases, one where the prestress is applied near the member edges, the other at the member center. Figure 2.7(a) shows the stress trajectories for elastic behavior. Note that the stresses are uniform for more than one-member depth from the ends. Figure 2.7(b) shows the stresses transverse to the longitudinal axis of the member. The location of the highest transverse tension stresses is where the transverse reinforcement should be provided. To assess the quantity of reinforcement necessary, a strut and tie model can be used as shown in Figure 2.7(c).

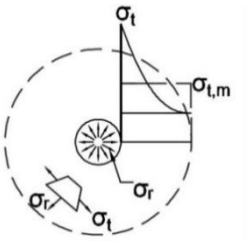

(a) Splitting Stress (Ujil, 1991)

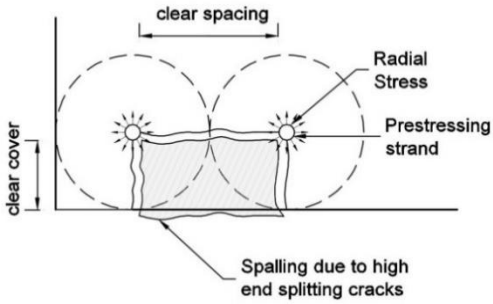

(b) Splitting cracks

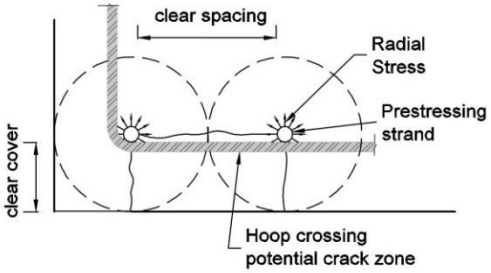

(c) Spalling prevented with reinforcement

Figure 2.6. Local effects of applied prestressing forces.

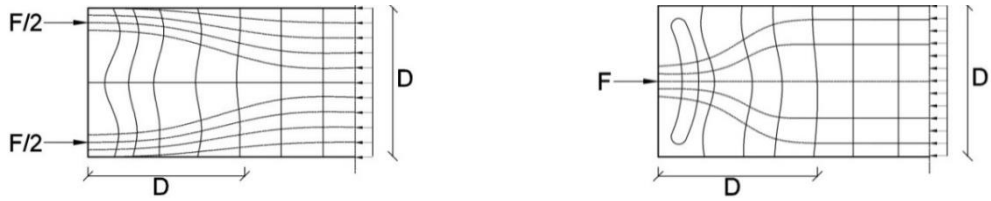

(a) Stress trajectories due to applied prestress

(b) Transverse stresses due to applied prestress

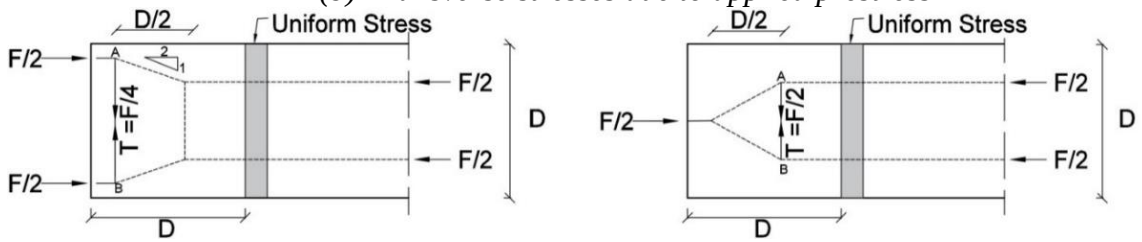

(c) Strut and tie model to assess reinforcement requirement.

Figure 2.7. Global effects of applied prestressing force.

For the case where there is an upper and lower layer of strands, a tension force denoted by the tie AB near the end of the member is equal to F/4, where F is the overall applied prestress at transfer. In contrast, for the case where there is a concentrated prestress force (F) applied at the center of the member, the strut and tie model shows bursting forces that must be restrained approximately D/2 away from the force application. The strut and tie model shows that the force denoted by the tie AB is equal to F/2.

2.5.2. *AASHTO and research recommendations*

AASHTO LRFD 5.10.10.1 specifies the splitting resistance provided by the end zone reinforcement in pretensioned beams as $P_r = f_s A_s$, in which f_s is the stress in steel not to exceed 20 ksi and A_s is the total area of reinforcement within a distance *D/4* from the member end, where *D* is the member depth. The reinforcement should be placed as close to the member end as practicable. The resistance should be considered not less than four percent of the prestressing force at transfer.

Experimental tests have shown that end zone reinforcement is more effective in controlling cracks if the reinforcement is concentrated at the member end and reduced gradually along the length of the member. Tuan et al. (2004) recommended that 50 percent of the end zone reinforcement be placed within *D/8* from the member end and the remaining 50 percent to be placed within *D/8* to *D/2* from the member end. Splitting reinforcement should not be needed beyond *D/2* from member end.

In TxDOT Project 05831-3, Avendano et al. (2013) conducted several experimental tests to evaluate end region detailing of box beams and the stresses at the

ends during prestress transfer. It was found that the bursting force in the region *D/4* from the beam end did not exceed 4 percent of the prestressing force. However, the bursting force beyond *D/4* from the beam end to approximately the transfer length of the beam exceeded 50 percent of the bursting force in the first *D/4* of the beam. This result is in accordance with O'Callaghan and Bayrak (2008) who found from their experimental tests on pretensioned I-beams that bursting stresses occur up to a distance of the transfer length from member ends. In their report, O'Callaghan and Bayrak mentioned that the AASHTO provision of reinforcement within *D/4* from the member end is in reality meant to handle spalling stresses that occur near the beam end. Bursting stresses reach a maximum value before the end of the transfer length and decreases rapidly to nearly zero some distance beyond the transfer length. The authors in both reports recommended that bursting reinforcement be placed immediately after spalling reinforcement, from *D/4* to the transfer length.

2.6. Connections

Precast bent caps have been used in bridges in a number of projects by various state Departments of Transportation (DOTs) due to several advantages such as Accelerated Bridge Construction (ABC), reduction of on-site hazards, improved economy, and reduction of cracking that leads to improved durability and quality. The main challenge in delivering a successful bridge project is in the design and construction of the connections between the precast cap and the pier columns whether they be cast-in-place or precast.

This section of the literature review describes several types of cap beam-to-column connections that may be used as a part of the bridge pier. These connections have been classified into emulative and jointed connections. An informative description has been first provided. Details of the different types of precast connections have been then presented, which includes a discussion of results of relevant research conducted and the state-of-the practice used by many state DOTs.

2.6.1. *Overview of column-to-bent cap connections*

For construction of traditional cast-in-place (CIP) bent caps, columns are constructed first with the longitudinal column reinforcement extended beyond the column top to form part of the connection of the column-to-cap joint. Following construction of the columns, the cap formwork is placed (typically on falsework), then the cap reinforcement is installed and finally the concrete is poured. As column reinforcement extending into the cap is bonded to the cap concrete, a monolithic (rigid) connection between the columns and cap beam is created.

The primary motivation for the use of precast bent caps is to facilitate improved construction, particularly to accelerate construction and to reduce worker exposure to potentially hazardous worksite conditions. Because the concrete for the bent cap is generally cast at an off-site location, a connection between column and cap needs to be formed on-site. In this study, the existing column-to-precast-cap connection types have been classified into two broad categories of emulative and jointed connections.

Emulative connections

In emulative connections, a rigid connection is formed to emulate customary CIP concrete bridge piers described above. To date, most bridge piers built with precast bent caps have been constructed using an emulative style of construction. For emulative connections, the cap beam is typically stronger than the column, particularly in seismic zones. Emulative connections include grouted pocket connection, grouted vertical duct connection, pocket connection, bolted connection, grouted sleeve coupler connection and socket connection.

- **Grouted pocket connection:** Reinforcing bars embedded into a column are projected above the column and inserted into pocket(s) built in the precast bent cap and then grouted. The pockets are unlined voids cast in the full depth of the bent cap. These pocket connections can have configurations in number of voids (for eg. single or double rectangular tapered pockets used in the tests by Matsumoto et al., 2001) and configurations in the cross section of the voids throughout the bent cap, both of which are project specific.
- **Grouted vertical duct connection:** Column bars or reinforcing bars embedded into the column core are projected from the column to create a connection with the bent cap. The extended bars are each inserted into individual corrugated ducts built in the precast bent cap. The connection is then grouted. TxDOT uses this connection as a standard connection between precast bent caps and columns. Details of TxDOT standard connection are discussed later in this section.

- **Pocket connection**: This connection is similar to the grouted vertical duct connection, but instead of individual ducts, a large corrugated pipe is built in the precast bent cap to which the column reinforcement projected from the column is inserted and is then filled with CIP concrete.
- **Bolted connection:** This connection is also similar to the grouted vertical duct connections. The difference is that threaded bars or post-tensioning bars embedded in the column are extended from the column into individual corrugated ducts present in the bent cap and are then anchored at the top of the cap with nuts. Alternatively, strands used in a precast column may be post-tensioned at the top of the cap.
- **Grouted sleeve coupler connection:** Sleeve couplers are embedded into a precast member (such as a bent cap) and reinforcing bars extended from an adjacent member (such as a column) are inserted into the sleeve and then grouted.
- **Socket connection:** The socket connection involves a member to be embedded to a certain length into an adjacent member. In a socket connection between precast bent cap and piles, a void is created at the bottom of the bent cap for the pile to be inserted. The void is then filled with grout. There is no reinforcement projecting from either member.

Jointed connections

Jointed connections are a relatively new concept and have had little field deployment. Nevertheless, considerable research has been conducted on jointed connections. Distinct from emulative constructions, the joints themselves are typically weaker than the adjoining columns and cap beam. Thus under either lateral load or differential

settlement, the joint may slightly open or close, thereby protecting the adjoining members from damage. Jointed connections include the following types: Partially prestressed (hybrid) connection, armored damage avoidance connections and pretensioned rocking bridge bent.

- **Partially prestressed (hybrid) connection**: The partially prestressed connection has a combination of both mild steel reinforcement and unbonded post-tensioning (PT) strands. It is often referred to as a hybrid connection. Unlike damage avoidance design, the reinforcement or strands may not be terminated at the column top and continue to the top of the bent cap. Mild steel dissipates inelastic energy; unbonded PT strands remain elastic and enable controlled rocking at the joints, thus leading to minimal residual lateral displacement.
- **Damage avoidance design (DAD)**: This is a design procedure to maximize post-earthquake serviceability requirements along with ensuring life safety. Reinforcement and post-tensioning strands (if used) are terminated at the column top which enables controlled rocking of the column at the joints. An armored steel interface is used to strengthen the joint to prevent damage due to development of high stress concentrations during rocking. Essentially no residual drift is observed after large earthquakes thus eliminating the need for any post-earthquake repairs.
- **Pretensioned rocking bridge bent**: Similar to damage avoidance design, pretensioned rocking bridge bent design dissipates energy by controlled rocking of the column at the ends. This results in minimal residual damage after an earthquake. The columns have pretensioned strands which are unbonded in the central region and

bonded at the ends, allowing the structure to return to its original position after an earthquake.

2.6.2. *Discussion of connection details*

The details of emulative and jointed connections are described in this subsection. Important conclusions for associated research projects and a discussion of use in DOT projects has been presented. The results of research studies are drawn from the relevant references. Much of the discussion on implementation by DOTs is based on the work of Culmo (2009). Summary of the state-of-the-art practice of connection details between prefabricated elements in ABC projects conducted under US DOT (US Department of Transportation) and FHWA (Federal Highway Administration) is presented in that report. The details were classified into three levels based on frequency of use and effectiveness. Information on performance rating by the agencies with respect to constructability, durability, cost, maintenance of the connection has been included. Connection details between precast bent cap with cast-in-place columns, precast columns, pile bents and precast concrete bent caps have been presented. In this research project, connection between a precast bent cap and columns will be discussed. Additionally, some of the connection details which are adopted by the state DOTs have been reproduced from the Scan Team report from Project 20-68A by Kapur et al. (2012) performed under NCHRP.

Grouted pocket connection

The grouted pocket connections use a column or pile longitudinal reinforcement or reinforcing bars embedded into the column and extended from the column. Pockets are

created in the precast bent cap. The noticeable difference between a grouted pocket and a grouted vertical duct connection is the absence of duct in the grouted pocket connection. Tapered pocket shapes were used in the tests conducted by Matsumoto et al.(2001). A single pocket is used in a single line pocket connection, while two pockets are present in a double line pocket connection. The embedded rebars project from the column. During placing of the bent cap, the bars are inserted into the pocket and the connection is then grouted. A similar connection configuration was used in the Red Fish Bay Project by TxDOT, in which #9 U-bars were epoxy grouted into precast piles and inserted into double line pockets present in the precast bent cap.

Matsumoto et al. (2001) examined both single and double line connections, conducted pull out tests during Phase 1 and full-scale bent cap to column connection tests in Phase 2 of their experimental program as shown in Figure 2.8.

Figure 2.9 presents a grouted pocket connection as used by various state DOTs and described in the synthesis report by Culmo, (2009). South Carolina DOT used this connection in the Carolina Bays Parkway Project.

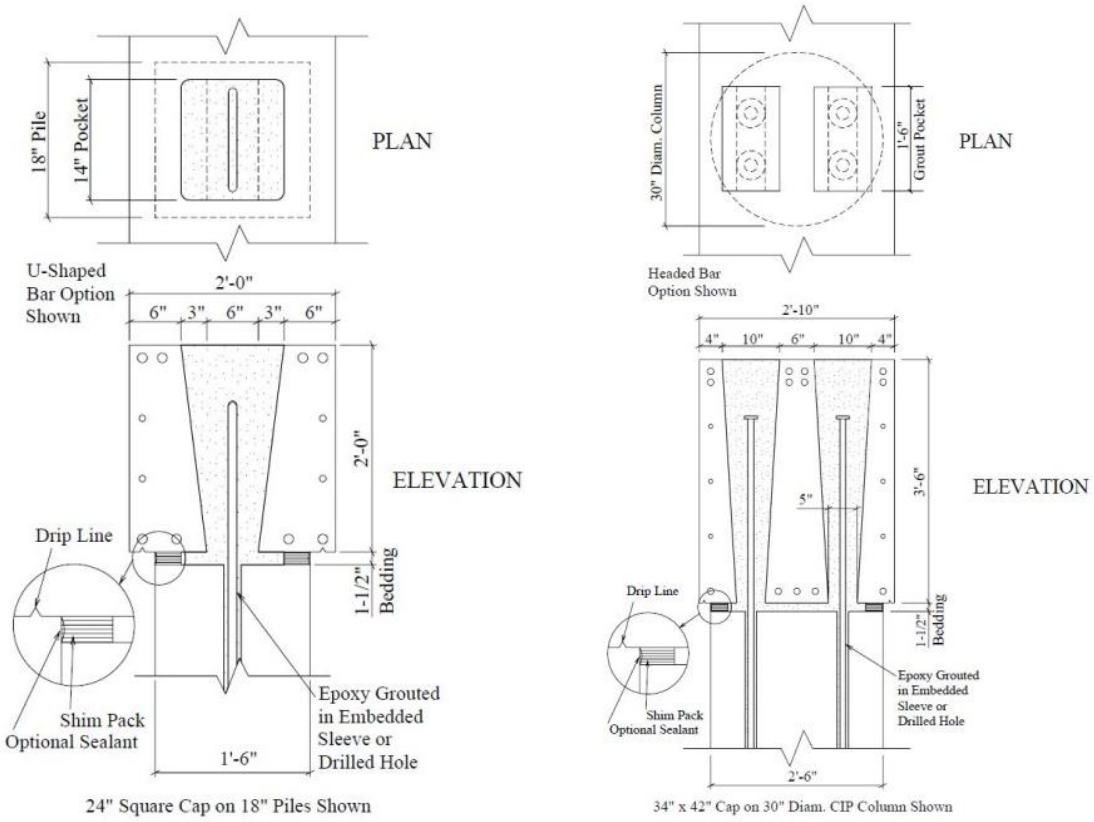

(a) Single Line Grouted Pocket *(b) Double Line Grouted Pocket*

Figure 2.8. Grouted pocket connection (Matsumoto et al. 2001).

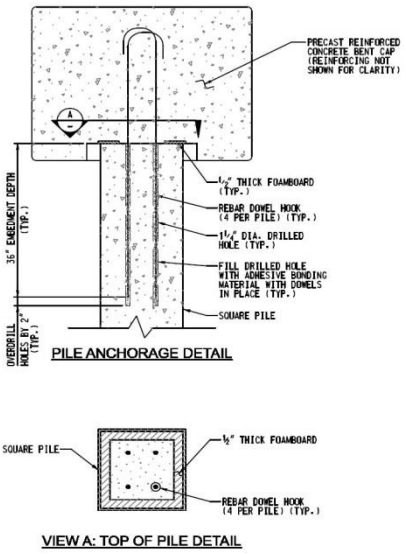

Figure 2.9. Carolina Bays Parkway project – SCDOT (Culmo, 2009).

Grouted vertical duct connection

The grouted vertical duct connections are commonly used as a standard TxDOT connection type for RC bent caps. This connection consists of column bars or reinforcing bars embedded into the column core and extended from the column into individual corrugated ducts built in the precast bent cap. The duct is then grouted.

The grouted vertical duct connection has been investigated and tested under several research studies. Matsumoto et al. (2001) conducted an experimental test program and formally investigated the grouted vertical duct connection along with three other connection types. The behavior of the connection in pull-out tests, gravity loads and wind lateral loading was examined. Brenes et al. (2006) under TxDOT Project 0-4176, conducted research on grouted vertical duct connections and tested 12 bent cap specimens for 32 pullout tests to understand the influence of a list of parameters. These research projects led to the development of the current TxDOT precast connection option for standard bent caps. Two options exist, one for square piles and one for round columns. As the two studies on the grouted vertical duct connection discussed above were confined to non-seismic regions such as Texas, Restrepo et al. (2011) conducted 42 percent scaled tests to evaluate the seismic performance of this precast connection. Failure of the test specimen occurred by low cyclic fatigue of the column longitudinal reinforcement. The connection was deemed to achieve its intended emulative behavior.

Pang et al. (2008) investigated the seismic response of this connection built with large diameter bars such as #18 bars. As the embedment length required for #18 bars grouted in ducts was unrealized, Steuck et al. (2007) performed pull out tests and

determined that the embedment depth of bars grouted in ducts is less than that required in concrete and can easily be accommodated in a typical bent cap. Using the result, tests performed to evaluate the seismic performance of the proposed connection exhibited adequate ductility and response comparable to a cast-in-place connection. With the concepts developed in this research, Khaleghi et.al (2012) developed a bridge bent cap system supporting ABC in high seismic regions as a part of a 'Highway for life' project supported by FHWA. The bent-cap-to-column connection, with #18 diameter bars in 8.5 inch diameter corrugated pipes, was tested under cyclic loading and later implemented in a Washington bridge project in the replacement in I-5 (Stanton et al. 2012).

Early implementation of the grouted vertical duct connection by TxDOT was at Lake Belton and Lake Ray Hubbard projects in 2004 and 2002, respectively (Hewes,2013). Figure 2.10(a) and (b) show these connections, respectively. In Figure 2.11, a precast pretensioned bent cap is built with vertical ducts to create a connection (Miller et al., 2014).

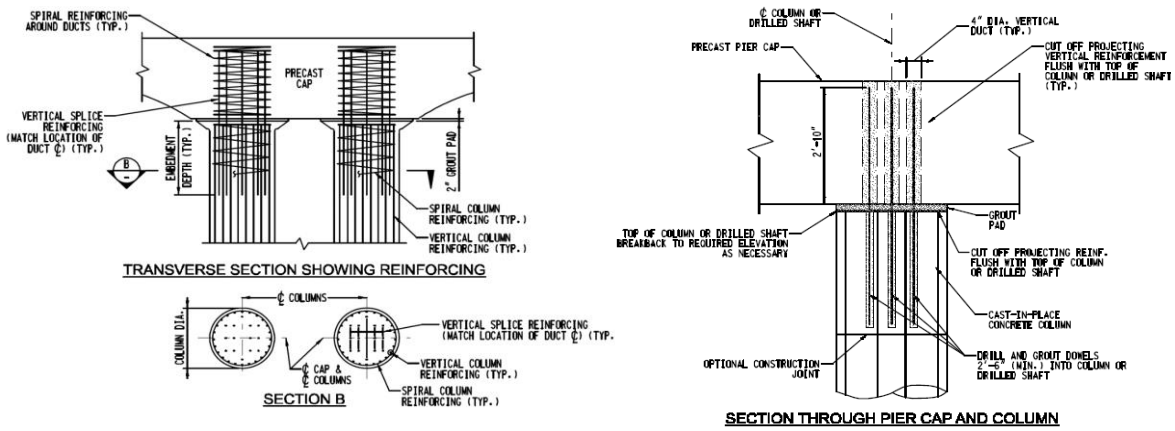

(a) Lake Belton Project *(b) Lake Hubbard Project*

Figure 2.10. Early use of grouted vertical duct connection by TxDOT (Culmo, 2009).

Figure 2.11. Pretensioned precast cap (Miller et al., 2014).

Pocket connection

The grouted vertical duct connection, used by TxDOT as standard connection type, consists of a number of corrugated ducts present in the precast bent cap to which reinforcing bars embedded in the column are inserted. Similar to this concept is a pocket connection. In this type of connection, one large corrugated metal pipe creates a pocket in the precast bent cap centered about the position of column. Longitudinal column reinforcement is extended from the column. During placement of the precast bent cap,

the reinforcing bars run through the large pocket to the top of the bent cap. The pocket is then filled with cast-in-place concrete.

In the research study reported in the National Cooperative Highway Research Program Report 681 (NCHRP 2011), Restrepo et al. (2011) examined this connection to test its suitability in high seismic regions. Examples of their test specimen are shown in Figure 2.12. The test specimen was 42 percent scaled and consisted of a bent cap, a column and a footing. An 18 inch nominal diameter corrugated metal pipe was used to create the pocket to house column reinforcement. The pipe is present between the top and bottom longitudinal reinforcement in the cap, hence drums made of cardboard were used above and below the pipe to make the pocket continuous along the depth of the bent cap. Two types of pocket connections were tested and examined; cap pocket full ductility (CPFD) intended for use in high seismic regions and cap pocket limited ductility (CPLD) for low to moderate seismic regions. The CPFD specimen was designed based on SDC D design which required significant joint reinforcement. The CPLD specimen was based on SDC B design which did not require any joint reinforcement other than the steel pipe. All dimensions and pipe size remained the same; thus CPLD differed from CPFD in terms of lack of joint confining reinforcement and reduction of cap longitudinal reinforcement. CPFD had additional hoops at both ends of the pipe and construction stirrups at the joint. After placement of the bent cap on the column, the pocket and bedding layer between the bent cap and the column were filled with concrete. Concrete compressive strength was intended to be achieved at least 0.5 ksi greater than the concrete in the bent cap.

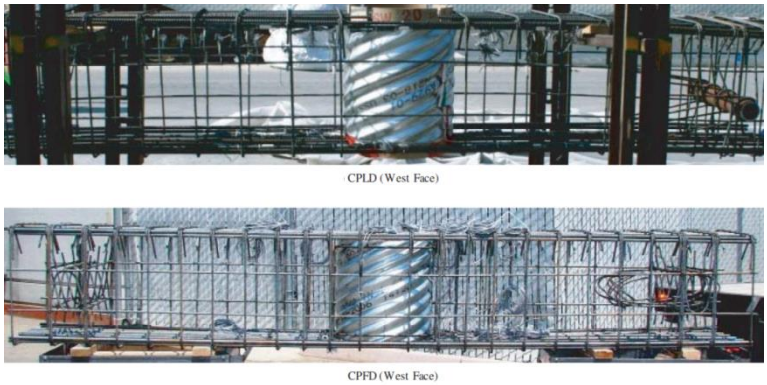

Figure 2.12. Reinforcement in CPLD (*top*) and CPFD- (*below)* (NCHRP 681).

Testing of the specimen was conducted in an inverted position. Force-controlled loading was applied until an expected first yield beyond which displacement-controlled loading was applied. Test results indicated plastic hinging of column, adequate ductility, and 'stable hysteretic behavior without appreciable strength degradation'. The limited ductility specimen (CPLD) showed more joint shear cracking and deformation in comparison to the full ductility specimen (CPFD) due to the intentionally reduced joint and flexural reinforcement. This proved that SDC B joint design should have at least minimum joint shear reinforcement. Both the specimens were able to emulate cast-in-place connections. Failure occurred by buckling followed by low cyclic fatigue of the longitudinal reinforcement.

Figure 2.13 presents a field implementation that is a similar arrangement of the pocket connection between precast concrete caps and steel pipe piles in Iowa DOT in their Boone County IBRC project. Concrete was filled in the interior of a steel pipe pile and #8 hooked bars were embedded. These bars were continued from the column top and

projected into the pocket created in the cap by a 21 inch corrugated metal pipe. Voids were filled with low shrinkage concrete.

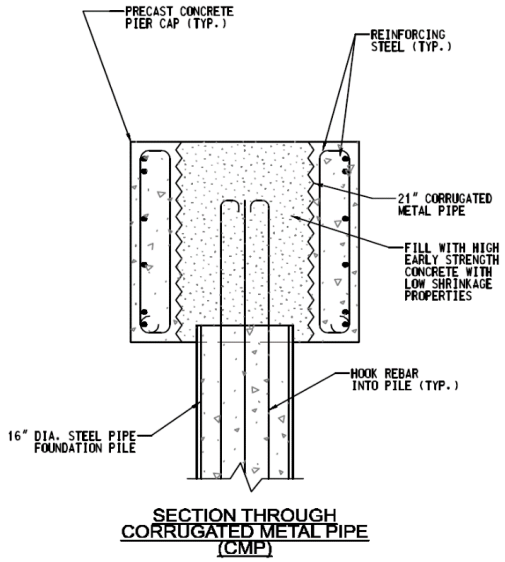

Figure 2.13. Boone County IBRC project- Iowa DOT (Culmo, 2009).

The primary advantage of a pocket connection with respect to current TxDOT design is the use of normal weight cast-in-place concrete rather than grout. Absence of grouting operation may result in improved economy and also mitigate durability concerns associated with formation of air voids during grouting operations. Large tolerances can be achieved for this class of connection as a large pocket can accept moderate misalignment of column reinforcement. This provides constructional advantage over grouted vertical duct connections which require the individual ducts to be precisely at the correct alignment with the projecting column reinforcement. The pocket connection showed favorable results during the inelastic cyclic loading tests representing high seismic regions, performed by Restrepo et al. (2011). The results of

their research show that the pocket connections can be transferred with confidence to a low seismic region such as Texas.

Bolted connection

A bolted connection is similar to a grouted vertical duct connection. Column longitudinal and spiral reinforcement are terminated at the top of the column. Threaded bars or post-tensioning bars embedded in sleeves or holes built in the column, extend above the column and provide connection to the bent cap. The precast bent cap is built with individual vertical steel ducts that align with the extended bars. The difference from a grouted vertical duct connection is that the bars are anchored at the top of the cap with nuts in a bolted connection. The ducts and bedding layer between the column and bent cap are grouted. Tobolski et al. (2006) mentioned that this connection is advantageous over the grouted vertical duct connection because it provides stability during construction before grouting and anchoring provides secondary support in case of grout bond failure. Another variation of a bolted connection was reported in which strands instead of reinforcing bars are projected from the column and then the strands are post-tensioned at the cap top. This has been used in precast segmental columns.

In the three phase experimental program by Matsumoto et al. (2001) under Project 0-1748, a full scale beam column specimen with a bolted connection was tested in Phase 2 and were found to be an acceptable connection type for use in precast bent caps.

Figure 2.14 shows an implementation of bolted connection in the Bridge over BNSF railroad project by Wyoming DOT, as reported in the synthesis report by Culmo (2009).

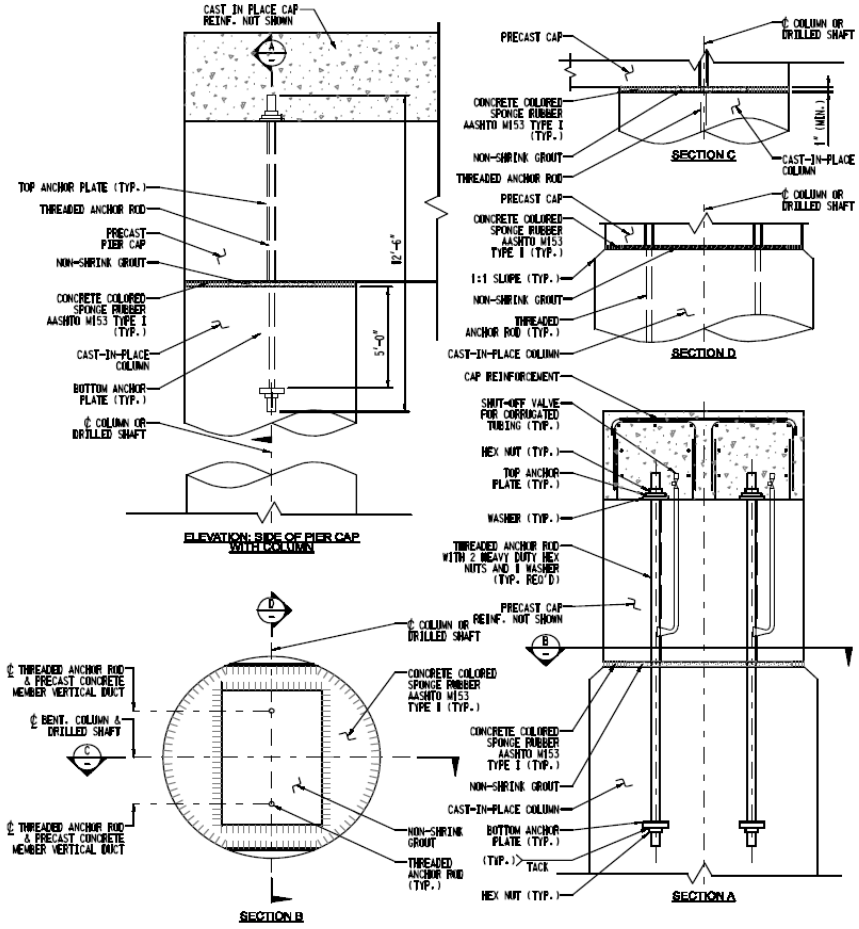

Figure 2.14. Bridge over BNSF Railway project- Wyoming DOT (Culmo, 2009).

Grouted sleeve coupler connection

In this connection, a grouted sleeve coupler is embedded in the bent cap and reinforcing bars from the column are extended and inserted into the sleeve. The connection is then grouted.

Features of this connection were reviewed in TxDOT Project 0-1748 by Matsumoto et al. (2001). This connection has been successfully used in the past in the building industry. But in the bridge industry, the minimal horizontal tolerance allowed in the connection causes concern during construction. Matsumoto et al. (2001) reported the constraints of tight tolerance in the connection, limited availability of proprietors offering mechanical sleeve couplers, and the need of separately grouting the connection and bedding layer between the bent cap and the column.

Although research has not been conducted particularly for bent cap-to-column connections with grouted sleeve couplers, studies have been done to evaluate the seismic behavior of this connection between columns and footings. Haber et al. (2013) conducted five experimental tests to evaluate the behavior of grouted sleeve coupler connections between precast columns and cast-in-place footings.

WisDOT in their Standard drawing No.7.04 has implemented grouted sleeve coupler as a standard connection between precast columns and precast bent caps/cast-in-place footings. The couplers are placed at the top and bottom ends of the column to create a connection with the bent cap and the column respectively.

Figure 2.15 shows a grouted sleeve coupler connection between an I-shaped precast column and a U-shaped precast bent cap in the Edison Bridge in Florida, as reported by Culmo (2009). The limitation of tight tolerance involved in this connection was resolved by using oversized splicers. However, to provide cover to the couplers the reinforcing bars were moved towards the center of the members. The Florida DOT commented that ‘quality control on bar and splicer locations’ were critical.

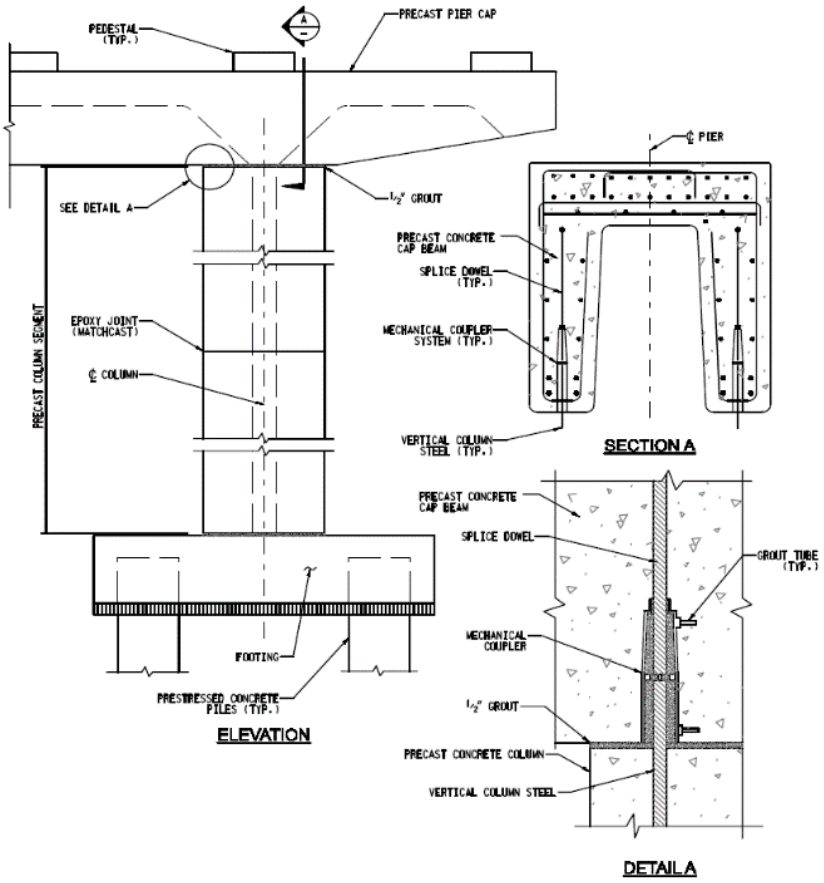

Figure 2.15. Edison bridge, Florida DOT (Culmo, 2009).

The Scan Team report under NCHRP Project 20-68A by Kapur at el. (2012) also reported on projects with implementation of this connection type. Utah has used this connection between column and pile shaft. A noticeable feature in this connection is placement of couplers in the plastic hinge region of the columns. This was based on some other codes, which unlike AASHTO, allowed placing of couplers in plastic hinge locations in high seismic regions.

Socket connection

In a socket connection one member is embedded to a certain length into an adjacent member. In a precast bent cap system, this connection is made between precast piles and precast bent cap. The connection is then grouted. The difference from a pocket connection is that there is no reinforcement projecting from the embedded member to make a connection. Marsh et al. (2011) in the NCHRP 698 report mentioned that the embedded member is anchored by the bond formed with grout and by the prying action. Bond resistance can be increased by roughening the connecting surfaces of both members.

Research has been performed to evaluate the seismic performance of a precast socket connection. Ziehl et al. (2011) conducted research on connections between prestressed concrete piles and precast concrete bent caps. The study focused on testing two full-scale single pile bent cap specimens, which included one interior (T-joint) and one exterior (knee joint) specimen. Ductility capacities of both the specimens were greater than the desired ductility, moment capacity exceeded desired value, cracks in the bent cap were small, and stresses at the joint were below allowable limits.

In the bridge bent system developed by Khaleghi et.al (2012) discussed earlier, a socket connection was used between footing and column. A socket connection was developed by placing the precast column, footing reinforcement in the excavation and then casting the footing concrete around the column. Although the same concept of embedment of the column into the adjacent member has been used, this detail is not directly applicable in a precast bent cap to column connection.

The synthesis report by Culmo (2009) indicates the use of this connection between precast bent caps and precast piles, by the state DOT's. Figure 2.16(a) show the connection used by the South Carolina DOT with large sized pocket connections built in the precast bent caps and a smaller hole built between the top of large pocket and cap top for grouting. Figure 2.16(b) show the connection used by Louisiana DOT.

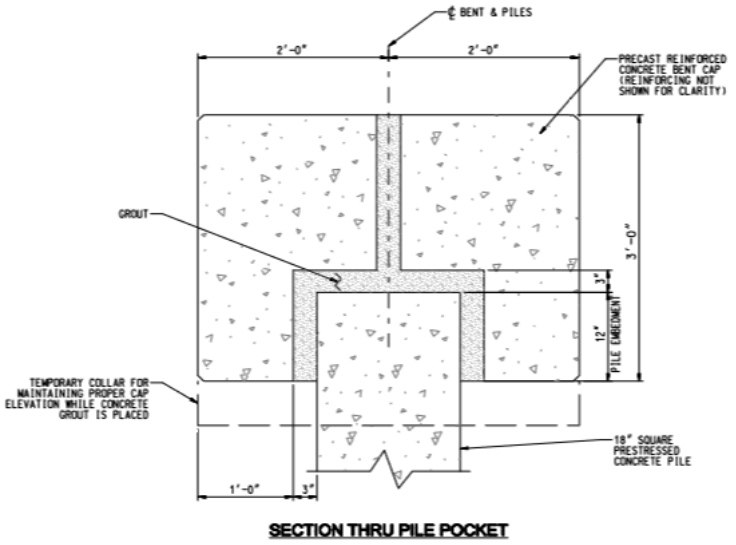

(a) South Carolina DOT

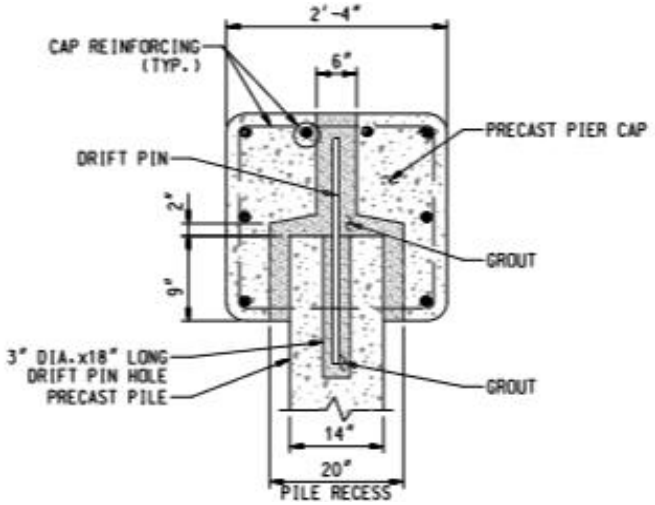

(b) Louisiana DOT

Figure 2.16. Socket connections used recently in two states (Culmo, 2009).

Partially prestressed (hybrid) connection

This connection is different from the connections described so far. As discussed earlier, those connections were emulative connection and are so named as they intend to perform or emulate a cast-in-place connection. The partially prestressed (hybrid) connections utilize both mild steel reinforcement and unbonded post-tensioning. Their design intent is particularly for seismic regions where large inelastic cyclic loading may be expected. Mild steel allows dissipation of energy, while unbonded post-tensioning strands combine both beam and column together and enables controlled rocking at the joint interface. Even if deformation is caused during seismic activity, since the strands remain elastic, the structure is re-centered back to original position. This ensures minimal residual damage in this connection.

Research and use of hybrid connections in building industry have been performed before the bridge industry. Stone et al. (1995) performed tests on precast moment resisting hybrid connections used in buildings in high seismic regions and found these connections yielded comparable results with a cast-in-place connection, showed minimal residual drift, and exhibited a large lateral drift capacity. Cheok et al (1998) analytically investigated precast moment resisting hybrid connections using a non-linear analysis computer program. Similar results were achieved which demonstrated that precast hybrid connections performed equivalent to or better than monolithic connections.

Restrepo et al. (2011) in NCHRP Report 681 classified and examined three types of hybrid connections for precast bent cap systems intended to be used in seismic

regions. Tobolski (2010) described the three types of hybrid connections investigated by Restrepo et al.(2011). The first type is the conventional hybrid connections shown in Figure 2.17(a), with reinforcement projected from the column to individual corrugated ducts present in the bent cap and a single post tensioning duct with strands located at the center; the second type is the concrete filled pipe hybrid connection shown in Figure 2.17(b) and it differed from the conventional type as it consisted of an outer steel pipe filled with concrete; the third type referred as dual steel shell hybrid connection shown in Figure 2.17(c) was developed as a lighter alternative of the concrete filled pipe, in which an additional inner steel pipe was present inside the outer steel shell to form a void interior. Tests were conducted on 42 percent scaled specimens for each of the above three connections. All the specimens displayed excellent ductility, exhibited negligible damage and residual drift in comparison to a cast-in-place specimen.

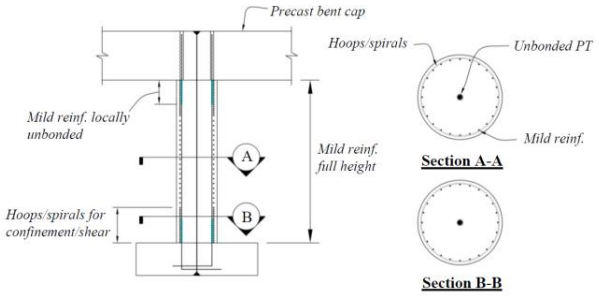

(a) Conventional hybrid

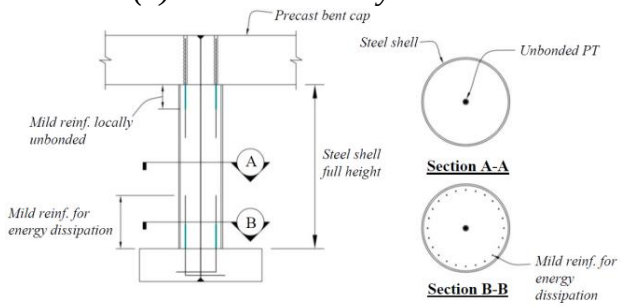

(b) Concrete filled pipe hybrid

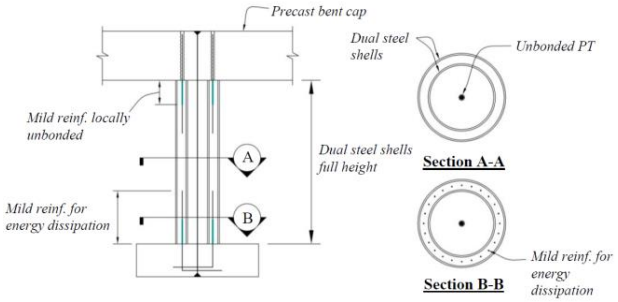

(c) Dual steel shell hybrid

Figure 2.17. Hybrid connection (Tobolski 2010).

Damage avoidance design

The concept of Damage Avoidance Design (DAD) is functionally different than the partially prestressed (hybrid) connections discussed above. The column reinforcement is anchored to and within armor plates terminated at the column top. A similar plate is in the cap beam. Under lateral load the column rocks from head-to-toe, column steel plate-

to-beam steel plate. The concrete remains in the elastic range due to the armoring thereby avoiding damage, by design. Post tension strands are used to provide a moment connection, increase lateral restraint and prevent overturning of the column in large earthquakes. In DAD, a 'steel-steel rocking interface' is provided at the joint region as shown in Figure 2.18 to prevent damage in concrete due to rocking. Mander and Cheng (1997) proposed this design philosophy for connections between column-to-bent cap and column-to-footing, particularly for moderate to high seismic zones, to maintain post-earthquake serviceability along with life safety in subsequent large earthquakes. In contrast to conventional systems designed for plastic hinging at columns, DAD involves special detailing of the connection enabling rocking of the column at the joints to allow inelastic energy dissipation and minimal strength degradation. DAD prevents the inelastic deformation occurring after a major earthquake which mostly needs member retrofitting or replacement/rebuilding the whole bridge.

Mander and Cheng (1997) conducted tests on a full scaled precast concrete rocking column under seismic loading to validate the proposed model. Results were in agreement with the predicted performance and hence validated the design philosophy.

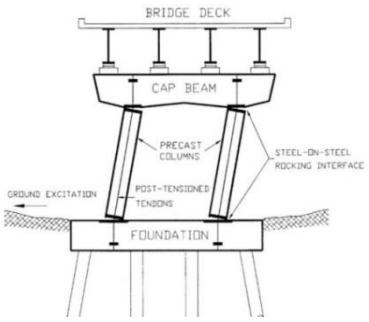

Figure 2.18. Design based on Damage Avoidance Design (Mander and Cheng, 1997).

Li et al. (2008) assessed the performance of an 80 percent scaled precast prestressed beam to column connection of a frame designed in accordance to the DAD philosophy. Results showed good performance of the specimen up to four percent drift with no damage or cracking in the column and minor flexural cracking in the precast bent cap.

Pretensioned rocking bridge bent

A similar connection concept to the DAD was recently developed by Stanton et al. (2014), which dissipates seismic energy by controlled rocking at the joints between the column and the bent cap/footing. However, it should be noted that this solution is not strictly damage free. The column ends are detailed so that the column can rock as a rigid body at the cracks produced near the ends. Figure 2.19 shows the steel toe or shoe reinforced at column ends to prevent damage to the concrete due to rocking. Pretensioned strands present in the center of the column, unbonded in the middle and bonded at the ends, are designed for the system to return to original position after ground motion stops. The reinforcing bars are debonded at the ends to prevent premature bar fracture.

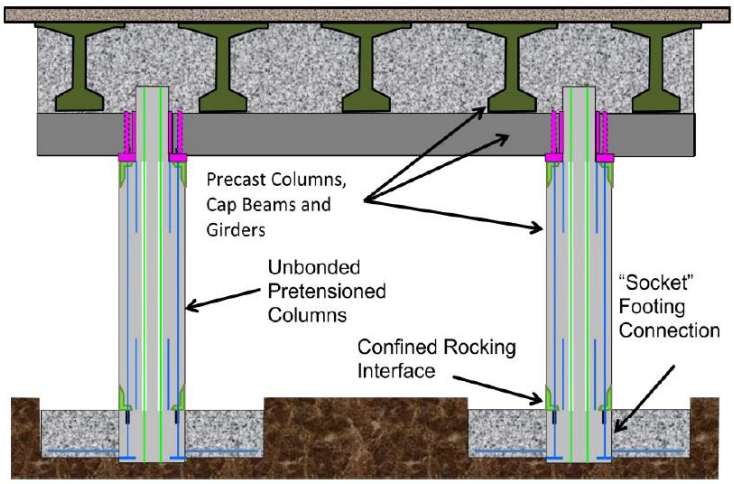

Figure 2.19. Precast, pretensioned rocking column (Stanton et al., 2014).

Stanton et al. (2014) performed cyclic tests on cap-column and column-footing connections. Connection types included large diameter bar connection and socket connection between column-to-bent cap and column-to-footing respectively. An octagonal column was used and reduced in section at the interface with the bent cap. Results showed that the column returned to its original position at unloading even at high drifts and lateral load resistance continued even at drift ratios of 10.4 percent after two cycles of deformation. Spalling and buckling were not visible. Thus it was observed that cyclic performance of the sub-assemblies was better than the conventional reinforced concrete connection, but not damage free as in DAD.

3. DESIGN CONSIDERATIONS

To develop designs for precast, pretensioned concrete bent caps it is first necessary to identify potential design challenges and opportunities for improvements in design efficiency. This chapter is devoted to a preliminary investigation of design challenges.

This chapter provides an overview of the TxDOT design requirements for RC bent caps. This is followed by a summary of the design objectives for pretensioned bent caps. Flexural design considerations, including a proposed design procedure, an alternate design procedure and an extension of the proposed procedure using Magnel diagram have been discussed. An investigation on the impact of strand configuration is also presented in this chapter.

3.1. TxDOT reinforced concrete bent caps

The motivation for investigating the design of pretensioned bent caps is to provide an alternative to reinforced concrete designs. For a pretensioned alternative, it is desirable to provide improved constructability and performance under service and ultimate loads. As such, a summary of RC bent cap design requirements and standard practice are presented here.

Unless higher strength materials are needed for special cases, Class C concrete with a compressive strength of 3.6 ksi and Grade 60 reinforcing steel are used. Bent cap width is based on the size of the columns, with the cap width at least 6 inch wider than the column. For I-girder bridges with Tx-62 girders, a 42 inch diameter column and a 48 inch cap width is used. For other I-girder bridges, a 36 inch diameter column and a 42 inch bent cap is used. The depth of the cap is required to be in 3 inch increments, but

not less than the width of the cap except when the width is widened to accommodate a precast connection.

Analysis of multi-column caps is done as simply supported beams on knife-edge supports at the center of columns or piles with moments taken at the center of the column except for bent caps widths of 4 ft or larger, in which case the moment at the face of the support is used for design. TxDOT uses in-house bent cap analysis program CAP18 to establish demands for dead, service and ultimate loading. Loading on the bent cap considered for design consists of dead and vehicular live load with impact.

Both Strength I and Service I limit state load combinations are considered for design. Under the Service I load combination, the tensile stress in the steel reinforcement is limited to $0.6f_y$. Previously, an additional serviceability limit of 22 ksi under service dead load was considered; however, this provision was removed in the 2015 update to the design guidelines.

Flexural reinforcement is typically #11 bars, although smaller bars can be used to satisfy development length requirements; mixing of bars sizes is prohibited. Longitudinal skin steel is required along the sides of the cap; typically, this is provided as #5 bars.

Monolithic connections for cast-in-place bent caps consist of an extension of the column longitudinal reinforcement into the cap. An alternative connection detail is provided to allow construction of precast reinforced concrete bent caps; details of this connection are discussed in Section 6.2.1.

3.2. Design objectives for pretensioned bent caps

The primary design objective for precast, pretensioned bent caps is to provide at least equivalent, but preferably superior, performance to reinforced concrete designs. To achieve this, one key limit on stresses in the bent cap is introduced in this research: no tension stress is permitted under dead load. This ensures any unexpected cracks will close under the removal of applied load. At service, the stresses are limited to the AASHTO LRFD tension and compression stress limits of $0.19\sqrt{f'_c\,(ksi)}$ and $0.45\,f'_c$ respectively.

Provisions for compressive strength requirements for prestressed concrete bent caps are not explicitly stated in AASHTO LRFD and TxDOT standards. The TxDOT Design Manual specifies the use of Class H concrete for pretensioned concrete beams with a minimum f'_{ci} = 4 ksi and f'_c = 5 ksi, and a maximum f'_{ci} = 6 ksi and f'_c = 8.5 ksi. This provision has been adopted for the design of prestressed concrete bent caps and is in conformity with the requirement in AASHTO LRFD which specifies the use of a minimum specified compressive strength of 4 ksi for prestressed concrete members and decks. Due to common use of 0.6 inch diameter strands in the TxDOT prestressed concrete I-girder standard designs, 0.6-inch diameter low relaxation strands with a specified tensile strength of f_{pu} = 270 ksi are adopted herein.

Prestressing losses of 20 percent are conservatively assumed for pretensioned members and is used in the design. The design of the cap to resist the bursting and spalling stresses at the ends of prestressed members is considered, with reinforcement designed to prevent cracking under these stresses.

3.3. Flexural design

The design approach for reinforced concrete bent caps selects top and bottom flexural reinforcement to provide sufficient strength; skin reinforcement is not considered to contribute to the strength of the specimen. The design is then checked for stresses in the reinforcement at dead and service loads, resulting in an increase in reinforcement in some cases. The dead load stress is intended to limit the observed cracking under dead load.

In establishing a flexural design procedure for pretensioned bent caps, it is desired to provide equivalent or superior performance to reinforced concrete bent caps. To improve the performance, it is necessary to limit the extent of cracking in the bent cap. In exploring potential design procedures, a number of approaches were considered. These approaches generally focused on achieving target stress levels under dead, service, and/or ultimate loads. The proposed design procedure, presented in detail in Section 3.3.1, was found to be simple while achieving the design objectives of providing strength and limiting the cracking in the bent cap. An alternative approach, presented in Section 3.3.2, serves as a useful approach when a pretensioned design is developed as an alternative to an existing design for a reinforced concrete bent cap. Section 3.3.3 provides an extension of the proposed design procedure to include the option of eccentric prestressing with the use of Magnel diagrams.

The proposed design procedure was developed for solid, square cross-sections with strands located primarily at the top and bottom of the section. To provide flexibility in construction, modifications in the strand arrangement to better accommodate the

cap-to-column connection is considered. The impact of strand configuration on the strength and serviceability of bent caps is presented in Section 3.3.4.

3.3.1. *Proposed design procedure*

The following design procedure for pretensioned bent caps is based on the simple philosophy of no tension permitted under dead load. The steps in the design procedure are detailed below, with in-depth discussion presented in the subsequent paragraphs.

STEP 0: Determine minimum number of strands

STEP 1: Calculate number of strands for zero tension under dead load

STEP 2: Determine required minimum concrete compressive strength

STEP 3: Check ultimate strength capacity

STEP 4: Check deflections

Step 0: Determine minimum number of strands

To preclude a brittle failure of the section it is necessary to check that the flexural resistance is greater than the cracking moment.

AASHTO LRFD Section 5.7.3.3.2 specifies that the amount of prestressed tensile reinforcement shall be adequate to develop a factored flexural resistance, M_r, which is at least equal to the lesser of (a) 1.33 times the ultimate moment and (b) cracking moment. The cracking moment is given by:

$$M_{cr} = (f_t A + F) S_x \qquad (3\text{-}1)$$

in which M_{cr} = cracking moment (k-in); $f_t = 0.24\sqrt{f_c'(ksi)}$ (AASHTO LRFD 5.4.2.6); A = area of cross section (in^2); F = prestressing force (k); and S_x = section

modulus (in^3) (for a rectangle $S_x = BD^2/6$ where B = width and D = overall depth). Note the sign convention of *tension positive* is used throughout this work.

The number of strands for which Eq. (3-1) equals the nominal moment capacity is determined and increased by a factor of 1.33 (AASHTO LRFD 5.7.3.3.2) to evaluate the minimum number of strands.

STEP 1: Calculate number of strands for zero tension under dead load

The first step in design is to select the number of strands to achieve zero tension under dead load. The flexural stresses under dead load should remain compressive at the extreme tension fiber (see Figure 3.1)

$$-\frac{F}{A}+\frac{M_{DL}}{S_x}<0 \tag{3-2}$$

and within the normal service limits at the extreme compression fiber

$$-\frac{F}{A}-\frac{M_{DL}}{S_x}>-0.45 f_c' \tag{3-3}$$

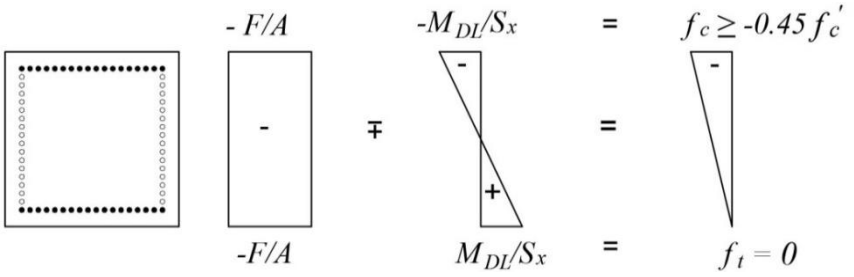

Figure 3.1. Stresses under dead load: No tension.

in which F = prestress force after losses (k); M_{DL}= dead load moment (k-in); f'_c = specified compression strength of the concrete (ksi).

From Eqs. (3-2) and (3-3) it follows that the required prestressing force is

$$F \geq 6\frac{M_{DL}}{D} \tag{3-4}$$

with an upperbound value determined by the limits on compressive stresses:

$$F \leq 0.45 f_c' A - 6\frac{M_{DL}}{D} \tag{3-5}$$

In Eq. (3-5), only a provisional value for f'_c (6 ksi - 8.5 ksi) needs to be selected at this stage of the design. The concrete compressive strength should be sufficiently strong to prevent time dependent losses. Excessive concrete strength results in a higher cracking moment and thus greater minimum reinforcement to prevent a brittle failure.

The number of strands is calculated as:

$$n = \frac{F}{T_{strand}} \tag{3-6}$$

where T_{strand} = prestressing force per strand and is calculated as:

$$T_{strand} = f_{pbt} A_{PS} (1 - \Delta f_{pT}) \tag{3-7}$$

in which $f_{pbt} = 0.75 f_{pu}$ = stress limit in low relaxation strand immediately prior to transfer (ksi); f_{pu} = specified tensile strength of prestressing strand = 270 ksi (AASHTO LRFD Table 5.4.4.1-1); A_{ps} = area of each strand = 0.217 in^2 for 0.6 inch diameter strand; and Δf_{pT} = prestress loss in pretensioned members = 20 percent.

The number of strands from Eq. (3-6) is rounded up to the nearest multiple of 2 or 4 for symmetric arrangement of strands in the bent cap.

STEP 2: Determine required minimum concrete compressive strength

To ensure that the bent cap does not crack at service, a minimum concrete compressive strength should be provided such that the service stresses are less than or equal to the service stress limits specified in AASHTO LRFD.

As shown in Figure 3.2, the tensile and compressive stresses are calculated from the service moments

$$f_t = -\frac{F}{A} + \frac{M_{DL+LL+IM}}{S_x} \tag{3-8}$$

$$f_c = -\frac{F}{A} - \frac{M_{DL+LL+IM}}{S_x} \tag{3-9}$$

where $M_{DL+LL+IM}$ = moment due to dead load and live load with impact (k-in); f_t = tension stress (ksi); and f_c = compression stress (ksi).

The design concrete compressive strength must be selected such that the AASHTO tension (Table 5.9.4.2.2-1) and compressive (Table 5.9.4.2.1-1) service stress limits are met:

$$f_t \le 0.19\sqrt{f_c'} \tag{3-10}$$

$$f_c \ge -0.45 f_c' \tag{3-11}$$

If the necessary strength is $f'_c <$ 6 ksi, then a minimum design concrete compressive strength of f'_c = 6 ksi is recommended.

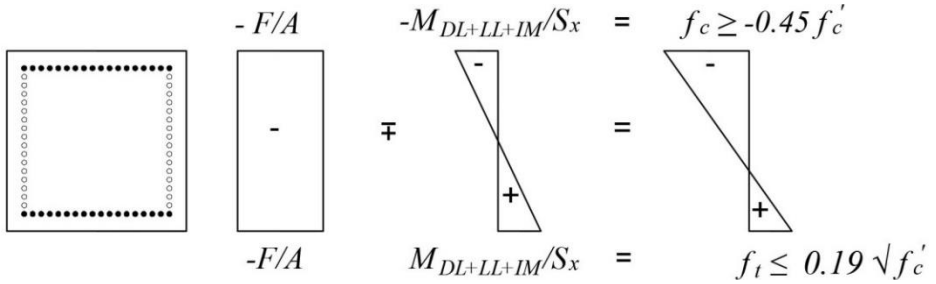

Figure 3.2. Stresses under service load and establish minimum concrete strength.

STEP 3: Check ultimate strength capacity

The bent cap should have at least the nominal strength capacity such that it does not fail under the ultimate flexural demand. The ultimate flexural moment capacity (M_n) is calculated from AASHTO LRFD 5.7.3.2 (see Figure 3.3) and evaluated against the demands:

$$\phi M_n \geq M_u \tag{3-12}$$

where M_u = flexural demand under ultimate loads; ϕ = 1 for tension-controlled prestressed concrete sections (AASHTO LRFD 5.5.4.2.1). If $\phi M_n < M_u$, the prestressing force should be increased such that Eq. (3-12) is satisfied.

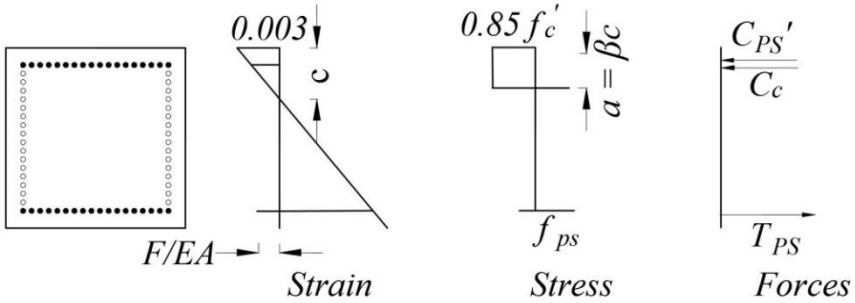

Figure 3.3. Ultimate strength capacity.

STEP 4: Check deflections

To ensure that the deflection of the bent cap does not affect serviceability, the deflection should be checked to be within the specified limit.

The deflection, Δ under vehicular loading should be less than the limit specified in AASHTO LRFD 2.5.2.6.2, specifically

$$\Delta < Span/800 \tag{3-13}$$

3.3.2. *Alternate design approach*

An alternate design approach is to replace Step 1 of the proposed design procedure with another method of selecting the number of strands. In this approach, the proposed prestressed solution is determined to provide an equivalent reinforcement capacity. The approach would allow the use of existing designs, thereby preventing the need to start the design from the beginning. Standard TxDOT practice is followed for the reinforced concrete solution to determine the amount of reinforcing steel. The equivalent reinforcement capacity is provided as the prestressed solution:

$$A_{PS}\,0.75\,f_{pu} = A_S\,f_y \tag{3-14}$$

The number of strands is determined by:

$$n = \frac{A_{PS}}{A_{strand}} \tag{3-15}$$

in which A_{strand} is the area of each strand (in^2). Eq. (3-15) is the alternative to Eq. (3-6) in the design procedure; all other steps remain unchanged.

3.3.3. *Magnel diagram*

The proposed design procedure in Section 3.3.1 may be further extended to introduce eccentric prestressing thereby economizing the total number of strands required. In this approach, equations such as those given by (3-2), (3-3), (3-10) and (3-11) are recast in terms of e as a function of other geometric parameters and 1/F. These equations are plotted as e vs. 1/F and a feasible domain identified. The graph is known as a Magnel diagram.

During prestressing, there are two critical loading stages. At initial prestressing when the concrete is not strong, the stresses are due to prestress and self-weight of the member; at this point there is no prestress loss. When the component is in service, the stresses are due to prestress, self-weight of the member, superimposed dead loads or full service loads or ultimate loads; at this point the prestressing force is reduced due to losses. It is necessary that the stresses in these stages do not exceed the allowable stresses. From AASHTO LRFD provisions, an allowable stress of $0.6f'_{ci}$ in compression under self-weight is considered. Consistent with the proposed design procedure, an allowable stress of zero tension under dead; $0.19\sqrt{f'_c\,(ksi)}$ and $0.38\sqrt{f'_c\,(ksi)}$ under service and ultimate loads respectively in tension; $0.45f'_c$ in compression under dead and service loads; and $0.60f'_c$ under ultimate load in compression is considered.

The two critical stress locations in pretensioned bent caps are the maximum negative moment at the columns and the maximum positive moment in the span. At both locations the tension and compression stresses under each loading condition are checked with the allowable stresses resulting in 14 stress inequality equations.

Table 3.1 summarizes the stress inequality conditions, in which e = eccentricity assumed positive below the neutral axis (inch); D = depth of section; f'_c = concrete compressive strength; S_x = section modulus; F = applied prestressing force; M_{DL} = moment under dead load; M_{SL} = moment under service load; M_{UL} = moment under ultimate load; and M_{SW} = moment under self-weight. For simplicity, the equations emphasize the unknowns e and $1/F$. Stress conditions I to III and IV to VII represent tension under negative and positive moments respectively. Stress conditions VIII to X and XI to XIV represent compression under negative and positive moments respectively.

Table 3.1. Inequality stress equations.

Stress condition	Inequality equation
I	$e \leq D/6 - M_{DL}/F$
II	$e \leq D/6 + (0.19\sqrt{f'_c}S_x - M_{SL})/F$
III	$e \leq D/6 + (0.38\sqrt{f'_c}S_x - M_{UL})/F$
IV	$e \geq -D/6 + 0.8M_{SW}/F$
V	$e \geq -D/6 + M_{DL}/F$
VI	$e \geq -D/6 - (0.19\sqrt{f'_c}S_x - M_{SL})/F$
VII	$e \geq -D/6 - (0.38\sqrt{f'_c}S_x - M_{UL})/F$
VIII	$e \leq -D/6 - (-0.45f'_cS_x + M_{DL})/F$
IX	$e \leq -D/6 - (-0.45f'_cS_x + M_{SL})/F$
X	$e \leq -D/6 - (-0.60f'_cS_x + M_{UL})/F$
XI	$e \geq D/6 + 0.8(-0.60f'_{ci}S_x + M_{SW})/F$
XII	$e \geq D/6 + (-0.45f'_cS_x + M_{DL})/F$
XIII	$e \geq D/6 + (-0.45f'_cS_x + M_{SL})/F$
XIV	$e \geq D/6 + (-0.60f'_cS_x + M_{UL})/F$

A graphical representation of the equations with *1/F* in the x-axis and *e* in the y-axis form straight lines creating the Magnel diagram (Magnel 1948). Each line passes through one of the kern points ($e = S_x / A$) when 1/F = 0. Four of the 14 inequalities govern a feasible region which gives the most valid combination of *e* and *1/F*. The allowable stresses are met within this feasible domain. Figure 3.4 shows an example Magnel diagram presenting the four lines governing the feasible domain. The optimal solution occurs when *1/F* is maximized.

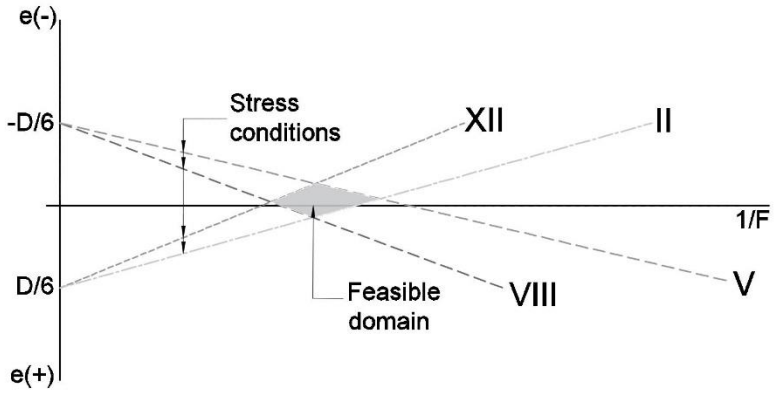

Figure 3.4. Magnel diagram construction.

3.3.4. *Effect of strand configuration*

The design procedure proposed in Section 3.3.1 was developed for solid square cross sections with strands located primarily at the top and bottom of the section. To prevent interference of the bent cap-to-column connection on the strand layout, rearrangement of the strands to the sides has been considered.

In the top and bottom configuration, the primary reinforcement is placed at the top and bottom and secondary reinforcement in the form of skin steel is provided on the sides for crack control. The current TxDOT design of reinforced concrete bent caps have

the same configuration of flexural reinforcement. Figure 3.5(a) shows a general strand layout in the top and bottom configuration.

In the side configuration, the primary reinforcement is placed on the sides. It can serve as an alternative to top and bottom configuration when constraints in the layout of reinforcement is faced due to pockets created for precast connection in bent caps. Figure 3.5(b) shows a general strand layout in the side configuration. The strands on the sides will not pose any interference to the bent cap-to-column connection.

It should be noted that prior to cracking, both sections have the same performance because their cgs is identical. Slight differences emerge after cracking commences.

A brief analysis of the impact of the strand configuration is presented here; the strand layouts shown are for illustrative purposes only and should not be considered a recommendation for implementation in a pretensioned cap design.

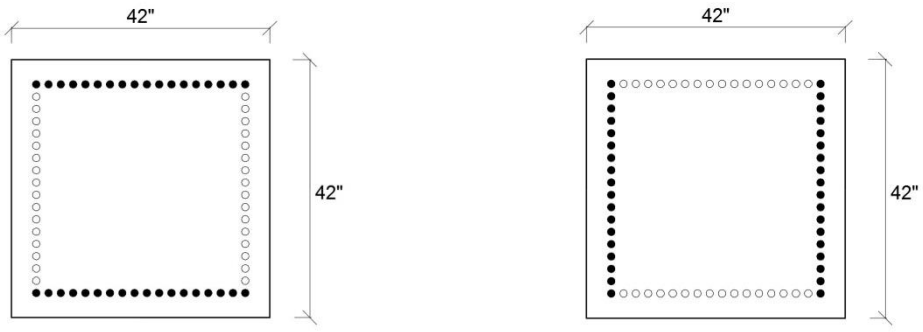

(a) Top/bottom configuration *(b) Side configuration*

Figure 3.5. General strand layouts.

Figure 3.6 shows the full moment-curvature response of a 42 inch bent cap with 18 numbers of strands obtained by fiber-section analysis (OpenSees Version 2.4.6). Three critical points are indicated: 1) cracking, 2) yield f_{py}, and 3) nominal strength. As mentioned above, both configurations have the same behavior prior to cracking. After cracking occurs, the stiffness is greater for the top/bottom configuration. At yield, the curvature is same in both the configurations, with a higher moment in the top/bottom configuration. At the nominal strength, the top/bottom configuration has slightly larger moment and curvature. This is due to a lower number of strands in tension than the side configuration, resulting in a smaller concrete compression stress block and thus higher curvature.

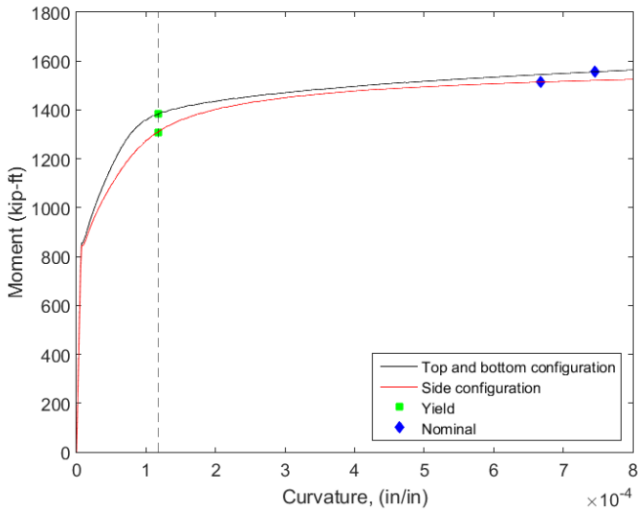

Figure 3.6. Moment curvature.

The most important effect of the configuration of strands is the nominal strength, particularly the sensitivity to the number of strands. Figure 3.7 illustrates the impact of the amount of prestressing on the moment strength for the 42 inch and 48 inch square

bent caps for a concrete compressive strength of 8.5 ksi. To eliminate the impact of the cross-section dimensions, the nominal strength is normalized by *AD* and the area of prestressing is normalized by *A* (same as reinforcement ratio). The solid black line represents the top and bottom configuration, and the dashed red line represents the side configuration. The range of variation in strength between the two configurations increases with the increase in the area of prestressing, but the strength of the side configuration is not more than 5 percent less than the strength of the top/bottom configuration.

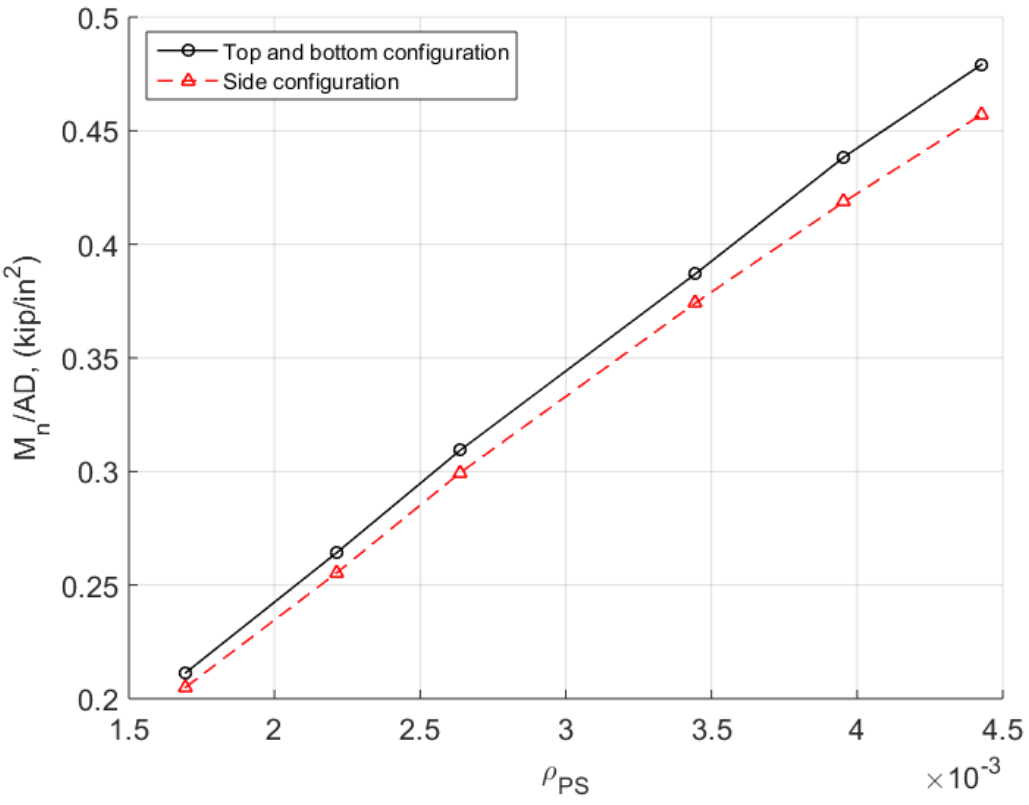

Figure 3.7. Nominal strength vs. area of prestressing.

4. OVERVIEW OF BRIDGE INVENTORY

To evaluate the application of the proposed design procedures, the TxDOT standard bent designs for bridges with I-girders, box beams and X-beams are used as a demonstration bridge inventory. Additionally, two nonstandard bridges which do not conform to the TxDOT bridge inventory have also been considered. In this chapter, the bridge characteristics, summary of the sources of loads and method of analysis and an overview of the demands for the bridge inventory is discussed.

4.1. Bridge characteristics

The bridge characteristics for I-girders, box beams, X-beams and nonstandard bridges are presented in the subsections below.

4.1.1. *Non-skewed I-girder bridges*

The roadway widths of the TxDOT I-girder bridges are 24 ft, 28 ft, 30 ft, 32 ft, 38 ft, 40 ft and 44 ft. In this research, three span lengths are considered for each bridge width: minimum, intermediate and maximum span length. For Tx-28 to Tx-54 girders, the minimum, intermediate and maximum span lengths considered are 40ft, 80 ft and 120 ft respectively. For Tx-62 girders, the minimum, intermediate and maximum span lengths considered are 60 ft, 95 ft and 130 ft respectively.

The non-skewed I-girder bridges consist of three unique bent configurations shown in Figure 4.1. Figure 4.1(a) shows the three column, four girder configuration (24 ft, 28 ft, 30 ft, and 32 ft bridge widths). Figure 4.1(b) shows the three column, five

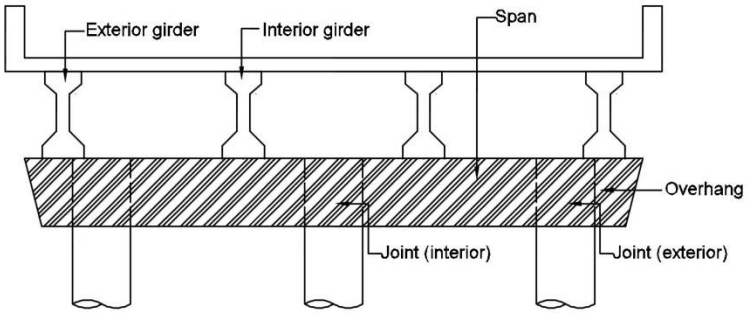

(a) 3 column, 4 girder

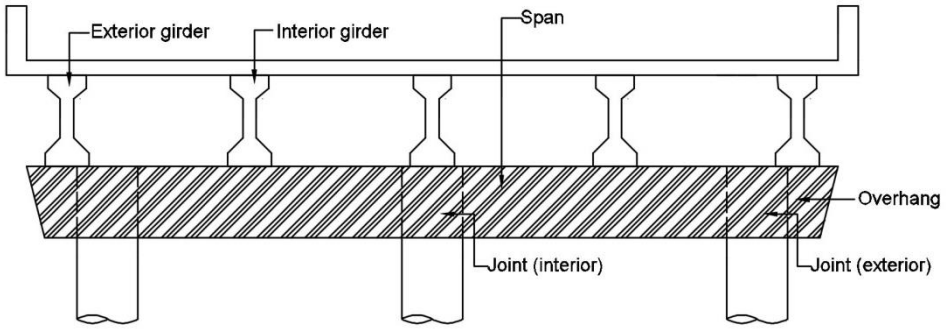

(b) 3 column, 5 girder

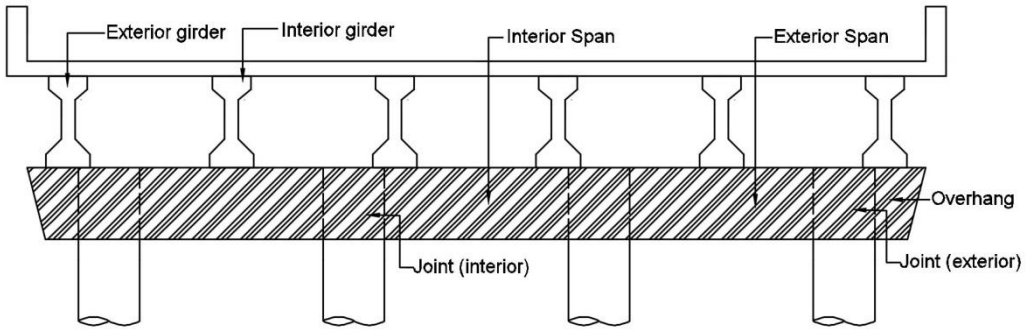

(c) 4 column, 6 girder

Figure 4.1. Bent configurations in bridge inventory for non-skewed I-girders.

girder configuration (38 ft, and 40 ft bridge widths). Figure 4.1(c) shows the four column, six girder configuration (44 ft bridge width). The column spacing for the bridges vary from 8 ft to 12 ft, except for the 38 ft and 40 ft width bridges in which the column spacing are 15 ft and 16 ft respectively. The girder spacing for the bridges vary from 6.67 ft to 9.33 ft. The exterior girders in all non-skewed bridges are located 2 ft from the edge of the bent cap and 2 ft from the center of the exterior column.

The column dimensions in the standard TxDOT bridge inventory are based on the girder sizes. For girder sizes of Tx-28 to Tx-54 the columns are 36 inch diameter, while for Tx-62 girder the columns are 42 inch diameter. TxDOT design requirements specify that the width of the bent cap be 6 inch greater than the column dimension. For girder sizes of Tx-28 to Tx-54 the bent cap is of 42 inch width. For Tx-62 girder the bent cap is of 48 inch width. A square shape is preserved for aesthetics.

4.1.2. *Skewed I-girder bridges*

Skew angles of 15, 30 and 45 degrees are used with TxDOT standard I-girders. In lieu of all the skew angles, the 45 degree skewed I-girder bridges will be discussed in this research. Similar to the bridges with non-skewed I-girders, the minimum, intermediate and maximum span length for Tx-28 to Tx-54 girders are 40 ft, 80 ft and 120 ft respectively, and for Tx-62 girders are 60 ft, 95 ft and 130 ft respectively.

The girder spacing in the skewed bridges is the same as the non-skewed bridges. The distance of exterior girder/column from edge of bent cap and column spacing increases by the reciprocal of the cosine of the skew angle. To restrict the column spacing to the 18 ft limit used by TxDOT, an additional column is added in the 45

degree skew of the 38 ft roadway and in the 30 and 45 degree skews of the 40 ft roadway.

For the 45 degree skew, the I-girder bridges consist of three unique bent configurations shown in Figure 4.2. Figure 4.2(a) shows the three column, four girder configuration (24 ft, 28 ft, 30 ft, and 32 ft bridge widths). Figure 4.2(b) shows the four column, five girder configuration (38 ft and 40 ft bridge widths). Figure 4.2(c) shows the four column, six girder configuration (44 ft bridge width). The column spacing for the

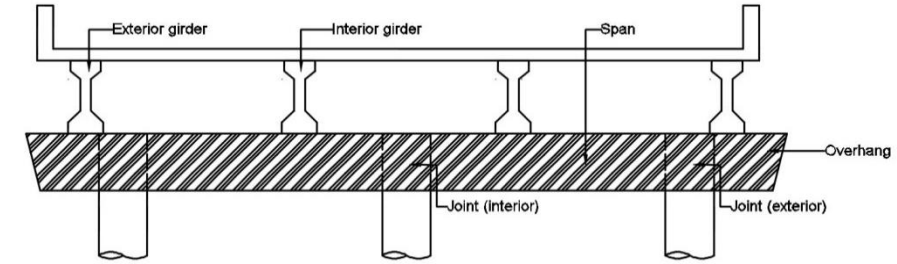

(a) 3 column, 4 girder

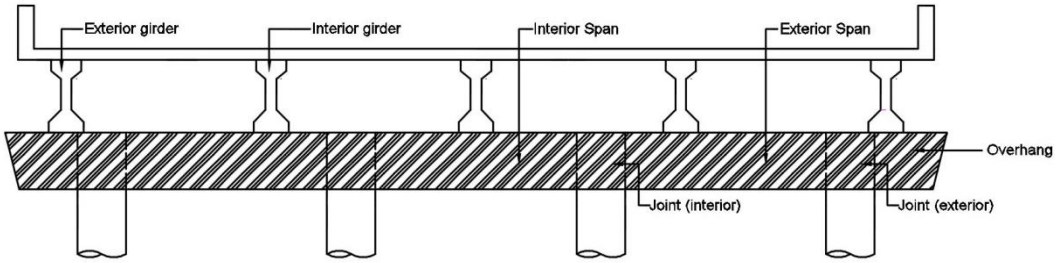

(b) 4 column, 5 girder

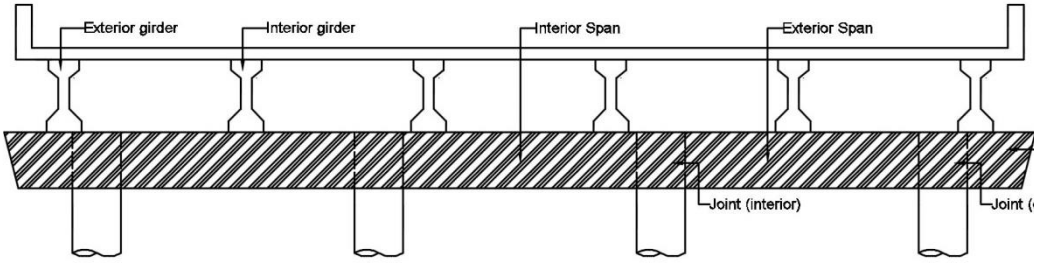

(c) 4 column, 6 girder

Figure 4.2. Bent configurations in bridge inventory for 45 degree skewed I-girders.

bridges vary from 12 ft to 17.5 ft. The girder spacing for the bridges vary from 9.42 ft to 13.19 ft. The locations of the exterior girders in the 45 degree skewed bridges vary from 3.70 ft to 3.86 ft from the edge of the bent cap. The centers of the exterior columns are located 6 ft from the edge of the bent cap.

The column dimensions and bent cap sizes in the skewed I-girder bridges are the same as the non-skewed I-girder bridges.

4.1.3. *Bridges with box beams*

The roadway widths of the TxDOT bridges for box beams are 24 ft, 28 ft and 30 ft. The span lengths vary from 30 ft to 95 ft for the box beams (B20, B28, B34 and B40). In this research, three span lengths are considered for each bridge width: minimum, intermediate and maximum span lengths of 30ft, 60 ft and 95 ft respectively.

The box beam bridges consist of two unique bent configurations shown in Figure 4.3. Figure 4.3(a) shows the three column, six girder configuration (24 ft and 28 ft bridge widths). Figure 4.3(b) shows the three column, seven girder configuration (30 ft bridge width). The column spacing for the bridges vary from 10 ft to 13 ft. The girder spacing for the bridges vary from 4.30 ft to 5.10 ft. The exterior girders are located 3.53 ft from the edge of the bent cap and the center of the exterior column varies from 4.29 ft to 4.38 ft from the edge of the bent cap. The columns are 30 inch diameter, and the bent caps are 2.75 ft wide and 3 ft deep.

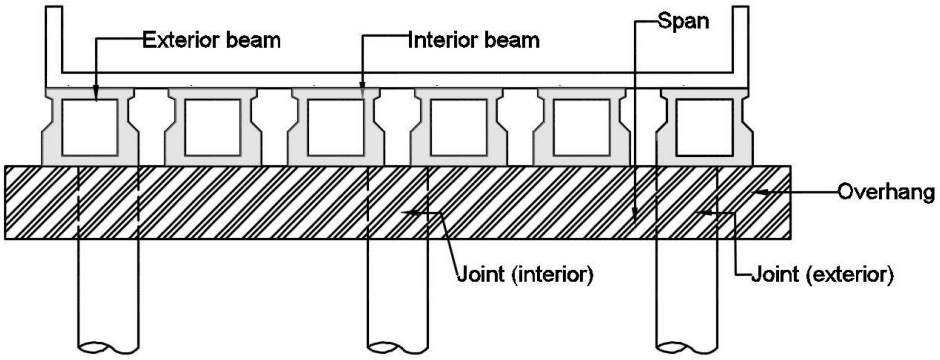

(a) 3 column, 6 girder

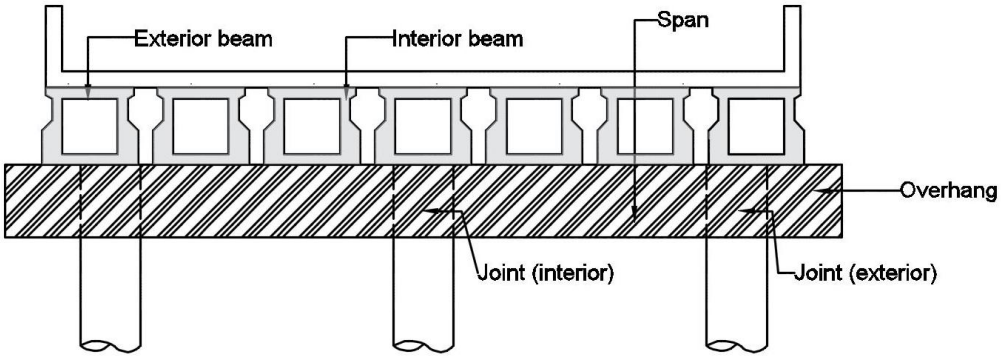

(b) 3 column, 7 girder

Figure 4.3. Bent configurations in bridge inventory for box beams.

4.1.4. *Bridges with X-beams*

The roadway widths of the TxDOT bridges for X-beams (spread box beams) are 32 ft, 38 ft, 40 ft and 44 ft. The span lengths vary from 40 ft to 105 ft for the XB20, XB28, XB34 and XB40 X-beams. In this research, three span lengths are considered for each bridge width: minimum, intermediate and maximum span lengths of 40ft, 70 ft and 105 ft respectively.

The X-beams bridges consist of three unique bent configurations shown in Figure 4.4. Figure 4.4(a) shows the three column, four girder configuration (32 ft bridge width). Figure 4.4(b) shows the three column, five girder configuration (38 ft and 40 ft bridge

widths). Figure 4.4(c) shows the four column, six girder configuration (44 ft bridge widths). The column spacing for the bridges vary from 12 ft to 16 ft. The girder spacing for the bridges vary from 7.6 ft to 8.67 ft. The exterior girders are located 3.5 ft from the edge of the bent cap and 1 ft from the center of the exterior column.

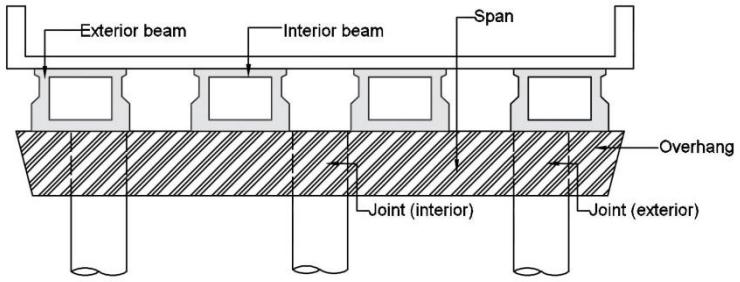

(a) 3 column, 4 girder

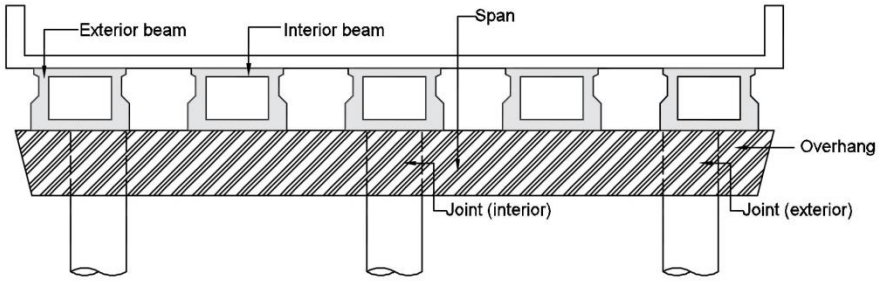

(b) 3 column, 5 girder

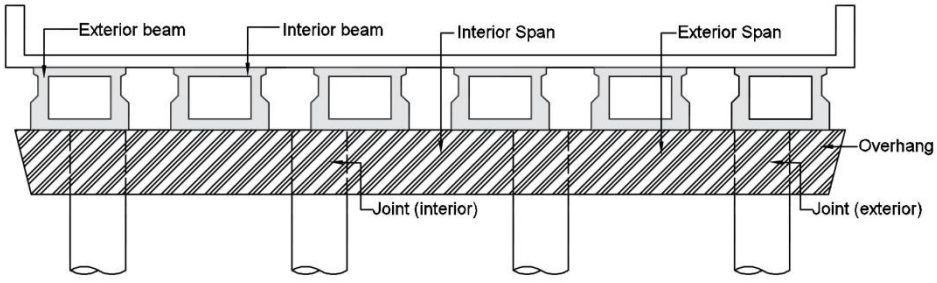

(c) 4 column, 6 girder

Figure 4.4. Bent configurations in bridge inventory for X-beams.

The column dimensions in the standard TxDOT bridge inventory for bridges with X-beams is 36 inch diameter. The bent caps are square of 42 inch width.

Skew angles of 15 and 30 degrees are considered in bridges with X-beams. The skewed bridges for the 32 ft, 38 ft, 40 ft and 44 ft roadway widths have the same bent configuration as the corresponding roadway widths in skewed bridges with I-girders. The skewed X-beam bridges are not studied in this research.

4.1.5. *Non-standard bridges*

TxDOT practice is to restrict standard bridges to a maximum non-skewed column spacing of 18 ft and girder spacing of 10 ft. This restriction is applied to readily implement standard girder and column designs without the need to redesign.

However, if the columns/girders are analyzed and designed, the maximum standard spacing could be increased. In this research, two bridge configurations not conforming to the standard spacing have been evaluated. Figure 4.5(a) shows a four column, seven girder configuration (68 ft bridge width) with column spacing of 19.67 ft. If standard spacing was used, the configuration would normally be a five column bent with 14.75 ft spacing. Figure 4.5(b) shows a five column, ten girder configuration (85 ft bridge width) with column spacing of 19 ft. If standard spacing was used, the configuration would normally be either six or seven column bent with 15.2 ft or 12.67 ft spacing, respectively.

The column dimensions in the nonstandard bridges with Tx-54 I-girders are 36 inch diameter. The bent caps are square of 42 inch width.

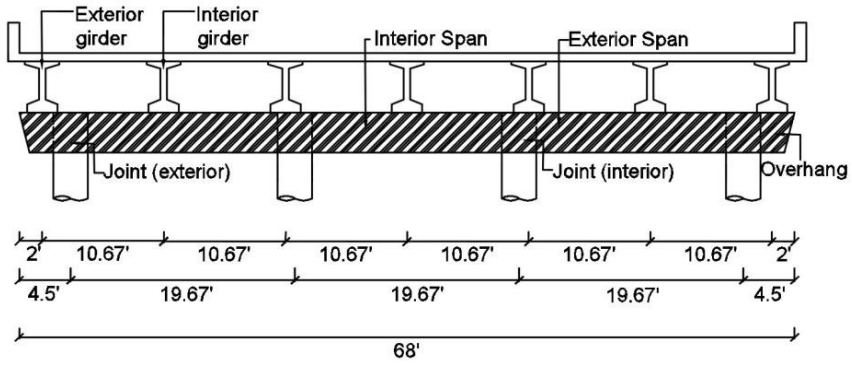

(a) 4 column,7 girder

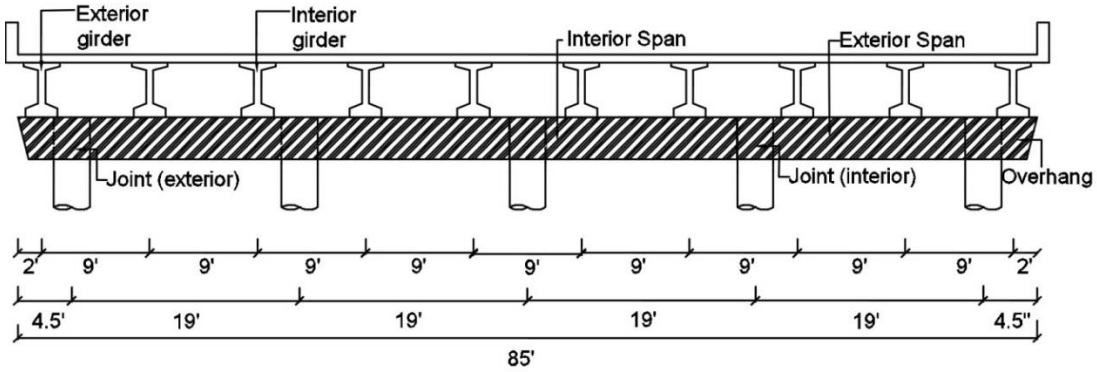

(b) 5 column, 10 girder

Figure 4.5. Bent configurations in nonstandard bridges.

4.2. Loads and analysis

Sources of loads on the bent cap used for structural design are the permanent dead load and the transient vehicular live load. The dead loads consist of loads from structural and non-structural attachments (DC) such as self-weight of all bridge elements i.e. slab, wearing surface (overlay), railing, girder and bent cap, and wearing surfaces and utilities (DW). Deck thickness is 8.5 inch for I-girder, 5 inch for box beams and 8 inch for X-beams. The vehicular live load is the combination of the design truck or tandem, and the design lane load, calculated with the AASHTO LRFD HL-93 design live load. The maximum live load reaction at an interior bent cap is always governed by the design

truck. The dynamic load allowance factor specified in AASHTO LRFD Table 3.6.2.1-1 is applied to the truck load to account for wheel load impact from moving vehicles. Multiple presence factors specified in AASHTO LRFD Table 3.6.1.1.2.1 are used for single or multiple lanes.

Flexural and shear demands were determined using the TxDOT bent cap analysis program CAP18 (CAP18 Version 6.2.2). The CAP18 program considers the bent cap as a continuous beam placed on knife-edge supports. The program analyzes dead and live loads that conform to AASHTO standard specifications. CAP18 has the unique feature of a movable load that runs across the width of the deck. The program determines the largest demands at the bent cap control points (such as column and girder positions) due to the movable load. This feature enables CAP18 to achieve conservative demands for the movable load.

The live load is a movable load to enable the program to determine the maximum demands. The live load model is stepped across the deck slab in user defined increments. The live load consists of a combination of concentrated load (P) and a uniform load (w) defined on a 10 ft design lane width. This load is used in combination with the dead loads to generate the service and ultimate shear and moment envelopes.

4.3. Summary of demands

The demands for the full bridge inventory were determined using CAP18. For comparison, demands were also evaluated by frame analysis of bents with 13.75 ft columns using SAP2000 (SAP2000 v.17.1.1). The live loads on the interior and exterior girders were determined from the live load distribution factor for shear in interior and

exterior beams from AASHTO LRFD Table 4.6.2.2.3a-1 and Table 4.6.2.2.3b-1 respectively.

Table 4.1 shows the maximum demands under dead, service and ultimate loads for the three bent configurations in non-skewed I-girders computed from CAP18 and frame analysis and the percentage by which CAP18 results are higher. It has been observed that the movable live load in CAP18 generates demands that result in a more conservative design than the live loads computed from AASHTO LRFD provisions for frame analysis.

Table 4.1 Comparison of flexural demands in non-skewed I-girders.

Roadway width		Maximum dead load moment	Maximum service load moment	Maximum ultimate load moment
32 ft	CAP18 (k-ft)	391	615	881
	Frame analysis (k-ft)	391	591	838
	% difference	0 %	4 %	5 %
40 ft	CAP18 (k-ft)	392	760	1133
	Frame analysis (k-ft)	393	656	951
	% difference	0 %	16 %	19 %
44 ft	CAP18 (k-ft)	351	557	780
	Frame analysis (k-ft)	351	530	752
	% difference	0 %	5 %	6 %

Sample results for each bent configurations in the non-skewed I-girders, skewed I-girders, box beams, X-beams and nonstandard bridges are discussed in Sections 4.3.1, 4.3.2, 4.3.3, 4.3.4 and 4.3.5 respectively.

4.3.1. *Non-skewed I-girder bridges*

Figure 4.6(a), (b) and (c) shows the bending moment diagrams under dead load for the 42 inch bent caps of 32 ft, 40 ft and 44 ft respectively. For the bents evaluated, two scenarios were observed for the location of maximum moment demands: (a) maximum moment at the column, and (b) maximum moment in the span. For most bridges with non-skewed I-girders, the maximum moment occurs at the exterior columns. The maximum moment occurs at the interior columns for dead loads on bridges with short spans and larger column spacing. The maximum moment occurs in the span for bridges with longer spans and larger column spacing, although not always for all load combinations. Table 4.2 summarizes the bridges and load combinations for which the maximum demand occurs in the span.

Table 4.3 provides a summary of the maximum moment demands in the 42 inch and 48 inch bent caps. The first three rows provide the largest values for dead, service and ultimate loads; these may be at different locations for each load combination. To facilitate a generalized evaluation of the demands between different size caps, the fourth row presents dead load moments normalized by AD in which A is the area of cross section and D is the depth of the bent cap. The moments at service and ultimate states are expressed as ratios to the dead load moments in the fifth and sixth rows of the table. Although the demands are larger for the 48 inch bent caps, the normalized values are actually lower for these larger bents, indicating the potential for a more favorable design and performance.

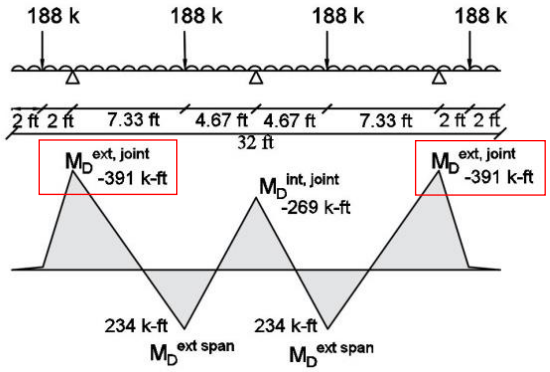

(a) 32 ft bent cap

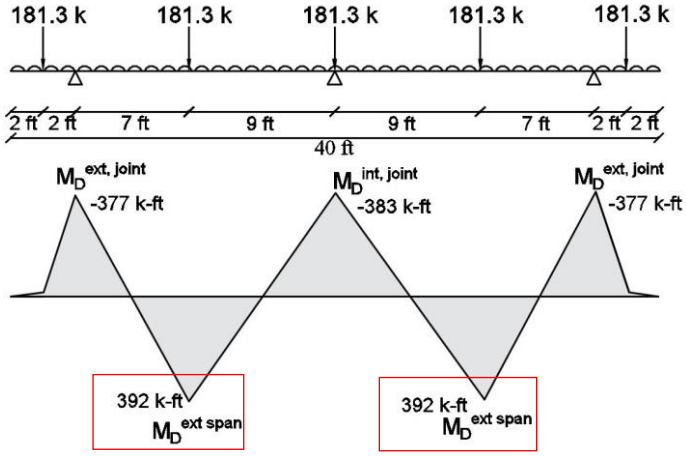

(b) 40 ft bent cap

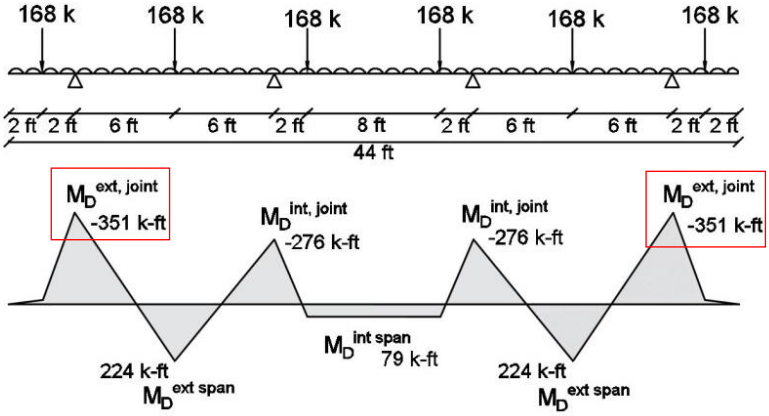

(c) 44 ft bent cap

Note: Moments are drawn on tension side. Values in the red boxes indicate maximum moments.

Figure 4.6. Bending moment diagram under dead load for 80 ft span length (non-skewed I-girder bridges).

Table 4.2. Scenarios at which span moment controls design or evaluation of the bent cap (non-skewed I-girder bridges).

Width (ft)	DL	DL + L	1.25 DL + 1.75 LL
38		✓	✓
40	✓ *	✓	✓

*Intermediate to maximum spans

For the bents evaluated, two scenarios were observed for the location of maximum shear demands: (a) maximum shear in the joint for exterior columns, and (b) maximum shear in the joint for interior column. For most bridges, the maximum shear occurs in the joint for exterior columns. Maximum shear occurs in the joint for interior columns for bridges of 44 ft roadway width.

Table 4.4 provides a summary of maximum shear demands in the 42 inch and 48 inch bent caps. The first three rows provide the largest values for dead, service, and ultimate loads. To facilitate a generalized evaluation of the demands between different size caps, the fourth row presents the dead load shear forces normalized by the area of cross section of the bent cap. The shear at service and ultimate are expressed as ratios to the dead load shear in the fifth and sixth rows respectively.

Table 4.3. Summary of maximum moment demands in 42 inch and 48 inch bent cap (non-skewed I-girder bridges).

	42 inch bent cap			48 inch bent cap		
Span Length	Minimum	Intermediate	Maximum	Minimum	Intermediate	Maximum
Configuration 1						
M_{DL} *(k-ft)*	173-203	331-391	489-579	268-313	413-484	559-656
$M_{DL+LL+IM}$ *(k-ft)*	310-370	516-615	713-850	431-511	613-727	791-938
M_U *(k-ft)*	457-547	737-881	1003-1198	621-739	866-1030	1105-1313
M_{DL}/AD *(k/in^2)*	0.028-0.033	0.054-0.063	0.079-0.094	0.029-0.034	0.045-0.053	0.061-0.071
$M_{DL+LL+IM}/M_{DL}$	1.80-1.83	1.56-1.57	1.46-1.47	1.61-1.63	1.48-1.50	1.42-1.43
M_U/M_D	2.64-2.70	2.22-2.25	2.05-2.07	2.31-2.36	2.10-2.13	1.98-2.00
Configuration 2						
M_{DL} *(k-ft)*	190-217	366-392	542-574	294-327	455-487	615-653
$M_{DL+LL+IM}$ *(k-ft)*	432-486	680-760	913-1021	578-647	793-885	1001-1118
M_U *(k-ft)*	664-746	1017-1133	1344-1499	869-972	1172-1306	1462-1631
M_{DL}/AD *(k/in^2)*	0.031-0.035	0.059-0.063	0.088-0.093	0.032-0.035	0.049-0.053	0.067-0.071
$M_{DL+LL+IM}/M_{DL}$	2.24-2.27	1.86-1.94	1.69-1.78	1.96-1.98	1.74-1.82	1.63-1.71
M_U/M_D	3.43-3.49	2.78-2.89	2.48-2.61	2.95-2.98	2.58-2.68	2.38-2.50
Configuration 3						
M_{DL} *(k-ft)*	183	351	519	283	437	590
$M_{DL+LL+IM}$ *(k-ft)*	334	557	768	466	660	850
M_U *(k-ft)*	498	800	1085	673	936	1193
M_{DL}/AD *(k/in^2)*	0.030	0.057	0.084	0.031	0.047	0.064
$M_{DL+LL+IM}/M_{DL}$	1.84	1.59	1.48	1.65	1.51	1.44
M_U/M_D	2.73	2.28	2.09	2.38	2.15	2.02

Table 4.4. Summary of maximum shear demands in 42 inch and 48 inch bent cap (non-skewed I-girder bridges).

	42 inch bent cap			48 inch bent cap		
Span Length	Minimum	Intermediate	Maximum	Minimum	Intermediate	Maximum
Configuration 1						
V_{DL} (k)	86-101	165-195	244-289	133-155	205-241	278-327
$V_{DL+LL+IM}$ (k)	154-184	257-307	355-424	214-255	305-362	394-468
V_U (k)	227-272	367-439	500-598	309-368	431-513	551-655
V_{DL}/A (k/in^2)	0.048-0.057	0.093-0.110	0.138-0.164	0.075-0.088	0.116-0.137	0.158-0.185
$V_{DL+LL+IM} / V_{DL}$	1.80-1.83	1.56-1.58	1.46-1.47	1.61-1.64	1.49-1.50	1.42-1.43
V_U / V_{DL}	2.66-2.71	2.23- 2.26	2.05- 2.07	2.33-2.37	2.10-2.13	1.98-2.01
Configuration 2						
V_{DL} (k)	94-97	182-188	270-278	146-150	226-233	306-316
$V_{DL+LL+IM}$ (k)	174-179	289-298	399-411	241-248	342-352	441-454
V_U (k)	258-265	415-427	563-581	348-358	485-499	618-637
V_{DL}/A (k/in^2)	0.053-0.055	0.103-0.106	0.153-0.158	0.083-0.085	0.128-0.132	0.174-0.179
$V_{DL+LL+IM} / V_{DL}$	1.85-1.85	1.59-1.59	1.48-1.48	1.65-1.65	1.51-1.51	1.44-1.44
V_U / V_{DL}	2.73-2.73	2.28-2.28	2.09-2.09	2.39-2.39	2.14-2.14	2.02-2.02
Configuration 3						
V_{DL} (k)	94	178	262	145	222	299
$V_{DL+LL+IM}$ (k)	174	285	392	240	238	434
V_U (k)	257	410	554	347	480	610
V_{DL}/A (k/in^2)	0.053	0.101	0.149	0.082	0.126	0.169
$V_{DL+LL+IM} / V_{DL}$	1.85	1.60	1.49	1.65	1.52	1.45
V_U / V_{DL}	2.73	2.30	2.12	2.39	2.16	2.04

4.3.2. *Skewed I-girder bridges*

For most I-girder bridges with a 45 degree skew, the maximum moment occurs at the exterior columns; however, it occurs in the span for bridges with larger column spacing, although not always for all load combinations. Table 4.5 summarizes the bridges and load combinations for which the maximum demand occurs in the span.

Table 4.6 provides a summary of the maximum moment demands in the 42 inch and 48 inch bent caps for a 45 degree skew I-girder bridges. The first three rows provide the largest values for dead, service and ultimate loads. The fourth, fifth and sixth rows provide the normalized dead load moment, ratios of moments at service and ultimate states to the dead load moments respectively.

For most bridges, the maximum shear occurs in the joint for exterior columns. Maximum shear occurs in the joint for interior columns for bridges of 44 ft roadway width.

Table 4.7 provides a summary of maximum shear demands in the 42 inch and 48 inch bent caps. The first three rows provide the largest values for dead, service, and ultimate loads. The fourth, fifth and sixth rows provide the normalized dead load shear, ratios of shear at service and ultimate states to the dead load shear respectively.

Table 4.5. Scenarios at which span moment controls design or evaluation of the bent cap (45 degree skewed I-girder bridges).

Width (ft)	DL	DL + LL	1.25 DL + 1.75 LL
40		✓	✓

Table 4.6. Summary of maximum moment demands in 42 inch and 48 inch bent cap (45 degree skewed I-girder bridges).

	42 inch bent cap			48 inch bent cap		
Span Length	Minimum	Intermediate	Maximum	Minimum	Intermediate	Maximum
Configuration 1						
M_{DL} *(k-ft)*	253-296	477-561	701-827	391-454	596-696	801-938
$M_{DL+LL+IM}$ *(k-ft)*	448-532	738-878	1017-1211	621-735	878-1039	1130-1338
M_U *(k-ft)*	657-784	1053-1257	1429-1705	892-1058	1239-1470	1577-1871
M_{DL}/AD *(k/in^2)*	0.041-0.048	0.077-0.091	0.113-0.134	0.042-0.049	0.065-0.076	0.087-0.102
$M_{DL+LL+IM}/M_{DL}$	1.77-1.80	1.55-1.57	1.45-1.46	1.59-1.62	1.47-1.49	1.41-1.43
M_U/M_D	2.59-2.65	2.21-2.24	2.04-2.06	2.28-2.33	2.08-2.11	1.97-1.99
Configuration 2						
M_{DL} *(k-ft)*	209-215	395-407	581-599	321-330	491-506	662-681
$M_{DL+LL+IM}$ *(k-ft)*	378-417	622-670	856-914	522-563	736-786	947-1005
M_U *(k-ft)*	560-624	891-982	1206-1319	753-828	1043-1139	1326-1439
M_{DL}/AD *(k/in^2)*	0.034-0.035	0.064-0.066	0.094-0.097	0.035-0.036	0.053-0.055	0.072-0.074
$M_{DL+LL+IM}/M_{DL}$	1.81-1.94	1.51-1.65	1.47-1.53	1.63-1.71	1.50-1.55	1.43-1.48
M_U/M_D	2.68-2.91	2.25-2.41	2.08-2.20	2.34-2.51	2.12-2.25	2.00-2.11
Configuration 3						
M_{DL} *(k-ft)*	267	505	742	411.2	628.7	846.2
$M_{DL+LL+IM}$ *(k-ft)*	485	796	1095	669.5	944.3	1210
M_U *(k-ft)*	715	1141	1545	966.1	1340	1700
M_{DL}/AD *(k/in^2)*	0.043	0.082	0.120	0.045	0.068	0.092
$M_{DL+LL+IM}/M_{DL}$	1.82	1.58	1.48	1.63	1.50	1.43
M_U/M_D	2.68	2.26	2.08	2.35	2.13	2.01

Table 4.7. Summary of maximum shear demands in 42 inch and 48 inch bent cap (45 degree skewed I-girder bridges).

	42 inch bent cap			48 inch bent cap		
Span Length	Minimum	Intermediate	Maximum	Minimum	Intermediate	Maximum
Configuration 1						
V_{DL} (k)	88-103	167-197	246-291	136-159	209-244	282-330
$V_{DL+LL+IM}$ (k)	157-187	260-309	358-427	218-258	309-366	398-471
V_U (k)	230-276	370-443	503-601	313-372	436-518	555-660
V_{DL}/A (k/in^2)	0.050-0.058	0.095-0.112	0.140-0.165	0.077-0.09	0.118-0.139	0.160-0.187
$V_{DL+LL+IM}/V_{DL}$	1.71-1.81	1.51-1.57	1.45-1.47	1.60-1.63	1.48-1.50	1.41-1.43
V_U / V_{DL}	2.61-2.67	2.22-2.25	2.04-2.07	2.30-2.35	2.09-2.12	1.97-2.00
Configuration 2						
V_{DL} (k)	96-98	184-189	271-280	148-152	228-235	308-317
$V_{DL+LL+IM}$ (k)	175-181	290-299	401-413	242-249	344-354	443-456
V_U (k)	259-267	416-429	565-583	350-360	487-502	621-639
V_{DL}/A (k/in^2)	0.054-0.056	0.104-0.107	0.154-0.159	0.084-0.086	0.129-0.133	0.175-0.180
$V_{DL+LL+IM}/V_{DL}$	1.84-1.84	1.58-1.58	1.48-1.48	1.64-1.64	1.51-1.51	1.44-1.44
V_U / V_{DL}	2.71-2.71	2.27-2.27	2.08-2.08	2.37-2.37	2.14-2.14	2.01-2.01
Configuration 3						
V_{DL} (k)	98	182	266	151	227	304
$V_{DL+LL+IM}$ (k)	178	289	396	245	343	439
V_U (k)	262	415	560	354	487	616
V_{DL}/A(k/in^2)	0.056	0.103	0.151	0.085	0.129	0.173
$V_{DL+LL+IM}/V_{DL}$	1.81	1.59	1.49	1.63	1.51	1.44
V_U / V_{DL}	2.67	2.28	2.10	2.35	2.14	2.03

4.3.3. *Box beam bridges*

Figure 4.7(a) and (b) shows the bending moment diagrams under dead load for the bent caps of 28 ft and 30 ft respectively in bridges with the B40 box beams. For the bents evaluated, the maximum moment occurs at the interior columns.

Table 4.8 provides a summary of the maximum moment demands in the bent caps for bridges with the B40 box beams. The three rows provide the largest values for dead, service and ultimate loads. The fourth, fifth and sixth rows provide the normalized dead load moment, ratios of moments at service and ultimate states to the dead load moments respectively.

For the bents evaluated, the maximum shear occurs at the interior columns. Table 4.9 provides a summary of the maximum shear demands in the bent caps for bridges with the B40 box beams. The three rows provide the largest values for dead, service and ultimate loads. The fourth, fifth and sixth rows provide the normalized dead load shear, ratios of shear at service and ultimate states to the dead load shear respectively.

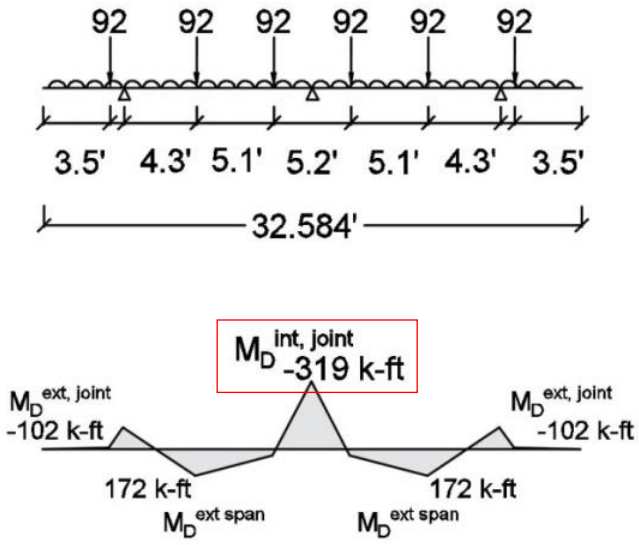

(a)28 ft bent cap

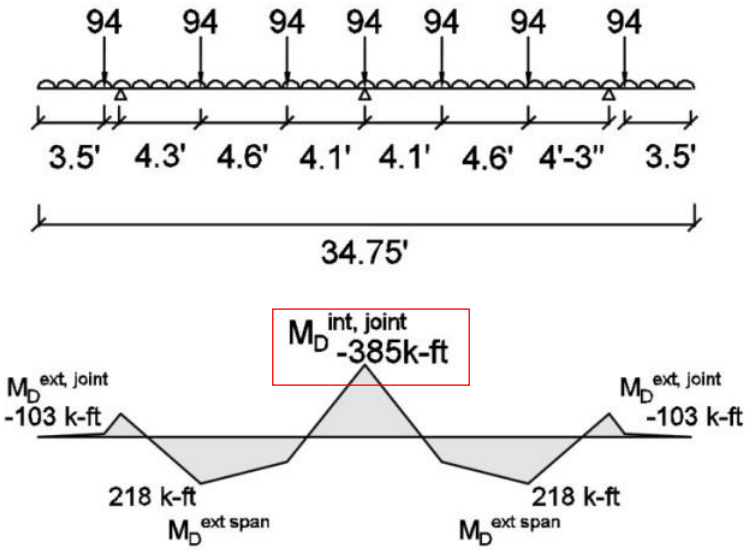

(b) 30 ft bent cap

Note: Moments are drawn on tension side. Values in the red boxes indicate maximum moments.

Figure 4.7. Bending moment diagram under dead load for 60 ft span length (box beams B40).

Table 4.8. Summary of maximum moment demands in bent cap (box beams B40).

Span Length	Minimum	Intermediate	Maximum
Configuration 1			
M_{DL} *(k-ft)*	130-168	251-319	392-496
$M_{DL+LL+IM}$ *(k-ft)*	238-324	397-529	571-752
M_U *(k-ft)*	350-483	569-766	803-1068
M_{DL}/AD *(k/in^2)*	0.037-0.047	0.070-0.090	0.110-0.139
$M_{DL+LL+IM}/M_{DL}$	1.82-1.93	1.58-1.66	1.46-1.52
M_U/M_D	2.69-2.88	2.27-2.40	2.05-2.15
Configuration 2			
M_{DL} *(k-ft)*	203	385	598
$M_{DL+LL+IM}$ *(k-ft)*	363	601	861
M_U *(k-ft)*	534	859	1208
M_{DL}/A *(k/in^2)*	0.057	0.108	0.168
$M_{DL+LL+IM}/M_{DL}$	1.79	1.56	1.44
M_U/M_D	2.63	2.23	2.02

Table 4.9. Summary of maximum shear demands in bent cap (box beams B40).

Span Length	Minimum	Intermediate	Maximum
Configuration 1			
V_{DL} (k)	70-72	134-137	209-213
$V_{DL+LL+IM}$ (k)	129-137	213-225	306-320
V_U (k)	190-204	306-325	430-453
V_{DL}/A (k/in^2)	0.059-0.061	0.113-0.116	0.176-0.179
$V_{DL+LL+IM}/V_{DL}$	1.84-1.89	1.59-1.64	1.47-1.50
V_U/V_{DL}	2.73-2.82	2.29-2.37	2.06-2.13
Configuration 2			
V_{DL} (k)	70	133	206
$V_{DL+LL+IM}$ (k)	123	204	292
V_U (k)	180	290	409
V_{DL}/A (k/in^2)	0.059	0.112	0.173
$V_{DL+LL+IM}/V_{DL}$	1.75	1.53	1.42
V_U/V_{DL}	1.46	1.42	1.40

4.3.4. *X-beam bridges*

Figure 4.8(a), (b) and (c) shows the bending moment diagrams under dead load for the 42 inch bent caps of 32 ft, 40 ft and 44 ft respectively. For most X-beam bridges, the maximum moment occurs at the interior columns. The maximum moment occurs in the span for bridges with larger column spacing. Table 4.10 summarizes the bridges and load combinations for which the maximum demand occurs in the span.

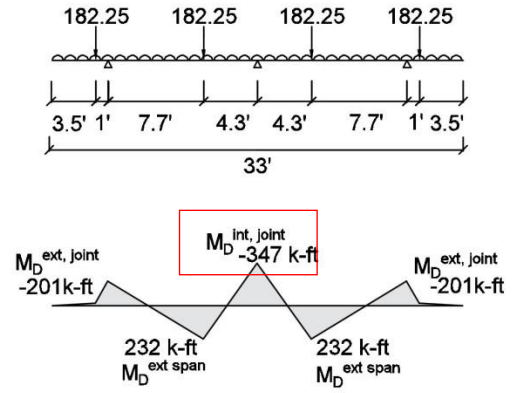

(a) 32 ft bent cap

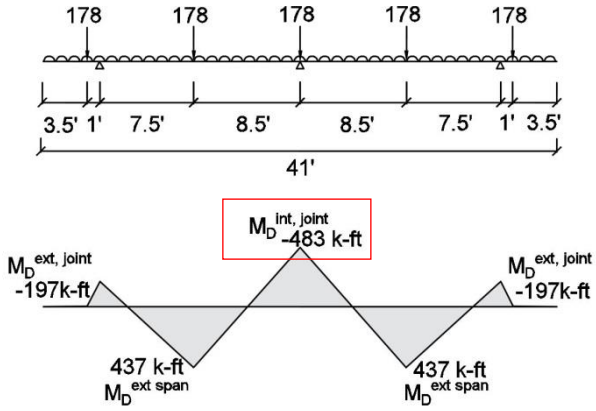

(b) 40 ft bent cap

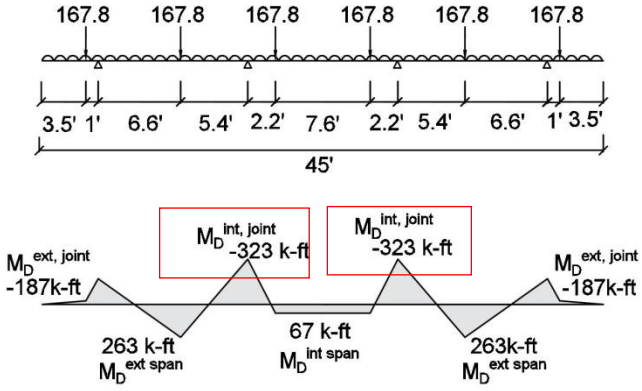

(c) 44 ft bent cap

Note: Moments are drawn on tension side. Values in the red boxes indicate maximum moments.

Figure 4.8. Bending moment diagram under dead load for 70 ft span length (X-beams XB40).

Table 4.10. Scenarios at which span moment controls design or evaluation of the bent cap (X-beams XB40).

Width (ft)	DL	DL + LL	1.25 DL + 1.75 LL
38		✓	✓
40		✓	✓

Table 4.11 provides a summary of the maximum moment demands in the bent caps for bridges with the XB40 X-beams. The three rows provide the largest values for dead, service and ultimate loads. The fourth, fifth and sixth rows provide the normalized dead load moment, ratios of moments at service and ultimate states to the dead load moments respectively.

For the bents evaluated, the maximum shear occurs in the joint for exterior columns.

Table 4.12 provides a summary of maximum shear demands in the bent caps. The three rows provide the largest values for dead, service, and ultimate loads. The fourth, fifth and sixth rows provide the normalized dead load shear, ratios of shear at service and ultimate states to the dead load shear respectively.

Table 4.11. Summary of maximum moment demands in bent cap (X-beams XB40).

Span Length	Minimum	Intermediate	Maximum
Configuration 1			
M_{DL} *(k-ft)*	209	347	508
$M_{DL+LL+IM}$ *(k-ft)*	386	571	778
M_U *(k-ft)*	571	827	1107
M_{DL}/AD *(k/in^2)*	0.034	0.056	0.082
$M_{DL+LL+IM}/M_{DL}$	1.85	1.65	1.53
M_U/M_D	2.73	2.38	2.18
Configuration 2			
M_{DL} *(k-ft)*	266-298	432-483	626-699
$M_{DL+LL+IM}$ *(k-ft)*	483-534	711-785	962-1062
M_U *(k-ft)*	726-803	1044-1153	1391-1535
M_{DL}/AD *(k/in^2)*	0.043-0.048	0.070-0.078	0.101-0.113
$M_{DL+LL+IM}/M_{DL}$	1.79-1.82	1.63-1.65	1.52-1.54
M_U/M_D	2.69-2.73	2.39-2.42	2.20-2.22
Configuration 3			
M_{DL} *(k-ft)*	197	326	476
$M_{DL+LL+IM}$ *(k-ft)*	349	520	709
M_U *(k-ft)*	513	746	1003
M_{DL}/AD *(k/in^2)*	0.032	0.053	0.077
$M_{DL+LL+IM}/M_{DL}$	1.78	1.60	1.49
M_U/M_D	2.61	2.29	2.11

Table 4.12. Summary of maximum shear demands in bent cap (X-beams XB40).

Span Length	Minimum	Intermediate	Maximum
Configuration 1			
V_{DL} (k)	112	190	281
$V_{DL+LL+IM}$ (k)	213	319	435
V_U (k)	318	463	622
V_{DL}/A (k/in^2)	0.063	0.107	0.159
$V_{DL+LL+IM}$ /V_{DL}	1.91	1.68	1.55
V_U / V_{DL}	2.85	2.44	2.21
Configuration 2			
V_{DL} (k)	106-109	181-185	267-274
$V_{DL+LL+IM}$ (k)	207-211	307-314	420-429
V_U (k)	308-314	448-457	600-613
V_{DL}/A (k/in^2)	0.060-0.062	0.102-0.105	0.152-0.156
$V_{DL+LL+IM}$ /V_{DL}	1.93-1.94	1.69-1.70	1.56-1.57
V_U / V_{DL}	2.88-2.90	2.46-2.48	2.23-2.25
Configuration 3			
V_{DL} (k)	106	178	262
$V_{DL+LL+IM}$ (k)	202	300	409
V_U (k)	302	438	587
V_{DL}/A (k/in^2)	0.060	0.101	0.149
$V_{DL+LL+IM}$ /V_{DL}	1.90	1.69	1.56
V_U /V_{DL}	2.85	2.46	2.24

4.3.5. *Nonstandard bridges*

Figure 4.9(a) and (b) shows the bending moment diagrams under dead load for the 42 inch bent caps of 68 ft and 85 ft respectively. For the bents evaluated, two scenarios were observed for the location of maximum moment demands: (a) maximum moment at the interior column or first interior column for bridges with multiple interior columns and (b) maximum moment in the span. Table 4.13 summarizes the bridge and load combinations for which the maximum demand occurs in the span.

Table 4.14 provides a summary of the maximum moment demands in the bent caps. The three rows provide the largest values for dead, service and ultimate loads. The fourth, fifth and sixth rows provide the normalized dead load moment, ratios of moments at service and ultimate states to the dead load moments respectively.

For the bents evaluated, the maximum shear occurs in the interior columns. Table 4.15 provides a summary of maximum shear demands in the bent caps. The three rows provide the largest values for dead, service, and ultimate loads. The fourth, fifth and sixth rows provide the normalized dead load shear, ratios of shear at service and ultimate states to the dead load shear respectively.

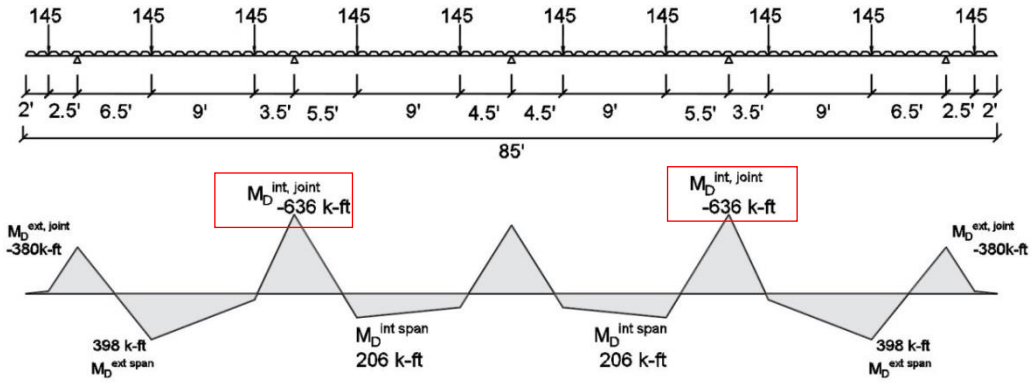

(a) 68 ft bent cap

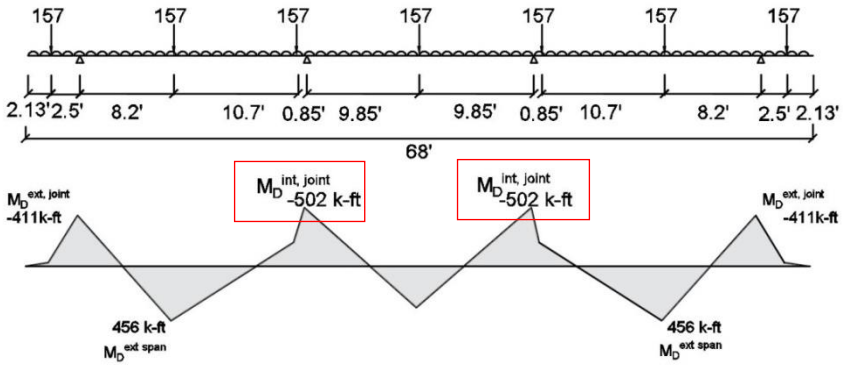

(b) 85 ft bent cap

Note: Moments are drawn on tension side. Values in the red boxes indicate maximum moments.

Figure 4.9. Bending moment diagram under dead load for 80 ft span length (nonstandard bridges).

Table 4.13. Scenarios at which span moment controls design or evaluation of the bent cap (nonstandard bridges).

Width (ft)	DL	DL + LL	1.25 DL + 1.75 LL
68		✓	✓

Table 4.14. Summary of maximum moment demands in bent cap (nonstandard bridges).

Span Length	Minimum	Intermediate	Maximum
Configuration 1			
M_{DL} *(k-ft)*	275	483	690
$M_{DL+LL+IM}$ *(k-ft)*	634	966	1274
M_U *(k-ft)*	988	1468	1909
M_{DL}/AD *(k/in^2)*	0.045	0.078	0.112
$M_{DL+LL+IM}/M_{DL}$	2.30	2.0	1.85
M_U/M_D	3.59	3.04	2.77
Configuration 2			
M_{DL} *(k-ft)*	351	636	921
$M_{DL+LL+IM}$ *(k-ft)*	635	1017	1383
M_U *(k-ft)*	936	1462	1959
M_{DL}/AD *(k/in^2)*	0.057	0.103	0.149
$M_{DL+LL+IM}/M_{DL}$	1.81	1.60	1.50
M_U/M_D	2.67	2.30	2.13

Table 4.15. Summary of maximum shear demands in bent cap (nonstandard bridges).

Span Length	Minimum	Intermediate	Maximum
Configuration 1			
V_{DL} *(k)*	105	190	276
$V_{DL+LL+IM}$ *(k)*	208	328	443
V_U *(k)*	312	479	637
V_{DL}/A *(k/in^2)*	0.088	0.160	0.232
$V_{DL+LL+IM}/V_{DL}$	1.98	1.73	1.61
V_U/V_{DL}	2.97	2.52	2.31
Configuration 2			
V_{DL} *(k)*	108	197	287
$V_{DL+LL+IM}$ *(k)*	222	349	471
V_U *(k)*	334	513	680
V_{DL}/A *(k/in^2)*	0.091	0.166	0.241
$V_{DL+LL+IM}/V_{DL}$	2.05	1.77	1.64
V_U/V_{DL}	3.09	2.60	2.37

4.3.6. *Summary*

Section 4.3 provides an overview of the flexural and shear demands in the bridges with I-girders, box beams and X-beams. For non-skewed I-girder bridges, maximum service and ultimate demands occurs in Configuration 2, as can be expected due to the large column spacing. The increase in bent cap length in the skewed I-girder bridges increases the dead load demands in these bridges. The addition of a bent in Configuration 2 reduces the service and ultimate demands, in comparison to the non-skewed bridges. The

bent caps in box beam bridges have a smaller cross-section than that in an equivalent bridge width (24 ft to 30 ft) with I-girders; consequently high normalized dead load demands are observed. For the same bridge widths (32 ft to 44ft), X-beams have the same configuration as the I-girder bridges except for larger exterior column/ girder edge distance and lower intermediate and maximum spans that results in lower dead load shear demands for these span lengths. The nonstandard bridges are an exceptional case of bridge configuration; the large column spacing generates high demands under service and ultimate loads.

5. FLEXURAL DESIGN FOR STANDARD BRIDGE INVENTORY

The recommended design procedure in Chapter 3 is based on the philosophy of zero tensile stresses under dead load to allow closure of cracks following removal of live load. In this chapter, the design procedure is evaluated for the bridge inventory summarized in Chapter 4. Section 5.1 discusses the selection of strands for the bridge inventory. Section 5.2 discusses the minimum concrete design strength for these designs. In Section 5.3, the stresses at service and ultimate loads are evaluated. In Section 5.4, the strength of the sections is assessed. Section 5.5 presents a comparison between performance of the reinforced concrete and prestressed concrete bent caps. Section 5.6 presents evaluation of a bent cap section with permanent void using the proposed design procedure.

5.1. Number of strands

This section discusses the minimum number of strands calculated by Step 0 of the proposed design procedure and the number of strands required to achieve the design objective of zero tensile stresses under dead load using the method established in Step 1.

5.1.1. *Bridges with non-skewed I-girders*

The minimum number of strands is sensitive to the design strength of the concrete. For a design strength of 6 ksi, the minimum number of strands is 14 for a 42 inch bent cap and 18 for a 48 inch bent cap. Naturally, if a higher strength were actually used, the minimum number of strands would also increase. Thus, for concrete with a compressive strength of 8.5 ksi, the minimum number of strands increases to 16 and 20 for 42 inch and 48 inch square bent cap sections, respectively. In evaluating the designs for the

standard bridge inventory in this study, the minimum strands associated with 6 ksi concrete strength are used. The configuration of the minimum strands for the two bent cap sizes is shown in Figure 5.1(a) and (b) respectively.

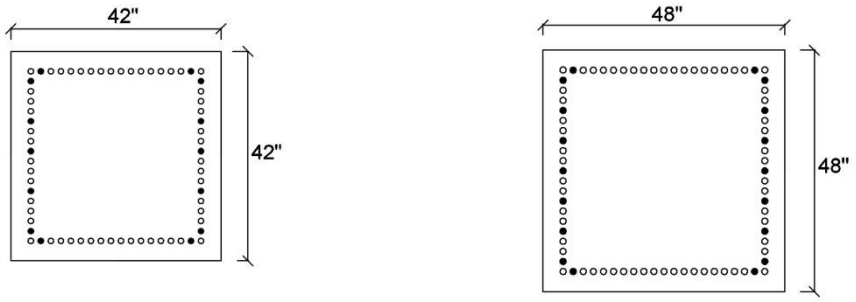

(a) 14 strands in 42 inch bent cap

(b) 18 strands in 48 inch bent cap

Figure 5.1. Minimum strands configuration for bent caps with I-girders.

After establishing the minimum number of strands in Step 0, the number of strands from Step 1 is calculated to range from 10 to 30 (see Figure 5.2(a)) for 42 inch sections and from 12 to 28 (see Figure 5.2(b)) for 48 inch sections. Bridges with the short span lengths are governed by the minimum strands.

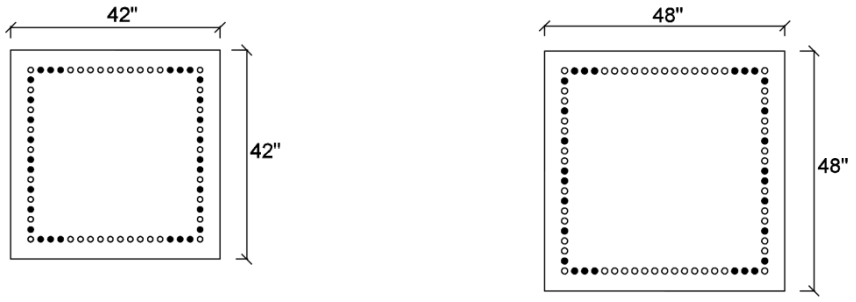

(a) 30 strands in 42 inch bent cap

(b) 28 strands in 48 inch bent cap

Figure 5.2. Configuration for highest strands in bent caps with non skewed I-girder bridges.

5.1.2. *Bridges with skewed I-girders*

The minimum number of strands for the skewed I-girder bridges is the same as that for the non-skewed bridges discussed in Section 5.1.1. For concrete design strength of 6 ksi and 8.5 ksi, the minimum number of strands is 14 and 16 for a 42 inch square respectively, and 18 and 20 for a 48 inch square respectively.

The number of strands from Step 1 is calculated to range from 12 to 42 (see Figure 5.3(a)) for 42 inch sections and from 14 to 42 (see Figure 5.3(b)) for 48 inch sections. In comparison to the non-skewed bridges, the increase in strands for a 42 inch bent cap in the 45 degree skewed 32 ft width bridge are 14 percent, 29 percent and 40 percent for the minimum, intermediate and maximum spans respectively. Bridges with the short span lengths are governed by the minimum strands.

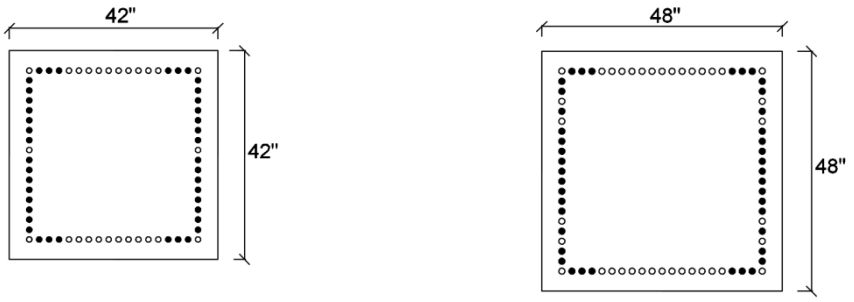

(a) 42 strands in 42 inch bent cap *(b) 42 strands in 48 inch bent cap*

Figure 5.3. Configuration for highest strands in bent caps with skewed I-girder bridges.

5.1.3. *Bridges with box beams*

For a concrete design strength of 6 ksi used in evaluating the designs of these bridges, the minimum number of strands is 10 for a bent cap of 33 inch width and 36 inch depth. For concrete with a compressive strength of 8.5 ksi which is more prudent in practice,

the minimum number of strands increases to 12. The configuration of the minimum strands is shown in Figure 5.4(a).

The number of strands from Step 1 is calculated to range from 10 to 36 (see Figure 5.4(b)). Bridges with the short span lengths are governed by the minimum strands.

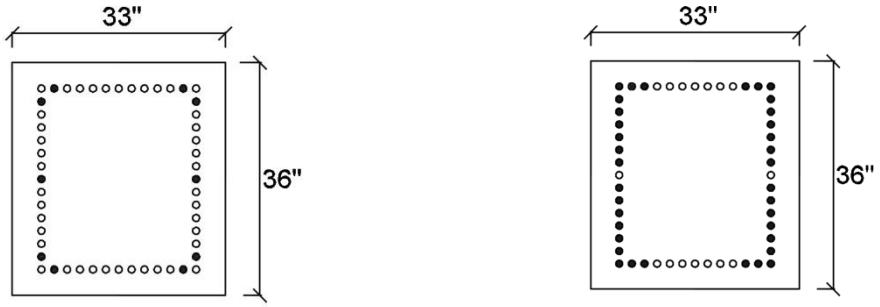

(a) 10 strands in 33" x 36" bent cap *(b) 36 strands in 33" x 36" bent cap*

Figure 5.4. Minimum and highest strands configuration for bent caps with box beams.

5.1.4. *Bridges with X-beams*

The minimum number of strands for the X-beam bridges is the same as the 42 inch bent cap for the non-skewed bridges discussed in Section 5.1.1. For concrete design strength of 6 ksi and 8.5 ksi, the minimum number of strands is 14 and 16 respectively.

The number of strands from Step 1 is calculated to range from 14 to 36. Bridges with the short span lengths are governed by the minimum strands.

5.1.5. *Nonstandard bridges with I-girders*

The minimum number of strands for the nonstandard bridges is the same as the 42 inch bent cap for the non-skewed bridges discussed in Section 5.1.1. For concrete design

strength of 6 ksi and 8.5 ksi, the minimum number of strands is 14 and 16 respectively. The number of strands from Step 1 is calculated to range from 18 to 56.

5.2. Minimum concrete strength

This section summarizes the minimum design concrete strength determined from Step 2 of the design procedure.

5.2.1. *Bridges with non-skewed I-girders*

For the non-skewed I-girder bridges, the highest minimum concrete strength calculated was 5.2 ksi, which occurred for the 42 inch square 40 ft bent cap with maximum span length. However, a concrete strength of 6 ksi is used as the design strength in evaluating the designs. For most bridge widths and span lengths, the minimum design concrete strength is governed by the compression limit. Minimum design concrete strength is governed by the tension limit for bridges with longer spans and larger column spacings such as the 38 ft and 40 ft roadway widths.

5.2.2. *Bridges with skewed I-girders*

For the 45 degree skewed I-girder bridges, the highest minimum concrete strength calculated was 4.5 ksi, which occurred for the 42 inch square bent cap for 32 ft width bridge and maximum span length. The variation from the non-skewed I-girder bridges is justified by the additional bent in the 40 ft width skewed bridge, resulting in the reduction of the service stress. A concrete strength of 6 ksi is used as the design strength in evaluating the designs. For all the 45 degree skewed I-girder bridges, the minimum design concrete strength is governed by the compression limit.

5.2.3. *Bridges with box beams*

For the B40 box beam bridges evaluated in this research, the highest minimum concrete strength calculated was 5.6 ksi, which occurred for the 30 ft bent cap with maximum span length. However, a concrete strength of 6 ksi is used as the design strength in evaluating the designs. For all the B40 box beam bridges, the minimum design concrete strength is governed by the compression limit.

5.2.4. *Bridges with X-beams*

For the XB40 beam bridges evaluated in this research, the highest minimum concrete strength calculated was 3.9 ksi, which occurred for the 40 ft bent cap with maximum span length. However, a concrete strength of 6 ksi is used as the design strength in evaluating the designs. For all the XB40 beam bridges, the minimum design concrete strength is governed by the compression limit.

5.2.5. *Nonstandard bridges with I-girders*

For the nonstandard bridges with I-girders, the highest minimum concrete strength for the number of strands computed from the proposed design procedure was 10.5 ksi, which occurred for the 68 ft bent cap with maximum span length. However, the number of strands was increased to maintain a minimum design concrete strength within 8.5 ksi. A concrete strength of 8 ksi is used as the design strength in evaluating the designs. For most span lengths of the nonstandard bridges, the minimum design concrete strength is governed by the tension limit. Minimum design concrete strength is governed by the compression limit for bridges with shorter spans of the 85 ft roadway width.

5.3. Service and ultimate stresses

This section presents the performance of pretensioned bent cap design for the bridge inventory, evaluated by assessing the stresses at service and ultimate loads. Figure 5.5 to Figure 5.11 show the tension stresses at service and ultimate versus the number of strands for the non-skewed I-girder bridges, skewed I-girder bridges, box beams, X-beams and nonstandard bridges with I-girders. For clarity, each bent configuration of the bridges is shown on a different subfigure. The tension stresses are calculated at the location of the maximum moments at service and ultimate; this may be a different location than the dead load moment used to select the number of strands. The solid markers indicate designs for which the minimum number of strands governs. The solid lines represent the service stresses and the dashed lines represent the ultimate stresses. The horizontal limits of $0.19\sqrt{f'_c\,(\text{ksi})}$ and $0.24\sqrt{f'_c\,(\text{ksi})}$ are the AASHTO service stress limit for tension and the cracking stress respectively. The horizontal limit of $0.38\sqrt{f'_c\,(\text{ksi})}$ is the stress limit beyond which the bent cap is assumed to behave as a cracked member (ACI 318-14 Section 24.5.2). If the stresses are between $0.24\sqrt{f'_c\,(\text{ksi})}$ to $0.38\sqrt{f'_c\,(\text{ksi})}$, the bent cap is assumed to be in transition between a cracked and uncracked member.

5.3.1. *Bridges with non-skewed I-girders*

Figure 5.5 and Figure 5.6 show the tension stresses at service and ultimate versus the number of strands for the 42 inch and 48 inch bent caps of non-skewed I-girder bridges. At service loads, the AASHTO stress limits enforce the expectation that stresses will be

less than the cracking stress of $0.24\sqrt{f'_c\,(\text{ksi})}$. The tensile service stress at the location of maximum service moment (exterior joint or span) for each of the designs of the non-skewed I-girder bridges are shown by solid lines. For bridges with the minimum span lengths, the design is controlled by the minimum number of strands (indicated by solid markers in the figures). In these bent caps, the service stresses are 67 percent below the expected cracking stress. As the span length increases, the number of strands in the design increases. The increase in strands is accompanied by a minor increase in the service stresses, but these stresses still remain well below the expected cracking stress. The highest service stress is 0.43 ksi in the 42 inch, 40 ft bent cap. This stress is 26 percent lower than the expected cracking stress.

At service loads, the tensile stresses are well below the cracking stress, thus providing a margin of over strength to prevent cracking under demands exceeding the expected service loads. For most of the bridges considered in this study, the over strength is sufficiently large to prevent cracking even under ultimate loads. The tensile ultimate stresses at the location of the maximum ultimate moment for each of the designs are shown by dashed lines in Figure 5.5 and Figure 5.6. For bridges with the

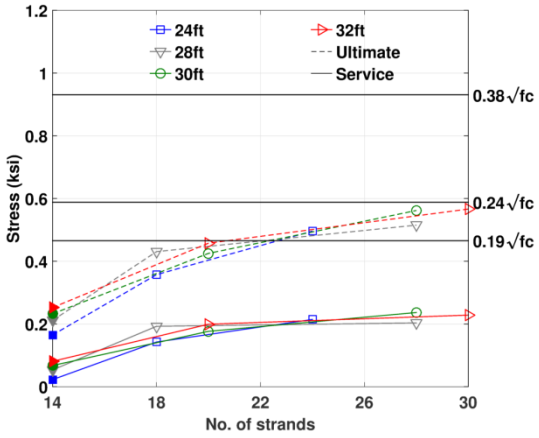

(a) Configuration 1: 3 column, 4 girder

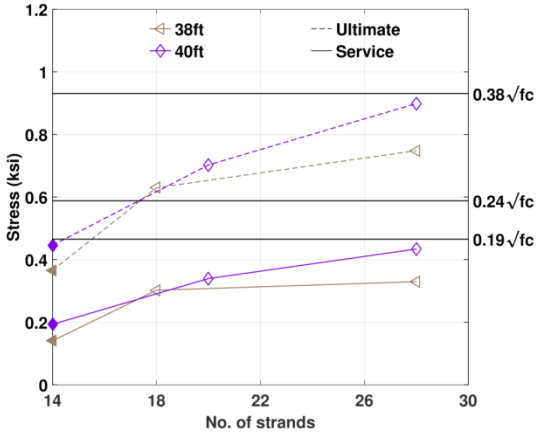

(b) Configuration 2: 3 column, 5 girder

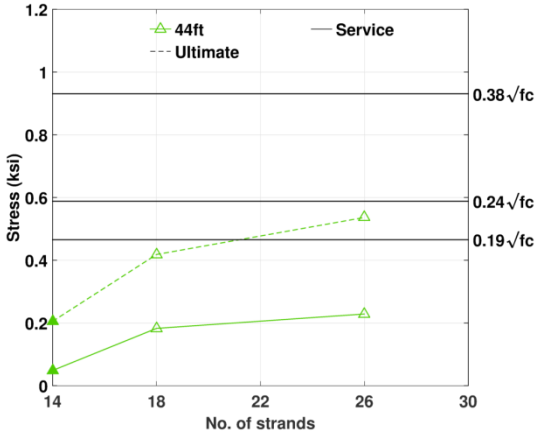

(c) Configuration 3: 4 column, 6 girder

Note: Solid markers indicate minimum strands control design.

Figure 5.5. Maximum tensile stress vs. number of strands for 42 inch bent cap (non-skewed I-girder bridges).

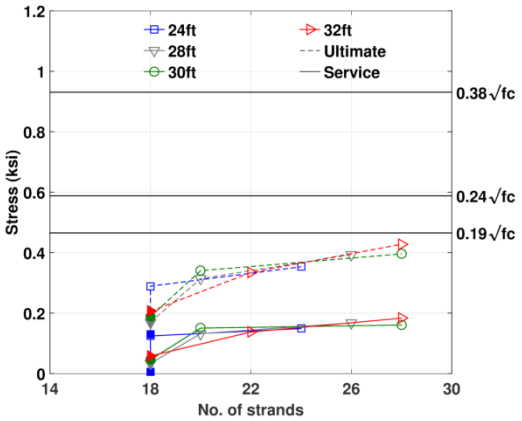

(a) Configuration 1: 3 column, 4 girder

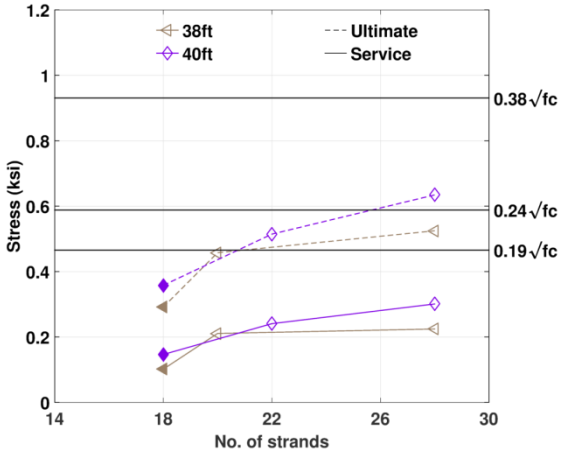

(b) Configuration 2: 3 column, 5 girder

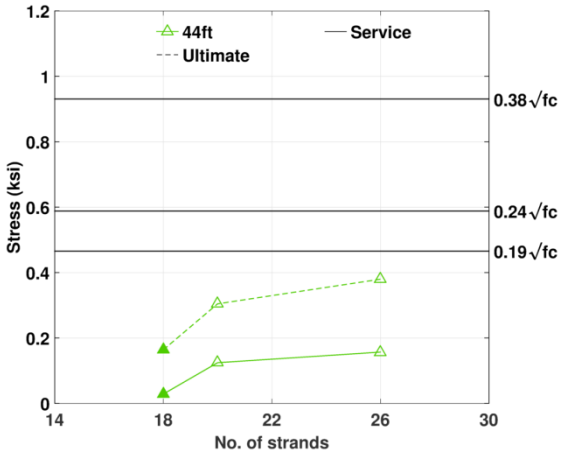

(c) Configuration 3: 4 column, 6 girder

Note: Solid markers indicate minimum strands control design.

Figure 5.6. Maximum tensile stress vs. number of strands for 48 inch bent cap (non-skewed I-girder bridges).

minimum span lengths, the design is controlled by the minimum number of strands (indicated by solid markers in the figures). In these bent caps, the ultimate stresses are 24 percent below the expected cracking stress. As the span length increases, the number of strands in the design also increases. This increase in strands number eventually leads to the possibility of cracking under ultimate strengths as shown (for example) for Configuration 2 in Figure 5.6. However, it should be emphasized that while some cracking may exist near ultimate loads, none of the solutions crack under normal service load conditions.

5.3.2. *Bridges with skewed I-girders*

Figure 5.7 and Figure 5.8 show the tension stresses at service and ultimate versus the number of strands for the 42 inch and 48 inch bent caps of 45 degree skewed I-girder bridges. The tensile service stresses at the location of maximum service moment (exterior joint or span) for each of the designs are shown by solid lines. Similar to the non-skewed I-girder bridges, the skewed I-girder bridges have service stresses below the expected cracking stress. The highest service stress is 0.34 ksi in the 42 inch, 32 ft bent cap. This stress is 42 percent lower than the expected cracking stress.

The tensile ultimate stresses at the location of the maximum ultimate moment for each of the designs are shown by dashed lines in Figure 5.7 and Figure 5.8. For the bridges with the minimum span lengths, the ultimate stresses are below cracking. For the intermediate and maximum spans of most bridges, the ultimate stresses exceed the expected cracking stress. The highest ultimate stress is 0.82 ksi in the 42 inch, 32 ft bent cap. While the stress is 40 percent higher than the expected cracking stress, it

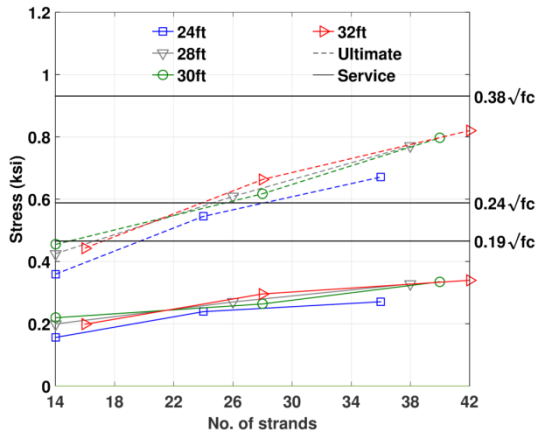

(a) Configuration 1: 3 column, 4 girder

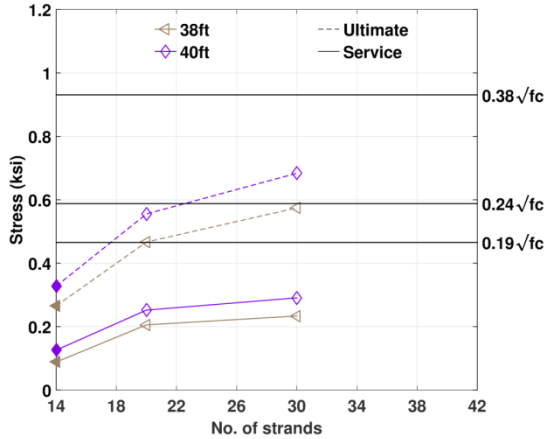

(b) Configuration 2: 3 column, 5 girder

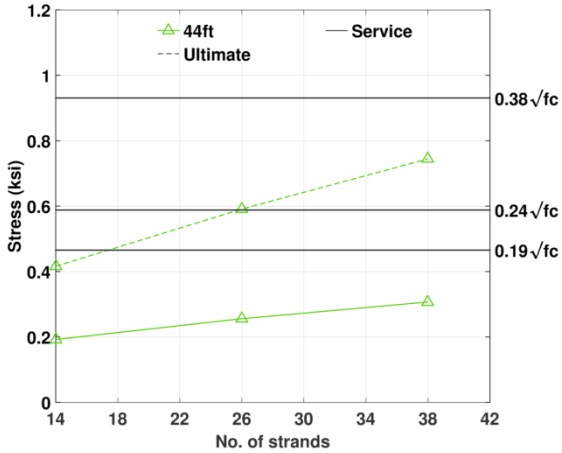

(c) Configuration 3: 4 column, 6 girder

Note: Solid markers indicate minimum strands control design.

Figure 5.7. Maximum tensile stress vs. number of strands for 42 inch bent cap (45 degree skewed I-girder bridges).

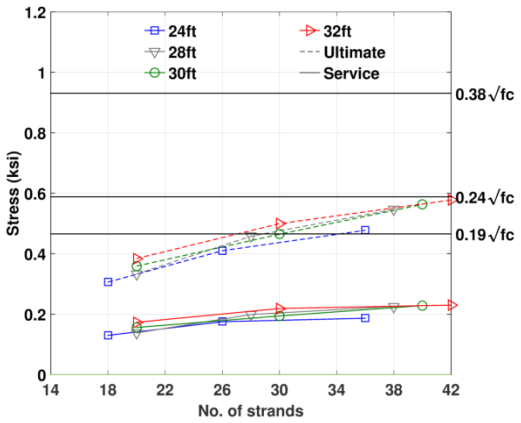

(a) Configuration 1: 3 column, 4 girder

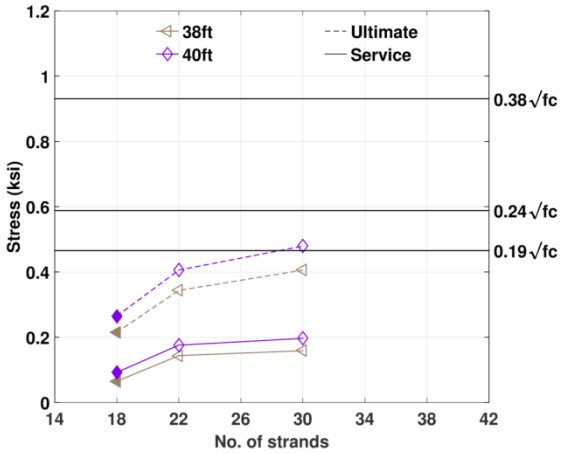

(b) Configuration 2: 3 column, 5 girder

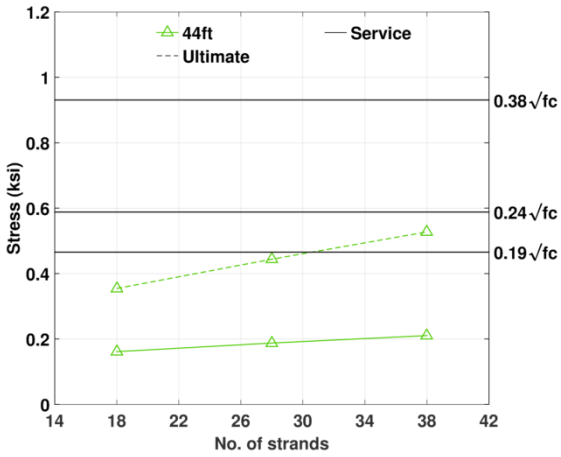

(c) Configuration 3: 4 column, 6 girder

Note: Solid markers indicate minimum strands control design.

Figure 5.8. Maximum tensile stress vs. number of strands for 48 inch bent cap (45 degree skewed I-girder bridges).

should be noted that cracking will not be severe as stress remains below $0.38\sqrt{f'_c\,(\text{ksi})}$. In other words, if a small crack did appear under such overload, the crack would close at removal of the load.

5.3.3. *Bridges with box beams*

Figure 5.9 shows the tension stresses at service and ultimate versus the number of strands for the box beam bridges. The tensile service stresses at the location of maximum service moment (interior joint) for each of the designs are shown by solid lines. Similar to the non-skewed I-girder bridges, the box beam bridges have service stresses below the expected cracking stress. The highest service stress is 0.38 ksi in the 30 ft bent cap. This stress is 35 percent lower than the expected cracking stress.

The tensile ultimate stresses at the location of the maximum ultimate moment for each of the designs are shown by dashed lines in Figure 5.9. For the bridges with the minimum span lengths, the ultimate stresses are below the expected cracking stress. For the intermediate and maximum spans of most bridges, the ultimate stresses exceed the expected cracking stress. The highest ultimate stress is 0.97 ksi in the 30 ft bent cap. This stress is 65 percent higher than the expected cracking stress and exceeds $0.38\sqrt{f'_c\,(\text{ksi})}$ (limit beyond which the member is not in the transition region but assumed to be a cracked member) by four percent. Efforts made to control such excessive cracking in these bridges are discussed later in Chapter 7 on the optimization of bridges.

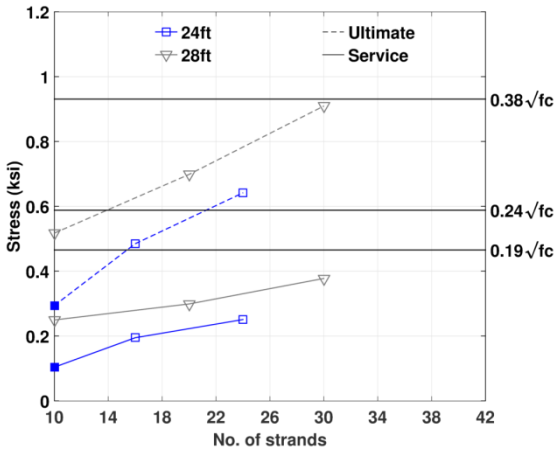

(a) Configuration 1: 3 column, 4 girder

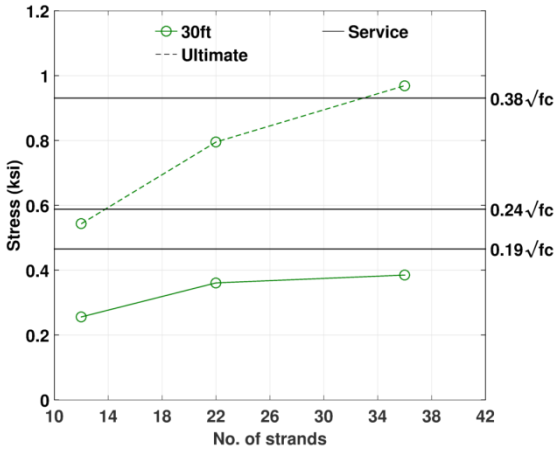

(b) Configuration 2: 3 column, 5 girder

Note: Solid markers indicate minimum strands control design.

Figure 5.9. Maximum tensile stress vs. number of strands for box beams.

5.3.4. *Bridges with X-beams*

Figure 5.10 show the tension stresses at service and ultimate versus the number of strands for the X-beam bridges. The tensile service stress at the location of maximum service moment (interior joint or span) for each of the designs is shown by solid lines. Similar to the non-skewed I-girder bridges, the X-beam bridges have service stresses

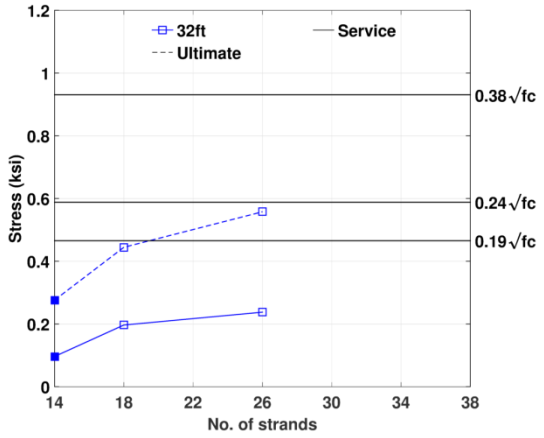

(a) Configuration 1: 3 column, 4 girder

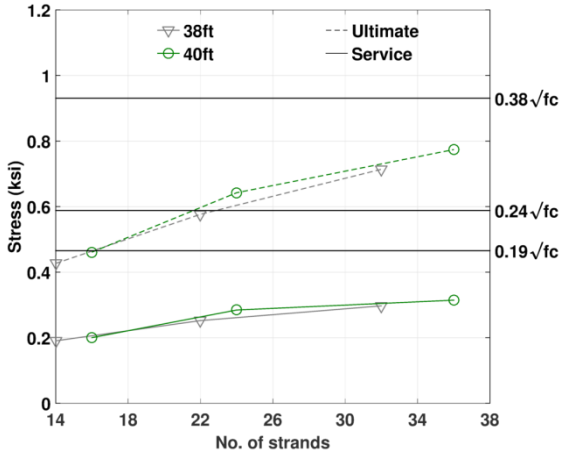

(b) Configuration 2: 3 column, 5 girder

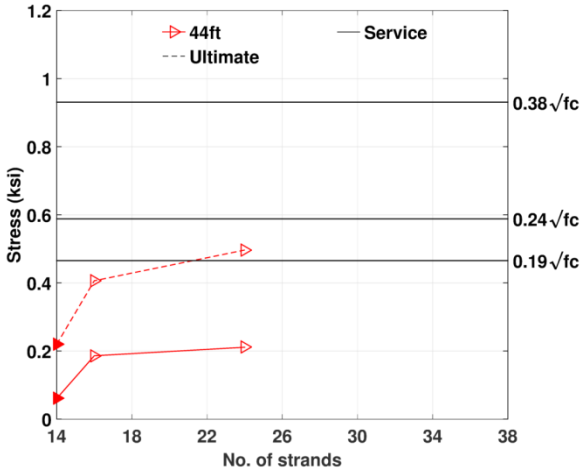

(c) Configuration 3: 4 column, 6 girder

Note: Solid markers indicate minimum strands control design.

Figure 5.10. Maximum tensile stress vs. number of strands for X-beams.

below the expected cracking stress. The highest service stress is 0.31 ksi in the 40 ft precast bent cap. This stress is 46 percent lower than the expected cracking stress.

The tensile ultimate stresses at the location of the maximum ultimate moment for each of the designs are shown by dashed lines in Figure 5.10. For the bridges with the minimum span lengths, the ultimate stresses are below the expected cracking stress. For the intermediate and maximum spans of the bridges with large column spacing, the ultimate stresses exceed the expected cracking stress. The highest ultimate stress is 0.77 ksi in the 40 ft bent cap. This stress is 32 percent higher than the expected cracking stress.

5.3.5. *Nonstandard bridges with I-girders*

Figure 5.11 show the tension stresses at service and ultimate vs. the number of strands for the nonstandard bridges. The tensile service stress at the location of maximum service moment (interior joint or span) for each of the designs is shown by solid lines. The designs in all the bridges are controlled by the number of strands for zero tension under dead load. Similar to the non-skewed I-girder bridges, the nonstandard bridges have service stresses below the expected cracking stress. The highest service stress is 0.53 ksi in the 68 ft bent cap. This stress is 21 percent lower than the expected cracking stress.

The tensile ultimate stresses at the location of the maximum ultimate moment for each of the designs are shown by dashed lines in Figure 5.11. For the bridges with the minimum span lengths, the ultimate stresses are 10 percent above the expected cracking stress. The highest ultimate stress is 1.24 ksi in the bridge with 68 ft bent cap and

maximum span length. This stress is 83 percent higher than the expected cracking stress, and exceeds $0.38\sqrt{f'_c\,(ksi)}$ (limit after which the member is beyond the transition region and assumed to be a cracked member) by 15 percent.

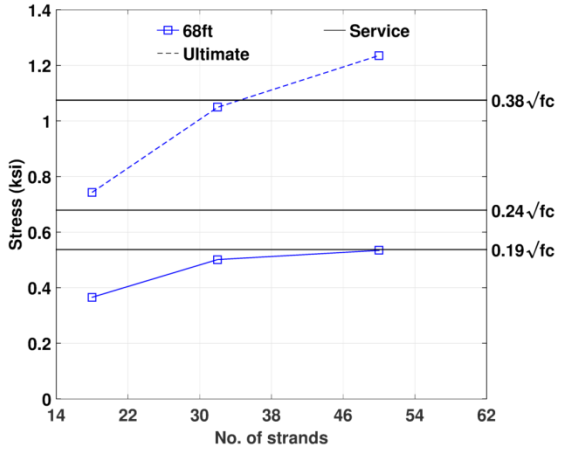

(a) Configuration 1: 3 column, 4 girder

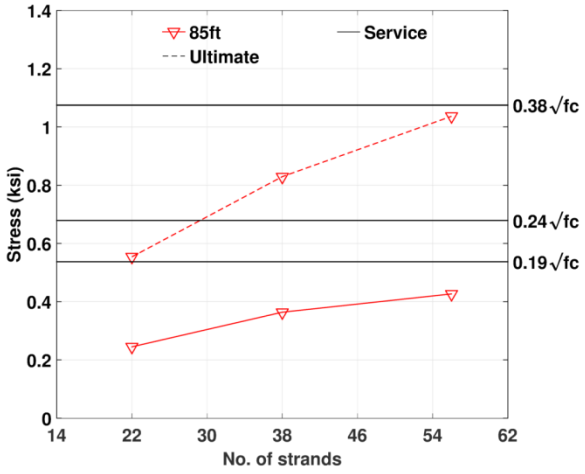

(b) Configuration 2: 3 column, 5 girder

Note: Solid markers indicate minimum strands control design.

Figure 5.11. Maximum tensile stress vs. number of strands for nonstandard bridges.

5.4. Provided overstrength

The concept of overstrength is hereby introduced to indicate the margin of reserve flexural capacity a section has at ultimate load. Overstrength is defined as

$$\Omega = \frac{\phi M_n}{M_u} \tag{5-1}$$

in which M_u = ultimate load demands; ϕM_n = factored capacity, where M_n = nominal flexural strength capacity and ϕ = capacity reduction factor (considered from AASHTO LRFD 5.5.4.2 as ϕ = 1 for prestressed concrete).

Step 3 of the design procedure requires the designer to check that the number of strands (Step 1) and concrete strength (Step 2) are sufficient to provide the necessary strength. For designs in the bridge inventory used in this study, the original design provided sufficient strength and no adjustments were needed.

Figure 5.12 to Figure 5.18 show plots of overstrength for the non-skewed I-girder bridges, skewed I-girder bridges, box beams, X-beams and nonstandard bridges with I-girders. Solid markers indicate designs that are controlled by the minimum number of strands.

5.4.1. *Bridges with non-skewed I-girders*

The overstrength factor is essentially the same for both bent cap sizes. Bent Configuration 1 (Figure 5.12(a) and Figure 5.13(a)) and Configuration 3 (Figure 5.12(c) and Figure 5.13(c)) have factors of safety between 1.8 and 2.1 for designs controlled by the number of strands for zero tension under dead load; the overstrength is as large as 2.92 when the minimum number of strands governs the design. For bent Configuration 2 (Figure 5.12(b) and Figure 5.13(b)), the overstrength

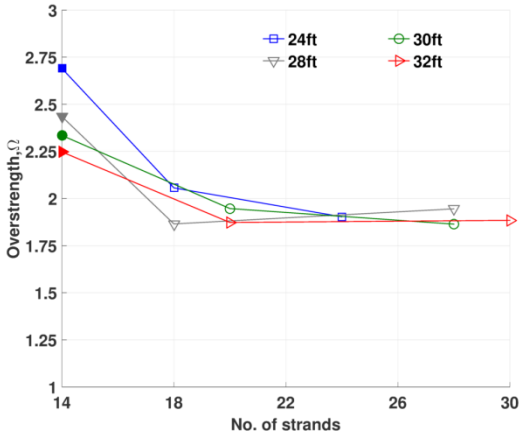

(a) Configuration 1: 3 column, 4 girder

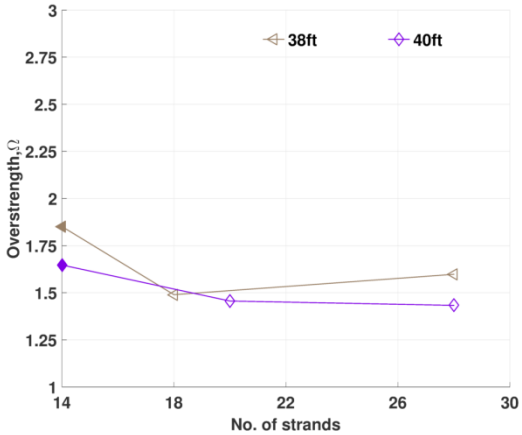

(b) Configuration 2: 3 column, 5 girder

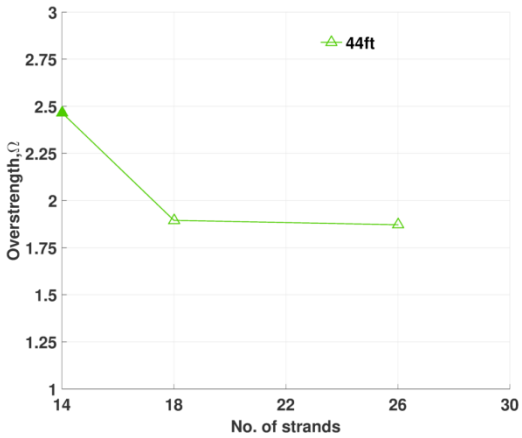

(c) Configuration 3: 4 column, 6 girder

Note: Solid markers indicate minimum strands control design.

Figure 5.12. Overstrength vs. number of strands for 42 inch bent cap (non-skewed I-girder bridges).

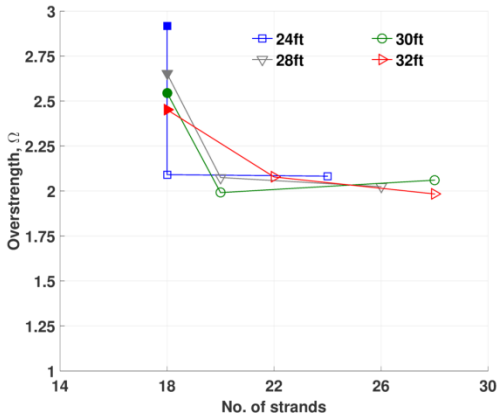

(a) Configuration 1: 3 column, 4 girder

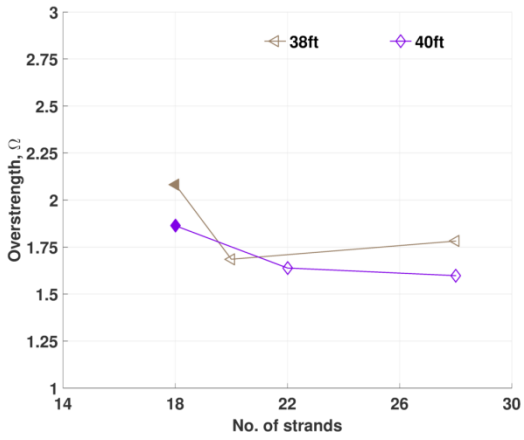

(b) Configuration 2: 3 column, 5 girder

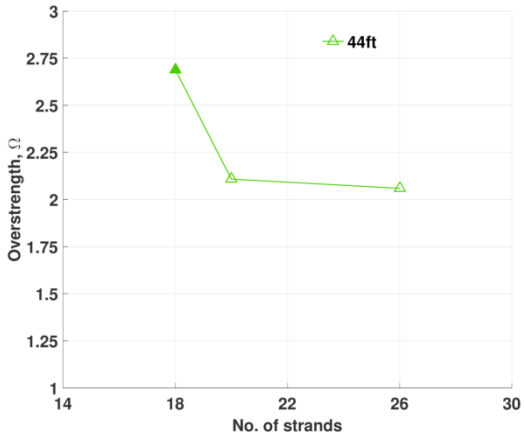

(c) Configuration 3: 4 column, 6 girder

Note: Solid markers indicate minimum strands control design.

Figure 5.13. Overstrength vs. number of strands for 48 inch bent cap (non-skewed I-girder bridges).

is not as large, with overstrengths between 1.4 and 1.8 for designs controlled by the number of strands for zero tension under dead load; the overstrength increases to as large as 2.1 when the minimum number of strands governs the design.

The lower overstrength for Configuration 2 is consistent with the increased tensile stresses and likelihood for cracking in these bents. While the overstrength and limited cracking under ultimate demands may be interpreted as an overdesign, it is important to assess this in regards to the original objective in developing the design procedure – zero tension under dead load. This ensures that if overloading resulting in cracking were to occur, the cracks would close under full removal of live load, thus preventing exposure of the steel to environment effects that may reduce the service life of the bent cap.

5.4.2. *Bridges with skewed I-girders*

The overstrength is essentially the same for both bent cap sizes. For all the three bent configurations in Figure 5.14(a), (b), (c) and Figure 5.15(a), (b), (c), the overstrength is between 1.6 and 2.1 for the designs controlled by the number of strands for zero tension under dead load. For bent Configuration 2 (Figure 5.14(b) and Figure 5.15(b)), the overstrength is as large as 2.4 when the minimum number of strands governs the design.

The higher overstrength for Configuration 2 is consistent with the reduced tensile stresses due to addition of a bent in the 45 degree skewed bridges.

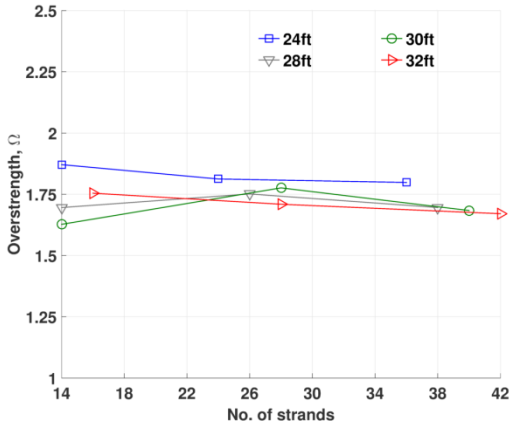

(a) Configuration 1: 3 column, 4 girder

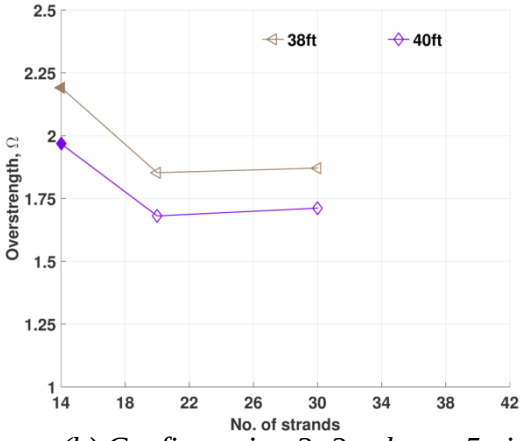

(b) Configuration 2: 3 column, 5 girder

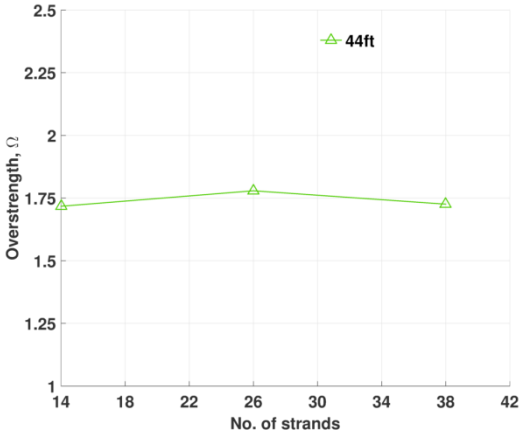

(c) Configuration 3: 4 column, 6 girder

Note: Solid markers indicate minimum strands control design.

Figure 5.14. Overstrength vs. number of strands for 42 inch bent cap (45 degree skewed I-girder bridges).

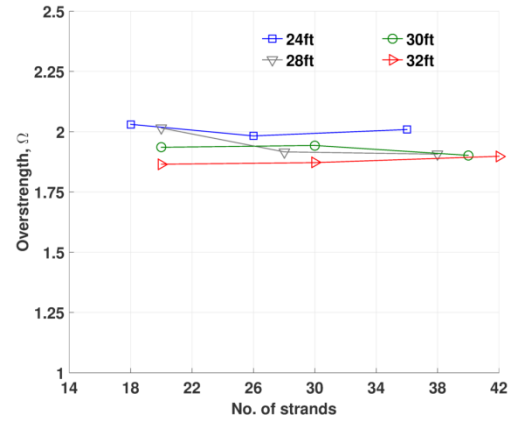

(a) Configuration 1: 3 column, 4 girder

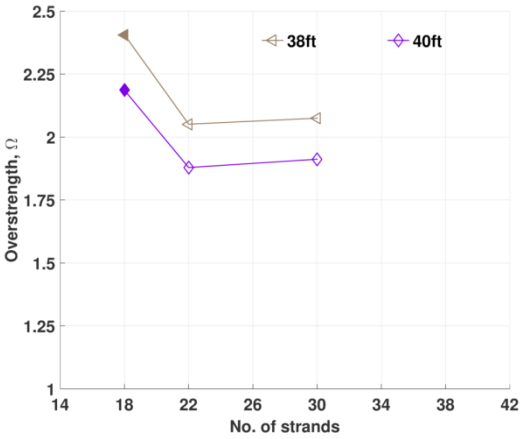

(b) Configuration 2: 3 column, 5 girder

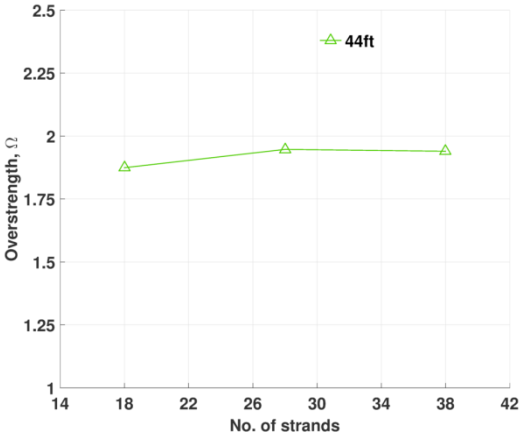

(c) Configuration 3: 4 column, 6 girder

Note: Solid markers indicate minimum strands control design.

Figure 5.15. Overstrength vs. number of strands for 48 inch bent cap (45 degree skewed I-girder bridges).

5.4.3. *Bridges with box beams*

The overstrength in Configuration 1 (Figure 5.16(a)) and Configuration 2 (Figure 5.16(b)) is between 1.5 and 1.9 for designs controlled by the number of strands for zero tension under dead load; the overstrength is as large as 2.1 when the minimum number of strands governs the design.

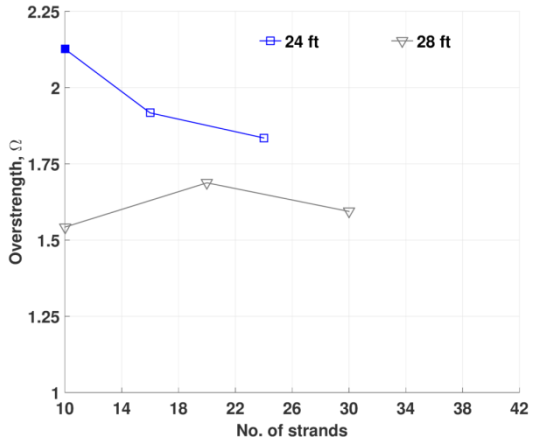

(a) Configuration 1: 3 column, 4 girder

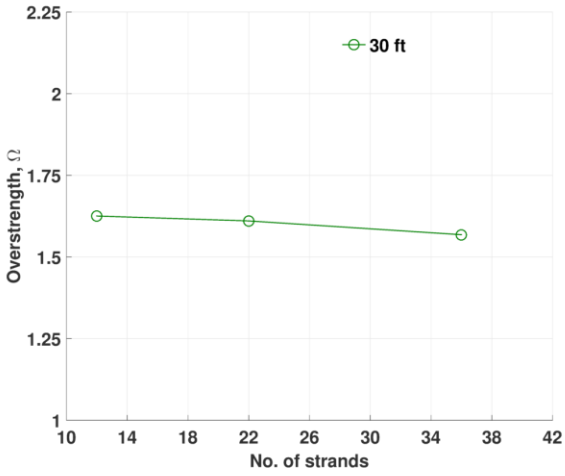

(b) Configuration 2: 3 column, 5 girder

Note: Solid markers indicate minimum strands control design.

Figure 5.16. Overstrength vs. number of strands for box beams.

5.4.4. *Bridges with X-beams*

The overstrength in all three bent configurations (Figure 5.17(a), (b), (c)) are between 1.6 and 1.9 for designs controlled by the number of strands for zero tension under dead load; the overstrength is as large as 2.4 when the minimum number of strands governs the design.

5.4.5. *Nonstandard bridges with I-girders*

For both bent configurations (Figure 5.18(a) and (b)) for the nonstandard bridges, the overstrength is not as large, with overstrength between 1.4 and 1.8 for all designs controlled by the number of strands for zero tension under dead load.

The lower overstrength for these bridges is consistent with the increased tensile stresses and likelihood for cracking in these bents.

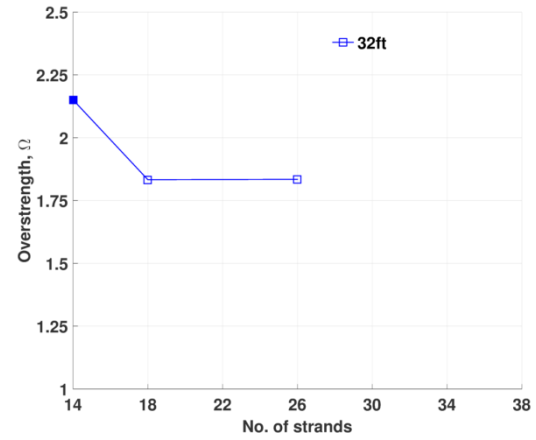

(a) Configuration 1: 3 column, 4 girder

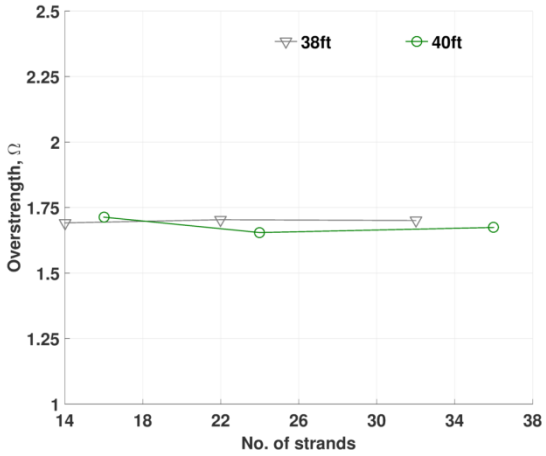

(b) Configuration 2: 3 column, 5 girder

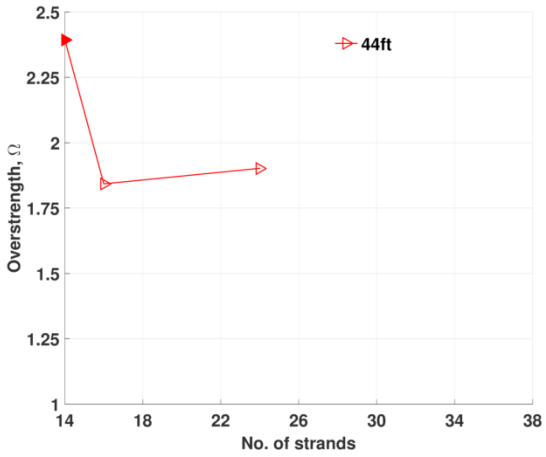

(c) Configuration 3: 4 column, 6 girder

Note: Solid markers indicate minimum strands control design.

Figure 5.17. Overstrength vs. number of strands for X-beams.

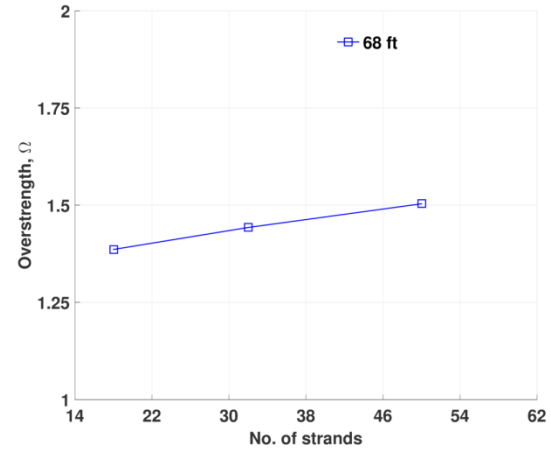

(a) Configuration 1: 3 column, 4 girder

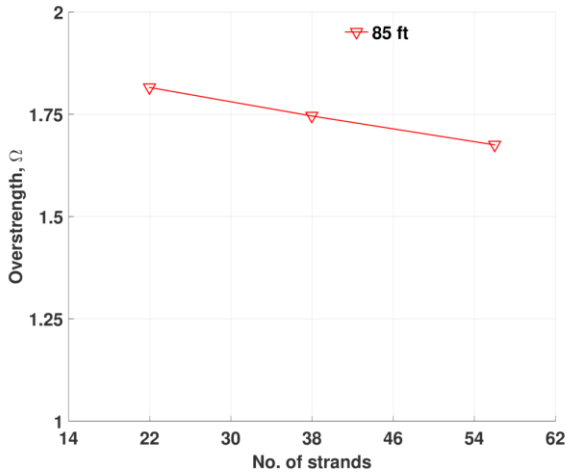

(b) Configuration 2: 3 column, 5 girder

Note: Solid markers indicate minimum strands control design.

Figure 5.18. Overstrength vs. number of strands for nonstandard bridges.

5.5. Comparison to RC design

The objectives of the research study will be met when the pretensioned, precast concrete bent cap has an equivalent or higher performance than a reinforced concrete bent cap. In lieu of a comparison of reinforced concrete and prestressed concrete for all bridges, comparison of the 42 and 48 inch square 40 ft bent caps for non-skewed I-girder bridges

with maximum span length is considered. These bridges have the largest stresses for 42 inch and 48 inch bent caps, respectively.

5.5.1. *Strength*

The reinforced concrete designs are adopted from the TxDOT standard drawing. For both bridges, the reinforcement consists of 6-#11 bars at the top, and 4-#11 bars at the bottom for the full length of the cap, with an additional 6-#11 bars at the bottom in the spans (does not continue through over the column). Skin reinforcement is provided as 5-#5 bars on each side face of the bent cap. The contribution of the skin reinforcement in flexural strength and cracking moment has not been considered. The prestressed concrete designs both require 28 strands, which are symmetrically placed at the top and bottom faces of the bent cap. Table 5.1 shows a comparison of the overstrength of the reinforced concrete and prestressed concrete bent caps.

Table 5.1. Comparison of strength between RC and PSC for the 40 ft bent cap.

	Reinforced concrete		Prestressed concrete	
	42 inch	48 inch	42 inch	48 inch
Moment capacity, M_n (k-ft)	2496	2929	2292	2747
Ultimate moment, M_u (k-ft)	1499	1631	1499	1631
Overstrength (M_n/M_u)	1.67	1.80	1.53	1.68

5.5.2. *Expected regions of cracking*

The cracking moment for a reinforced concrete bent cap can be determined from AASHTO LRFD equation 5.7.3.6.2.-2:

$$M_{cr} = f_r \frac{I_g}{y_t} \tag{5-2}$$

where, f_r = modulus of rupture of concrete (ksi); I_g = gross moment of inertia (in^4); and y_t = distance from the neutral axis to the extreme tension fiber (inch). For the

prestressed concrete bent cap, the cracking strength is determined from Eq. (3-1) in Section 3.3.1.

For reinforced concrete designs with 3.6 ksi concrete compressive strength, M_{cr} is 469 k-ft and 700 k-ft for the 42 inch and 48 inch bent caps respectively. For prestressed concrete bent caps with 28 strands, M_{cr} is 1179 k-ft and 1560 k-ft for the two sizes respectively. The bent caps will undergo cracking in the regions where the flexural demand is greater than the cracking moment.

Figure 5.19(a) and Figure 5.20(a) shows the regions of cracking of the bent cap at service for the 42 inch and 48 inch bent caps respectively. At service, the prestressed caps are uncracked, while the reinforced concrete caps are cracked at the regions of maximum positive (at girder in span) and negative moments (above the columns). Figure 5.19(b) and Figure 5.20(b) show the regions of cracking of the bent cap at ultimate for the 42 inch and 48 inch bent caps respectively. The extent of cracking in the reinforced concrete cap spreads. The prestressed cap now has cracking, but only where the maximum positive moment demands is located (at the girder locations in the span).

The bridges shown in Figure 5.19 and Figure 5.20 have the highest demands at service and ultimate and are the worst cases of cracking for the non-skewed I-girder bridges. For bent Configuration 1 and 3, the prestressed designs are not expected to crack at ultimate; companion reinforced concrete designs would be expected to have some regions of cracking. The intermediate and maximum span lengths of Configuration 2 undergo cracking in the span at ultimate.

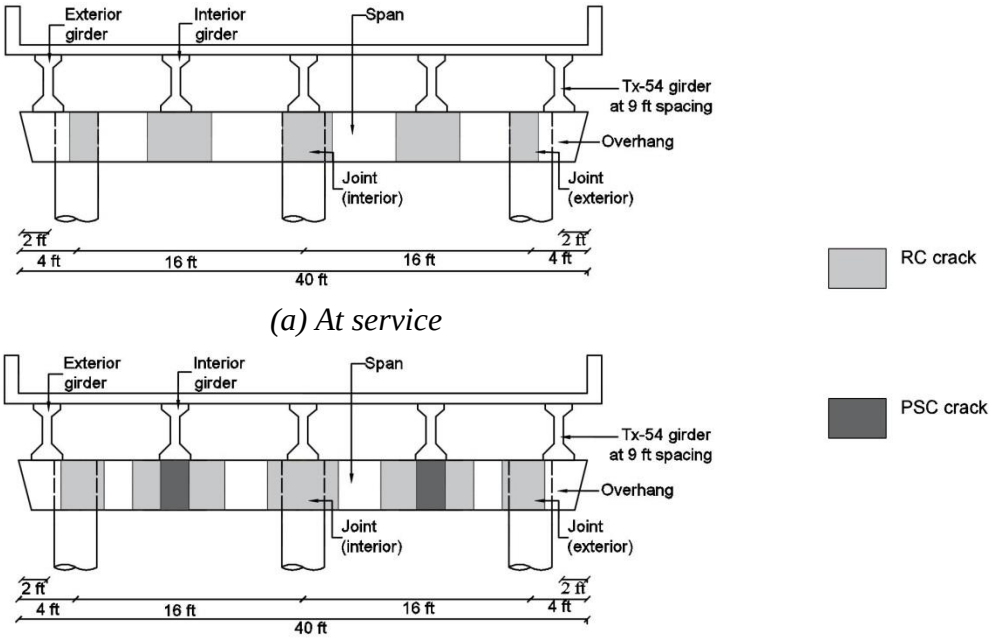

(a) At service

(b) At ultimate

Figure 5.19. Cracking of 40 ft, 42 inch bent cap (maximum span).

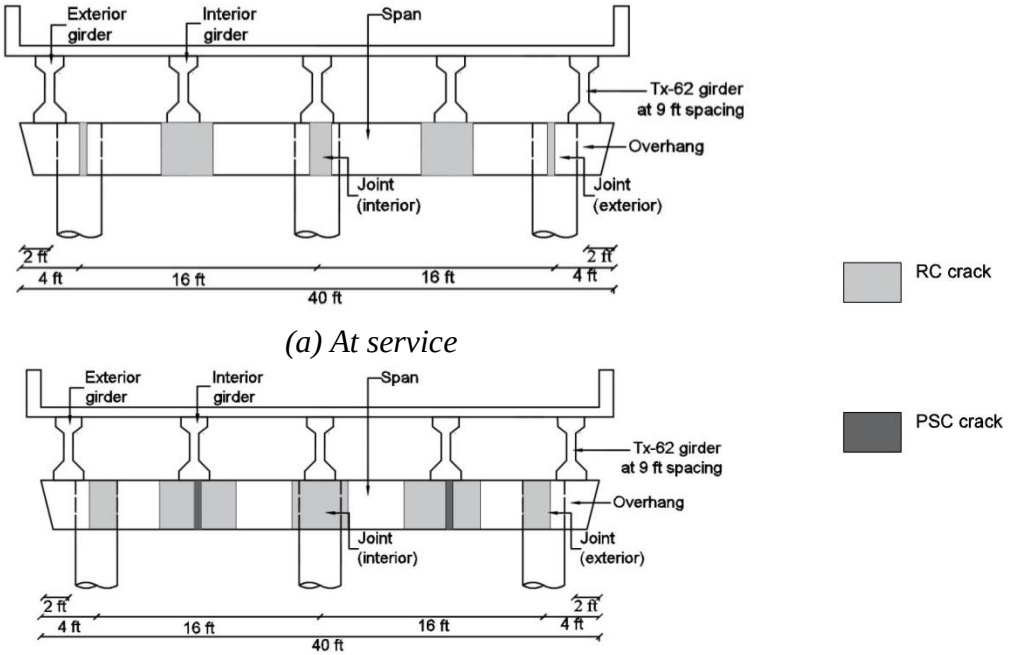

(a) At service

(b) At ultimate

Figure 5.20. Cracking of 40 ft, 48 inch bent cap (maximum span).

5.6. Design of void sections

The length of a large pretensioned bent cap is limited by weight restrictions due to shipping and placing requirements. To reduce bent cap weight, permanent interior voids can be introduced in the span region, while the overhang and connection remains solid. A voided bent cap with a cross section similar to a box-girder has somewhat less weight than a solid section; the top, bottom and the sides provide room for placing prestressing strands.

The proposed flexural design procedure can be used to evaluate a permanent void section, and determine the impact of voids in design and performance. In lieu of evaluating void pretensioned bent caps for all bridges, a 44 ft roadway width bridge with non-skewed I-girders, maximum span length (120 ft) and 42 inch square bent cap is considered. A 30 inch square void section is assumed; this is the maximum practical void size and the worst case scenario for permanent void sections.

A minimum of 8 strands is required in the void prestressed bent cap, less than the 14 strands required in an equivalent solid section. From Step 1 of the design procedure, 18 strands are required in the voided section; less than the 26 strands required in the solid section. Figure 5.21 shows the strands layout in the void section. The service and ultimate stresses in the void section are 0.27 ksi and 0.68 ksi respectively, indicating cracking under ultimate loads. This is in variation to a solid section, with service and ultimate stresses of 0.23 ksi and 0.54 ksi respectively, which does not crack under ultimate loads. In addition, the void pretensioned bent cap has a minimum concrete

strength of 3.8 ksi, higher than 2.8 ksi in the solid section. The overstrength is 1.4, lower than 1.8 in the solid section.

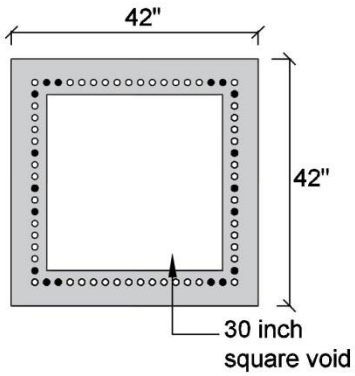

Figure 5.21. Void bent cap cross-section.

5.7. Summary of flexural design

The design of the entire bridge inventory by the proposed flexural design procedure (concentric prestressing) of zero tension under dead load required a feasible number of strands. The short span bridges are governed by the minimum number of strands. Service and ultimate stresses in these bridges are therefore well below the expected cracking stress. The intermediate to maximum span lengths of certain bridges have maximum stresses at ultimate loads that only marginally exceed the cracking stress; bridges with maximum stresses exceeding the $0.38\sqrt{f'_c\,(\text{ksi})}$ stress limit are assumed to behave as cracked members in that ultimate demand condition, but on removal of that load, cracks would be expected to close due to the action of the prestress. Such high tensile stress is observed in the box beam bridges and can be explained as a consequence of the smaller bent cap cross sections in these bridges.

The overstrength factor for all bridges is more than adequate; in most bridges the overstrength is at least 50 percent higher than required. While this overstrength achieved may be interpreted as an overdesign, it is essential to interpret it with respect to the objective of attaining zero tension under dead load. This has the added benefit of ensuring crack closure on removal of overload. The minimum concrete strength in all the bridges is less than 6 ksi, except for the nonstandard 68 ft roadway width bridge that requires a minimum concrete strength greater than 8.5 ksi. To limit the minimum concrete strength to a maximum 8.5 ksi, additional strands are necessary; the design is thus governed by the service stresses and is a variation from the proposed flexural design procedure. A comparison of performance between RC and PSC bent caps for an exemplar bridge showed that the RC bent cap cracked under service and ultimate loads; the companion PSC bent cap cracked only under ultimate loads.

Voids can be introduced in a pretensioned bent cap to mitigate weight exceedance. A void pretensioned bent cap is evaluated with the proposed flexural design procedure. In comparison to an equivalent solid section, the void section requires lower number of strands, has higher stresses under service and ultimate loads, higher minimum concrete strength, and lower overstrength.

6. DETAILING AND CONNECTIONS

With the previous focus on the flexural design of pretensioned bent caps it was established that prestressed concrete bent caps could be implemented in a wide variety of bridges. It follows that the pretensioned bent cap design be appropriately detailed to resist the end region tensile (bursting) stresses along with appropriate detailing for the bent cap-to-column connection. Therefore, this chapter focuses on detailing issues. Section 6.1 compares end region detailing requirements for end splitting, spalling and bursting with recommendations made for practical details. In Section 6.2, pocket connection details are established from first principles requirements and applied to bent caps.

6.1. End region detailing for pretensioned bent caps

Section 2.5 summarized the splitting, spalling and bursting stresses that occurs within the transfer length of pretensioned members. AASHTO LRFD provisions require end zone reinforcement to be provided, for splitting resistance, within a distance of *D/4* from the member end. The resistance should be at least four percent of the prestressing force at transfer. Besides this, there have been various research investigations conducted to determine effective detailing to control bursting stresses. Tuan et al. (2004) recommended that 50 percent of the end zone reinforcement be placed within *D/8* from the member end and the remaining 50 percent to be placed within *D/8* to *D/2* from the member end. O'Callaghan and Bayrak (2008) recommended that in addition to the reinforcement provided within *D/4* from the member end meant to handle spalling

stresses, bursting reinforcement needs to be placed immediately after spalling reinforcement, from *D/4* to the transfer length.

Figure 6.1 presents a comparison of the abovementioned recommendations applied to a bridge with 32 ft wide roadway, non-skewed I-girders and span length of 80 ft. The substructure consists of a 42 inch square bent cap prestressed with 20 strands. The exterior column face is 2.5 ft from the edge of the bent cap. Considering a 21 inch diameter pocket connection at the joint, 37.5 inches of length is available from the member end for detailing the end regions. Figure 6.1 shows 2-legged #5 stirrups provided as end zone reinforcement on a straight and a battered end, according to recommendations from (a) AASHTO LRFD, (b) Tuan et al. (2004) and (c) O'Callaghan and Bayrak (2008) respectively. In the battered end bent caps, first two stirrups are provided parallel to the battered end, followed by a transition stirrup and then the remaining are placed as vertical stirrups. The use of higher number of strands will require larger diameter bars or multi-legged stirrups, for example 30 strands require 4-legged #5 stirrups placed in the same spacing as Figure 6.1.

It is considered prudent that the more conservative recommendations of O'Callaghan and Bayrak (2008) be used for bent cap design. These recommendations are in keeping with the strut-and-tie models discussed earlier in Figure 2.7(c). The end region reinforcement provided up to the transfer length includes the region of high shear at the exterior girder location which may result in high stresses in the reinforcement. These stresses should be checked not to exceed 20 ksi. To prevent this, additional transverse reinforcement may be necessary.

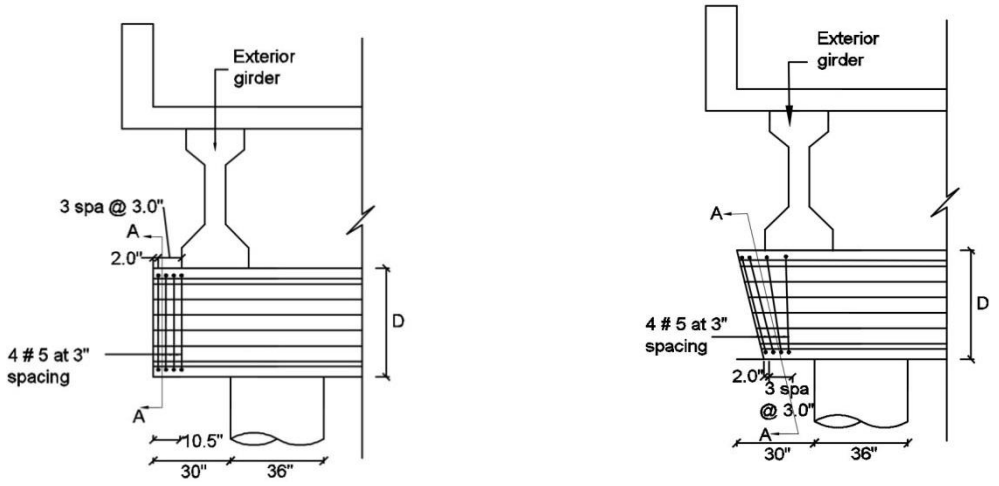

(a) AASHTO LRFD (2014)

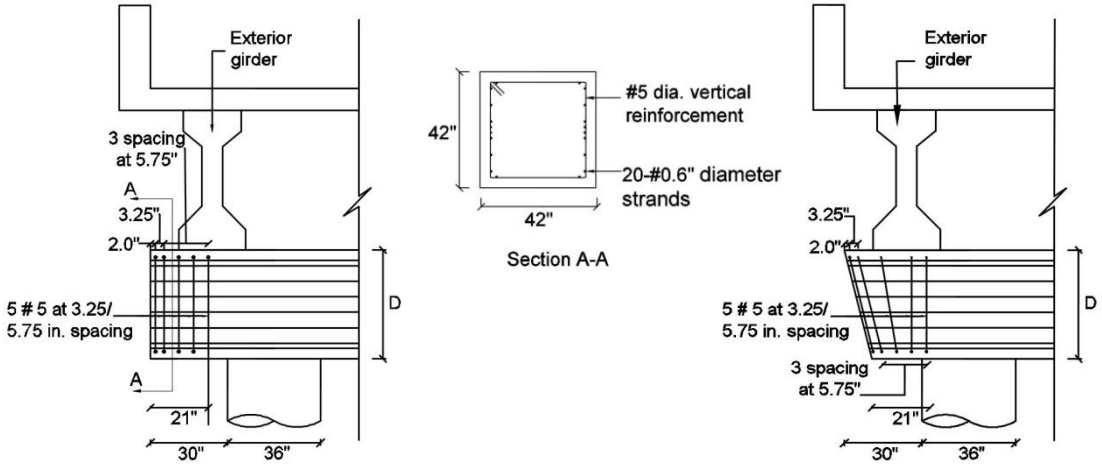

(b) Tuan et al. (2004)

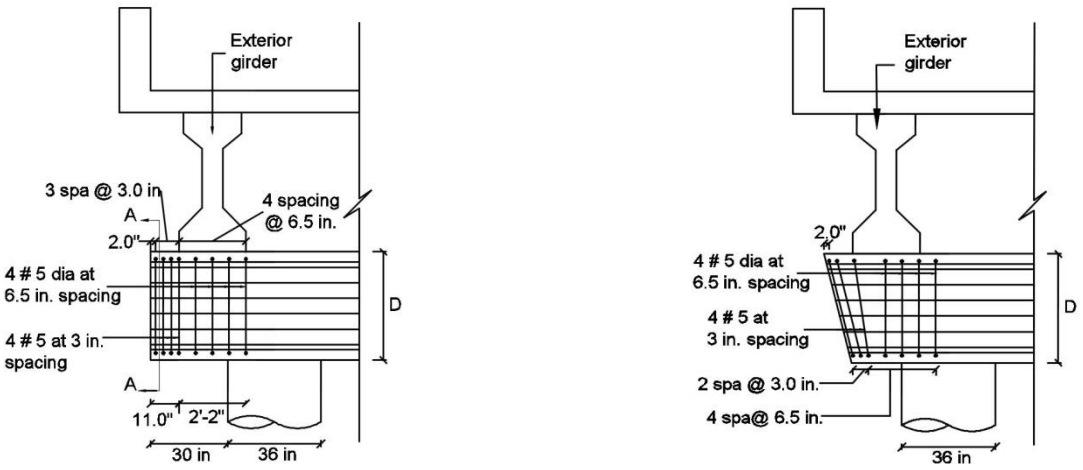

(c) O'Collaghan and Bayrak (2008)

Figure 6.1. Application of end region detailing provisions.

6.2. Pocket connections

The use of precast bent caps necessitates connections between the bent cap and columns. Ideally, precast connections should *emulate* the performance attributes of their monolithic counterparts, including the transfer of critical forces, elastic or inelastic behavior, joint shear resistance, and stability and ductility of the structure. It is also necessary that the connection design consider the construction of the structure with respect to time, cost, method of construction, type of material and the requirement of skilled labor. Two types of emulative connections are considered in this chapter- (a) grouted vertical duct connection, and (b) pocket connection.

In house design provided by TxDOT engineers currently focus on using grouted vertical duct connection as the standard connection between precast RC bent caps and columns. More recently private sector consultants have developed pocket connections for pretensioned bent caps which are now used in construction. In what follows is a discussion on the evolution of current practice and the changing trends toward prestressed bent caps and the associated detailing requirements.

6.2.1. *Discussion of current practice and previous research*

The investigations made in TxDOT Research Projects 0-1748 and 0-4176 led to the development of a connection known as the grouted vertical duct connection. This has been implemented by TxDOT as the standard connection detail for precast reinforced concrete bent caps, intended to be used with multi-column interior bent designs. In this connection, the column bars are terminated at the top of the column. Dowel bars are

embedded into the core of the column and extended above the column top into individual 4 inch diameter galvanized steel ducts precast in the bent cap.

TxDOT has identified a number of challenges in the use of the grouted vertical duct connection. This includes tight horizontal tolerances for alignment of bars with the corrugated duct, minimal room for accidental misalignment of column with respect to the bent cap and the issues associated with grouting of connection. Grouting operations require skilled labor, and special care and attention to ensure a successful mix. Improper grouting may lead to segregation of water from the grout. The migration of water to the surface of the grout is known as bleeding, which may result in voids created in the grout. These voids further lead to reduced strength of the grout and act as channels for ingress of unwanted materials into the grout possibly resulting in corrosion of the reinforcement.

To address these challenges, the large pocket connection developed by Restrepo et al. (2011) has been identified as an alternative connection. A corrugated steel pipe is used to form the void for the pocket connection within the precast concrete bent cap. In the field, the bent cap is placed over the column whose reinforcing bars, in the form of central dowel bars extend into the pockets. Rather than grout, normal concrete is used to fill the pocket connection. Sufficient clearance is available to accommodate accidental misalignment of column with respect to the bent cap. Due to the improved constructability attributes it is contended that the pocket connection should be a preferred option.

Restrepo et al. (2011) experimentally tested the pocket connection and reported its performance as satisfactory for use in seismic regions. Two pocket connections were

tested, which mostly differed in the amount of transverse and joint shear reinforcement. Results showed emulative behavior of the connection and emphasized the need for adequate joint reinforcement in the pocket connection implemented in seismic regions.

6.2.2. *Pocket size*

The question associated with the use of a pocket connection is "*How big does the pocket need to be?*" A general misconception is that a pocket may need to be as large as possible to directly accommodate the column bars. However, in this research it is contended that a pocket should be as small as practicable to maximize constructability. This feature is also important when switching from a reinforced to prestressed concrete bent cap; if the pocket is excessively large so will the stress concentration arising from the effect of prestressing in the neighborhood of the pocket. Moreover, an examination of Figure 6.2 indicates that those connections with relatively large pockets have very little construction tolerance to cope with misalignments. A small to medium diameter pocket, on the other hand, has markedly more latitude if any of the column heads are misaligned in a multi-column head, see Figure 6.3.

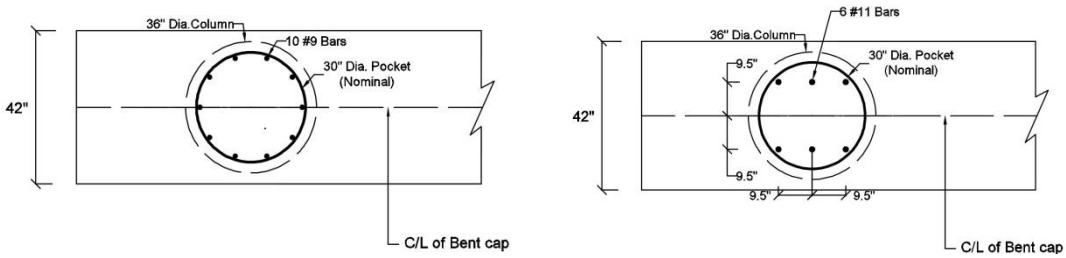

(a) Extension of column bars. *(b) Dowel bars for grouted vertical duct connection.*

Figure 6.2. Preliminary options of pocket connection for 36 inch diameter column around standard TxDOT bar configuration.

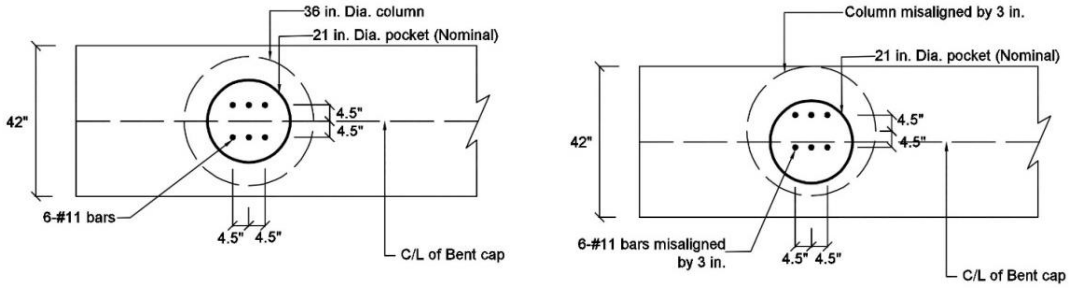

(a) Without misalignment *(b) With misalignment*

Figure 6.3. Geometry of 21 inch diameter pocket connection with 6-#11

Engineers may be predispositioned to think that the column/ dowel bars through the joint need to be on a large pitch diameter such as shown in Figure 6.2. Clustering the bars about a tight centroid, as shown in Figure 6.3, can also lead to a sufficiently strong joint connection. A minimum pocket size of 21 inches with a bar spacing of 4.5 inches (clear spacing of 2 d_b where d_b is the bar diameter) is adequate in a 36 inch diameter column for providing room for column misalignment.

6.2.3. *Moment capacity of the pocket connection*

The procedure followed for determination of moment capacity of the pocket connection is similar to the calculation of column flexural capacity. Figure 6.4 shows the section, strain, stress and internal forces acting in the joint.

The axial load (*N*) in the joint is assumed to result only from dead loads. To determine conservative results, the dead loads are combined using the minimum load factors corresponding to the Strength limit state load combination, for which the joint demand is the highest.

The tension force due to the dowel bars is determined by,

$$T = f_y A_s = \rho f_y A_g \tag{6-1}$$

in which ρ = joint reinforcement ratio, f_y = steel tensile stress (ksi) and A_g = gross cross-section area of column (in^2).

Lumping the bars at the column centroid (solid dot in Figure 6.4) and assuming all steel yields, equilibrium requires,

$$C_c = N + T = N + \rho f_y A_g \tag{6-2}$$

in which, C_c = concrete compression force considering core dimensions of joint (k); N = axial force from dead loads.

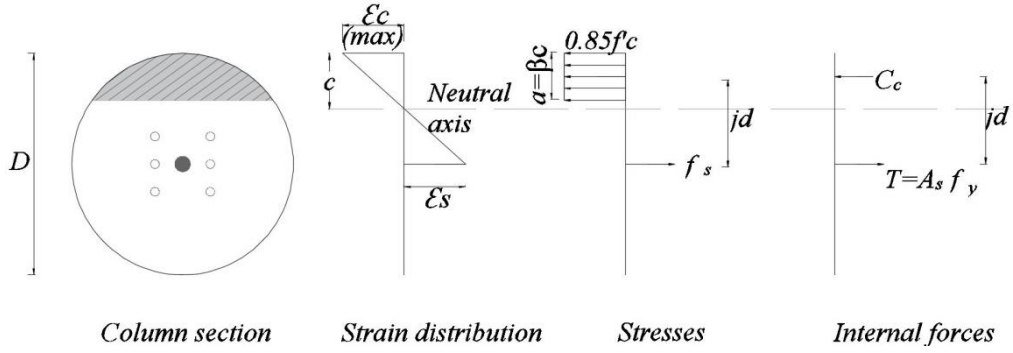

Figure 6.4. Calculation of moment capacity.

Dutta and Mander (2001) have shown that the concrete compression force in a circular configuration with an eccentric concrete stress block may be approximated as follows

$$\frac{C_c}{f'_c A_g} = 1.32\alpha\left(\beta\frac{c}{D}\right)^{1.38} \tag{6-3}$$

in which, D = diameter of the column; f'_c = unconfined compressive strength of concrete; α, β = stress block factors for unconfined concrete; and $a = \beta c$ where a = stress block depth and c = neutral axis depth.

Note, Eq. (6-3) is valid providing c/D < 0.5.

For $f'_c \leq 4$ ksi, β = 0.85 and α = 0.85. From Eq. (6-3),

$$C_c = 1.122 f'_c A_g \left(\frac{a}{D}\right)^{1.38} \tag{6-4}$$

Putting Eq. (6-2) in Eq. (6-4) and normalizing the axial load gives,

$$\frac{\phi N}{f'_c A_g} = 1.122\phi\left(\frac{a}{D}\right)^{1.38} - \frac{\phi\rho f_y}{f'_c} \tag{6-5}$$

where ϕ = undercapacity factor.

The depth of compression block from Eq. (6-4) is given by

$$\frac{a}{D} = 0.92\left(\frac{C_c}{f'_c A_g}\right)^{0.725} \tag{6-6}$$

The lever arm between tension and compression forces is computed as:

$$jd = \frac{D}{2} - 0.6a = \frac{D}{2}\left(1 - 1.2\frac{a}{D}\right) \tag{6-7}$$

The moment in the joint is given by:

$$M_j = C_C \; jd \tag{6-8}$$

Subtituting Eqs. (6-4) and (6-7) in Eq. (6-8) and normalizing the moment gives,

$$\frac{\phi M_j}{f'_c A_g D} = 0.561\phi\left(\frac{a}{D}\right)^{1.38}\left(1 - 1.2\frac{a}{D}\right) \tag{6-9}$$

The moment capacity of the pocket is compared with the column strength. Figure 6.5 shows a P-M interaction diagram for a 36 inch diameter column with 10-#9 bars and

3.6 ksi concrete compressive strength and for the associated pocket connection. The joint strength is determined for a specified a/D ratio ranging from 0 to 0.425 and one percent reinforcement ratio. For compressive loads, the joint strength is lower than that of a column, thus ensuring a strong column weak joint concept.

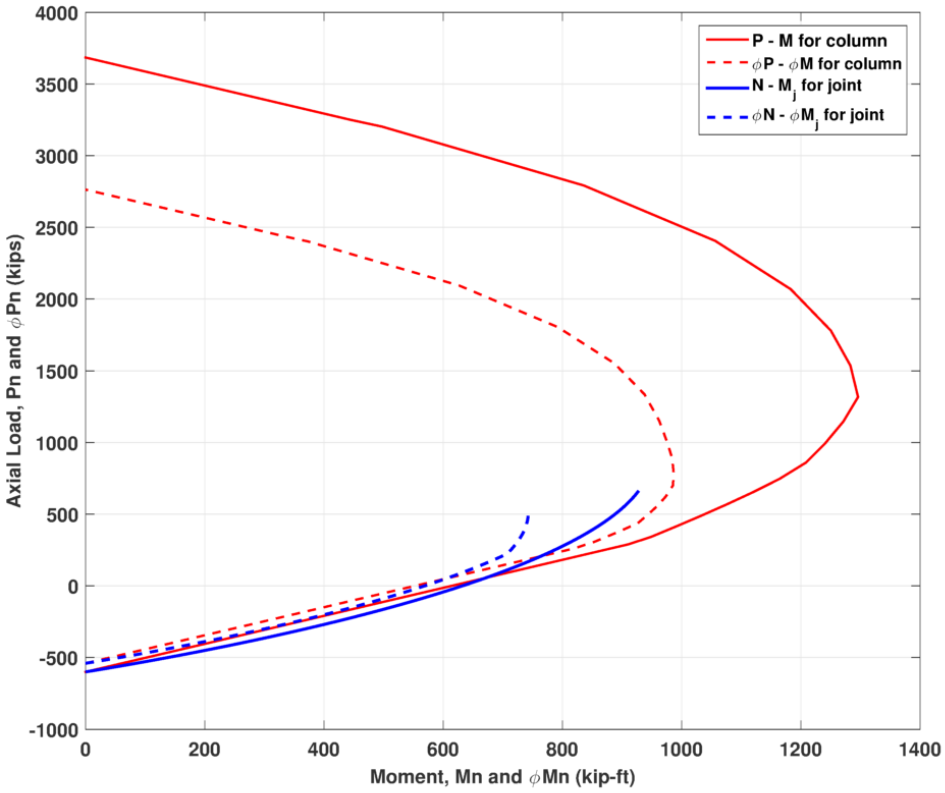

Figure 6.5. P-M interaction for column and joint.

6.2.4. *Connection demands*

The moment capacity of the pocket connection determined from the procedure in Section 6.2.3 should be adequate to transfer forces from the bent cap to the supporting columns. This section presents a summary of the demands in the joint that must be transferred.

The connection must transfer the gravity loads consisting of the dead and vehicular live loads used in designing the bent cap, and the wind loads acting on bridge members and on live loads. The dead load and vehicular live load with impact acting in the joint comprises the loads on the bent cap described in Section 4.2. The column moment is maximum when the live load is applied only at one exterior lane, therefore the live load is assumed from only one girder (either exterior or first interior whichever induces maximum column moment). Wind loads acting on the superstructure, bent cap, and live loads are calculated according to the provision of Section 3.8 in AASHTO LRFD. The dead, live and wind loads are combined in accordance with the load factors in AASHTO LRFD 2014 Table 3.4.1-1.

The joint shear is calculated from the joint moments and column axial forces. Figure 6.6 shows an indicative joint force calculation from (a) the compression forces in the joint due to the column axial force (R1, R2 and R3) and (b) the compression-tension couple, with a moment arm of 0.8 times the diameter of the column, formed by the joint moment (M1, M2 and M3). To determine the maximum possible joint shear, a full live load reaction along with dead load is considered in the girder (P1) for which a governing joint moment is obtained, and only dead load considered in all other girders

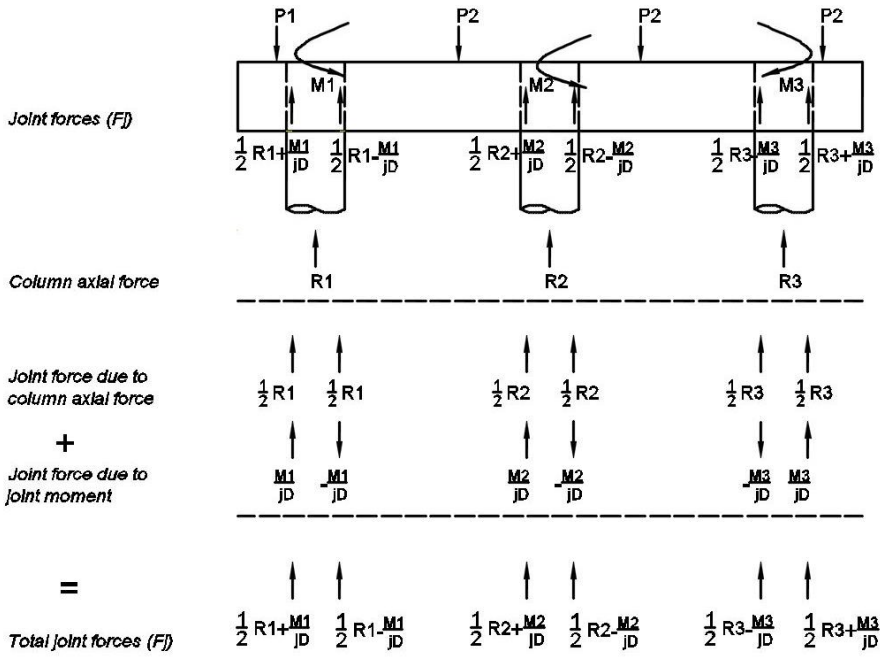

Figure 6.6. Determination of joint shear force.

(P2). These loads are multiplied with the load factors corresponding to the strength load combination for which the joint moment is the highest. From the joint forces and applied loads, the joint shear is determined.

Rigorous analysis shows that when sidesway is not present, the joint shear demands are small and similar to the shears encountered in adjacent beams. If sidesway occurs, which is a possibility under crash loads, joint opening (or closing) may occur. If there is substantial reinforcing steel from the column into the joint, an end couple of forces is formed (equivalent to the end moment within the column). This force couple introduces a high shear force within the cap-column joint region. The inherent shear strength of the concrete within the joint has limitations on the magnitude of shear force that can be transferred and without adequate transverse reinforcement within the joint

region, diagonal cracking may occur. Under these circumstances it is likely that a substantial amount of joint shear reinforcement may be necessary to inhibit concrete cracking.

6.2.5. *Connection performance under collision loads*

For bridges designed to resist vehicle collision loads, the proposed pocket connection should be examined for resistance against such loads. The failure of the structure under collision loads depends on the plastic hinge mechanisms formed. A plastic hinge mechanism is identified from the location of the plastic hinges. For a specific plastic hinge mechanism, a certain magnitude of lateral load will generate that mechanism; the mechanism with the lowest level of load (true collapse load) is critical mechanism. To provide resistance against vehicle collision, the true collapse load should be greater than the relevant component of the vehicle collision load. AASHTO LRFD 3.6.5.1 specifies a collision load of 600 k load applied at 5 ft above the ground and at an angle of zero to 15 degrees with the edge of the pavement in a horizontal plane. In this research, a 15 degree angle is assumed. The vehicle collision load can be resolved into two components: a 580 k force (F_x) acting in the transverse direction and a 155 k force (F_y) acting in the longitudinal direction of the bridge.

The joint design concept assumed in this research is of a strong column weak joint. The order of strength of the structure that is followed in this concept is:

$$M_j < M_c < M_b \tag{6-10}$$

where M_j, M_c, M_b are the moment capacities in the joint, column and bent cap respectively. A bent cap designed stronger than the column prevents plastic hinge

formation in the bent cap. Further, if the column is designed stronger than the joint, plastic hinge formation will be at the joint and vice versa.

Figure 6.7 show the failure mechanisms due to the vehicle collision load. Mechanism 1 is a global mechanism in which all the columns sway due to the lateral load. Mechanism 2 is a local mechanism affecting the column in which the collision occurs. Mechanism 3 is a combination of Mechanism 1 and 2, in which the column under collision has a local mechanism while the other columns have a global mechanism. Mechanisms 1, 2, and 3 are in the transverse direction. Mechanism 4 is a local column mechanism in the longitudinal direction of the bridge. Mechanism 2 always governs when $2h < H$, in which h = distance of 5 ft from the ground where the collision load is applied; H = height of column.

In bridges where the true collapse load in the critical mechanism is less than the vehicle collision load, the resistance against such loads can be increased by either providing higher column/connection reinforcement or reducing the column height.

6.2.6. *Pipe thickness*

The diameter and thickness of the corrugated pipe are critical parameters in the pocket connection that provides shear strength in the joint and resists the impact of stress concentrations due to prestressing; these issues are discussed here.

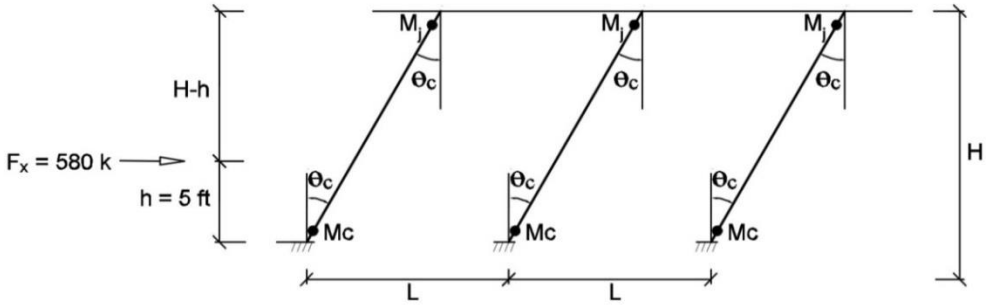

(a) Mechanism 1: Sidesway (transverse direction)

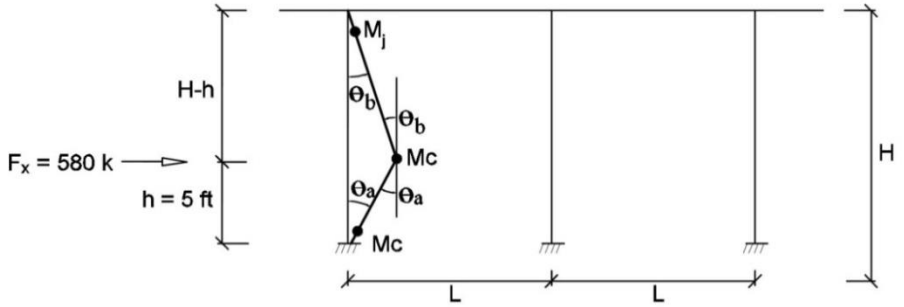

(b) Mechanism 2: Local column (transverse direction)

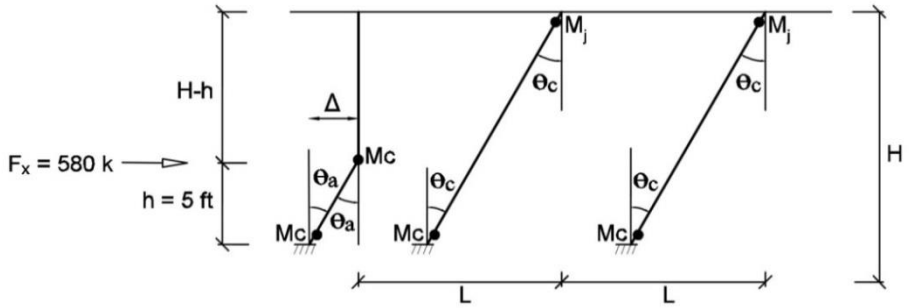

(c)Mechanism 3: Mixed column and sidesway (transverse direction)

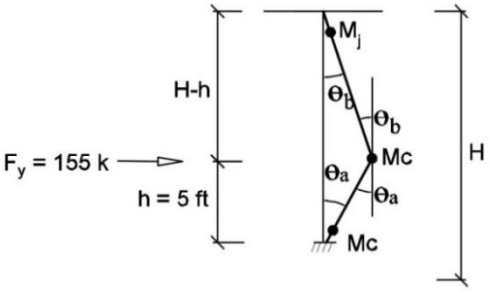

(d) Mechanism 4: Local column (longitudinal direction)

Figure 6.7. Failure mechanism due to vehicle collision load.

Joint shear

The joint should be provided with transverse reinforcement to ensure it is not a weak link in the structure. Minimum shear reinforcement can be provided in the form of stirrups, hoops, spirals, or the corrugated pipe used to form the pocket connection. In the current study on pocket connections, the corrugated pipe is used to satisfy the requirement of transverse reinforcement.

A pipe thickness is determined based on the assumption that it provides equivalent shear strength as the spiral reinforcement continued from the columns:

$$t_{pocket} = \frac{A_b}{s} \tag{6-11}$$

in which t_{pocket} = thickness of the corrugated pipe (inch); A_b = area of the spirals (in^2); and s = spiral spacing (inch).

The reinforcement ratio of the corrugated pipe is determined by:

$$\rho_t = \frac{4\,t_{pocket}}{d_{pocket}} \tag{6-12}$$

in which ρ_t = reinforcement ratio of the corrugated pipe; d_{pocket} = diameter of the pocket (inch).

The shear strength provided by the corrugated pipe is given by:

$$V_s = \frac{1}{2}\frac{\pi}{4}\rho_t\, d_{pocket}{}^2 f_{yp} \tag{6-13}$$

in which f_{yp} = nominal yield stress of the corrugated pipe (ksi).

The shear strength contribution from the concrete is computed as:

$$V_c = 2\sqrt{\frac{f'_{c\_pocket}}{1000}}A_v \tag{6-14}$$

in which f'_{c_pocket} = specified compressive strength of pocket fill (ksi); A_v = shear area = $0.8A_g = 0.8\frac{\pi}{4} D_{col}{}^2$ (in^2); A_g = gross area of the column(in^2); D_{col} = diameter of the column (inch).

The total shear strength V_r is the contribution from the steel and concrete

$$V_r = V_s + V_c \tag{6-15}$$

Prestressing impact on void

In a prestressed bent cap with concentric prestressing, compressive stresses equal to *F/A* are developed. A corrugated pipe precast in the bent cap for a pocket connection will be subjected to the same compressive stresses. As the corrugated pipe will be void at prestress release, there will be discontinuity in the stress flow, leading to local increase in stress intensity in the areas around the pipe. If this stress intensity exceeds the cracking stress, the bent cap will crack in those areas. To avoid such stress concentrations, the corrugated pipe should be provided with the thickness that would cause uniform stress in the bent cap (see Figure 6.8(a)).

From Figure 6.8(b), stress per unit length in the pocket due to prestressing need to be resisted by the corrugated pipe,

$$2 f_{st} t_{pocket} = \sigma_{ps} d_{pocket} \tag{6-16}$$

in which f_{st} = allowable stress of the corrugated pipe = 0.6 x nominal yield stress of the pipe; t_{pocket} = thickness of the corrugated pipe; σ_{ps} = F_i/BD = compressive stress due to initial prestressing, where F_i = initial prestressing force; B = width of bent cap; D = depth of bent cap; and d_{pocket} = diameter of the pocket.

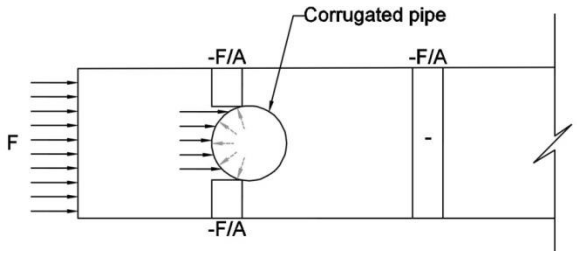

(a) Stresses in pretensioned bent cap

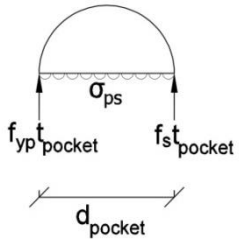

(b) Stresses acting on pipe

Figure 6.8. Corrugated pipe thickness required to minimize stress concentrations.

From Eq. (6-16), the required thickness of the pocket is

$$t_{pocket} = \frac{F_i d_{pocket}}{2 f_{st} BD} \tag{6-17}$$

For simplicity, the pocket diameter d_{pocket} can be considered as a factor λ of the width of the bent cap B,

$$t_{pocket} = \frac{F_i \lambda}{2 f_{st} D} \tag{6-18}$$

Eq. (6-18) recaptures earlier discussion on pocket sizes to be large enough for providing pocket thickness readily available in the market.

7. DESIGN OPTIMIZATION OF BRIDGES

The superior strength and stiffness of pretensioned prestressed concrete bridge bent caps presented in the foregoing work offers the opportunity to economize a design via optimization. Optimization can be achieved with modifications to the prestressing layout and the reconfiguration of the arrangement of columns. A discussion of the results from such modifications on three bridges selected from the bridge inventory is presented. Following an overview in Section 7.1, optimization in design with the use of eccentric prestress is discussed in Section 7.2. Section 7.3 discusses the effects of bent cap geometry on design and performance. In Section7.4, the evaluation of bridges where the bent is reconfigured is described. Section 7.5 presents a summary with limitations of the optimization procedure.

7.1. Overview of bridges considered for optimization

In lieu of optimizing all bridges, only three example bridges are considered herein. Table 7.1 presents an overview of the bridges. Example 1 is a 40 ft roadway width I-girder bridge and Example 2 is a 30 ft roadway width box beam bridge. Both bridges have large service and ultimate stresses that are expected to crack. Therefore additional strands, eccentricity and change in cross-section geometry may improve the expected performance. Example 3 is a 24 ft roadway width I-girder bridge, which is the smallest width in the bridge inventory. The bridge is not expected to crack and has a high overstrength and is thus a candidate for reducing the number of columns.

Table 7.1. Overview of example bridges for optimization.

	Width (ft) W	Girder type	Span length (ft)	Bent cap size (inch) B x H	No. of columns	Column spacing (ft)	Column edge distance (ft)
Example 1	40	Tx-54 I-girder	120	42 x 42	3	16	4
Example 2	30	B40 box beam	60	33 x 36	3	13	4.375
Example 3	24	Tx-54 I-girder	120	42 x 42	3	8	4

Table 7.2 presents bridges with variations to base example structures. These variations include increasing the total number of strands, introducing eccentricity to the prestress, increasing cross-section geometry, and changing the configuration by either removal of a column or increasing the cap overhang length.

Table 7.2. Variations in base example bridges for optimization.

Base Example	Example #	Strand Design		Geometry			Configuration	
		Increase Concentric	Eccentric	Increase H	Increase B	Increase column dia (D)	Remove column	Increase overhang
1	1(a)	✓						
	1(b)		✓					
2	2(a)	✓						
	2(b)		✓					
	2(c)				✓			
	2(d)			✓	✓			
	2(e)			✓	✓	✓		
	2(f)			✓	✓		✓	
	2(g)			✓	✓		✓	✓
	2(h)			✓	✓		✓	✓
3	3(a)						✓	
	3(b)			✓	✓		✓	

7.2. Optimization by change in strand layout

The design of the bridge inventory by the proposed flexural design procedure (concentric prestressing) can be further improved using the design space obtained from a

Magnel diagram. To be consistent with the proposed flexural design procedure, a concrete strength of 6 ksi is used.

Figure 7.1(a) and Figure 7.2(a) show Magnel diagrams with the eccentricity vs. the number of strands for Example 1 and Example 2, respectively. The dash, dash-dot and solid lines represent the load combinations under dead, service and ultimate states, respectively. Four sets of colored lines representing a stress condition are plotted; the red and magenta lines show the limits for tension stress under maximum negative and positive moments respectively, the blue and cyan lines show the limits for compression stress under maximum negative and positive moments respectively. A grey dashed line with each set under maximum positive moments represents the corresponding stress condition under self-weight. The grey shaded area represents the design space conforming to zero tension under dead load and the AASHTO LRFD compression and tension stress limits for the self-weight, dead and service loads. The region of the grey shaded area intercepted by the lines representing ultimate stress indicates the design space that conforms to the stress limits for ultimate loads in addition to self-weight, dead and service loads. Eccentricity is assumed as positive below the neutral axis (N.A) of the bent cap. Figure 7.1(b) and Figure 7.2(b) show the eccentricity achieved from strand layouts for Example 1 and Example 2, respectively.

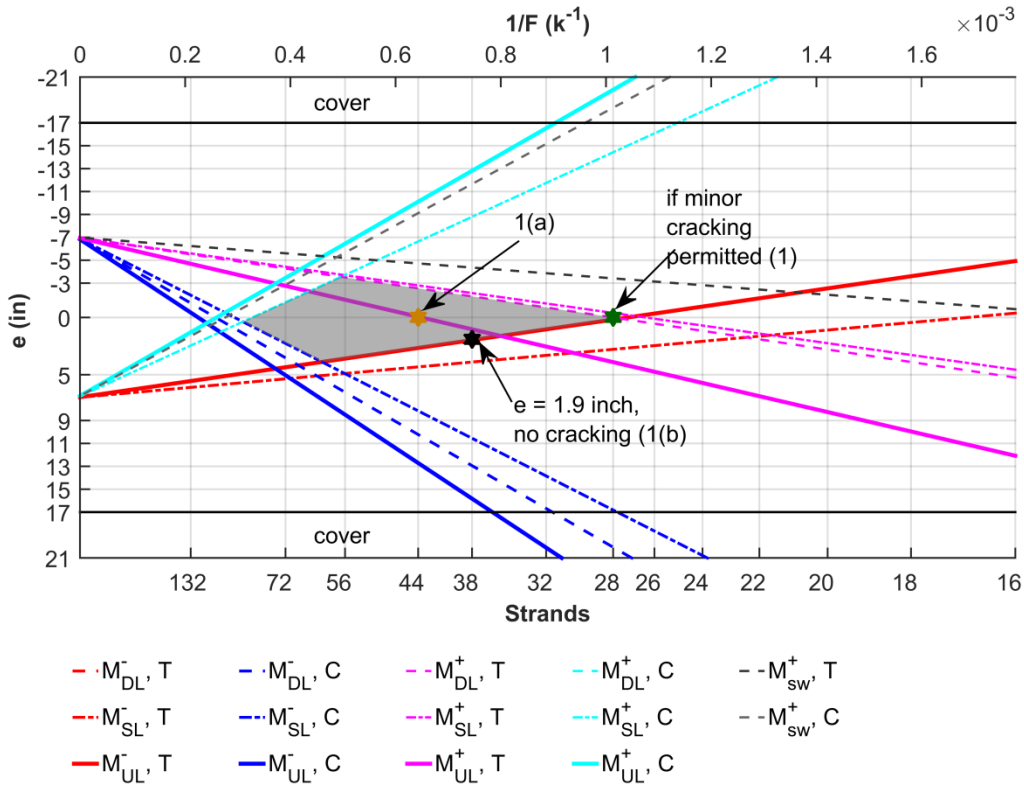

(a) Magnel diagram

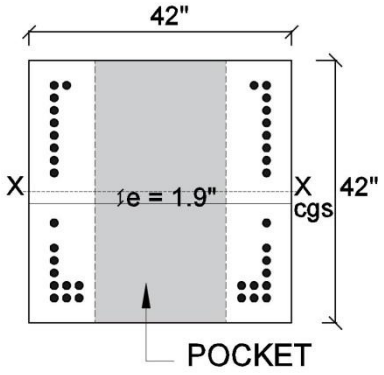

(b) Solution: 38 strands with 1.9 inch eccentricity

Figure 7.1. Optimal design for Example 1.

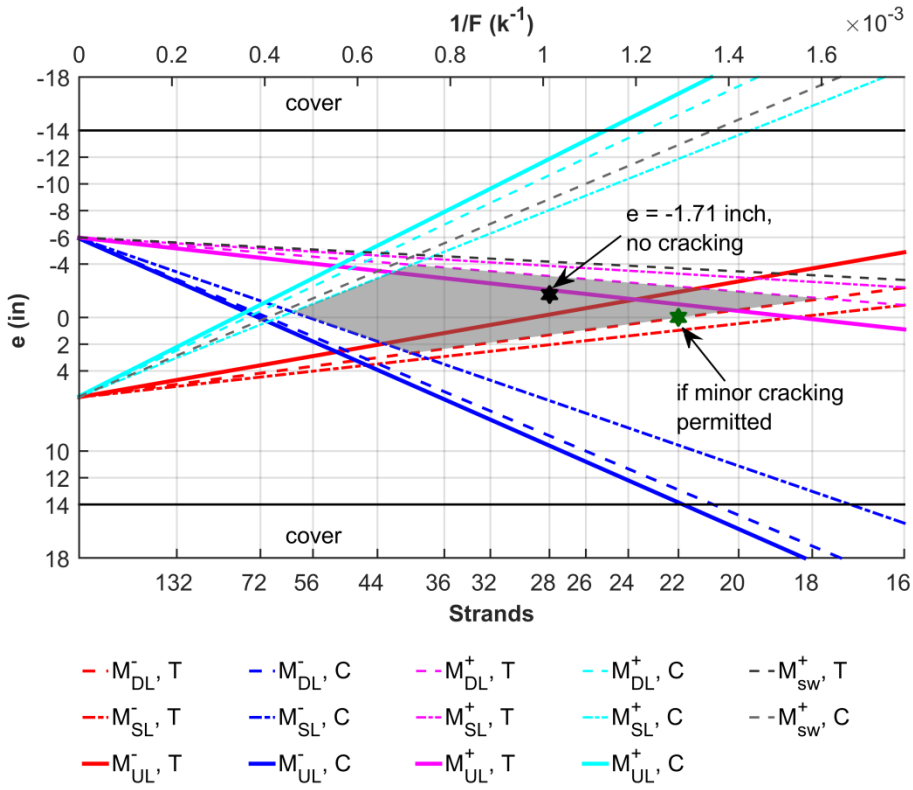

(a) Magnel diagram

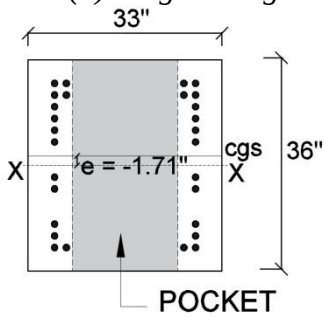

(b) Solution: 28 strands with -1.71 inch eccentricity

Figure 7.2. Optimal design for Example 2.

Table 7.3 presents strand design in Example 1 and Example 2 and variations in the design performed to eliminate cracking at ultimate. The variations include an increase in the number of concentric prestressing strands or use of an eccentric design.

Table 7.3. Summary of results for optimization by change in strand design.

Bridge name	Strand design			Cracking at ultimate?
	Concentric N	Eccentric N	Eccentricity (e)	
Example 1	28		0	Yes
Example 1(a)	44		0	No
Example 1(b)		**38**	**1.9**	**No**
Example 2	22		0	Yes
Example 2(a)	32		0	No
Example 2(b)		**28**	**-1.71**	**No**

For Example 1, the design space in Figure 7.1(a) shows 28 strands are required for concentric prestressing (shown by the solid green marker). The ultimate stress is 0.90 ksi, 53 percent higher than the expected cracking stress. To eliminate cracking at ultimate, two variations in strand design are evaluated. In Example 1(a), 44 strands are considered by concentric design resulting in an ultimate stress of 0.579 ksi. The performance can be improved by introducing an eccentricity of 1.9 inch (below N.A) in Example 1(b), which reduces the number of strands to 38, resulting in an ultimate stress of 0.49 ksi. The solid black marker in Figure 7.1(a) shows the eccentric design in Example 1(b). Figure 7.1(b) shows the strand configuration of the eccentric design. Table 7.4 shows that the positive and negative moment capacities in Example 1(b) are greater than the ultimate moment demands.

Table 7.4. Capacity ratio for Example 1(b).

	Positive	Negative
Moment capacity, M_n (k-ft)	2780	2725
Ultimate moment, M_u (k-ft)	1499	1164
Overstrength (M_n/M_u)	1.85	2.34

For Example 2, the design space in Figure 7.2(a) shows 22 strands are required for concentric prestressing (shown by the solid green marker). The ultimate stress is 0.80 ksi, 35 percent higher than the expected cracking stress. To eliminate cracking at ultimate, two variations in strand design are evaluated, i.e., Example 2(a) and Example 2(b). In Example 2(a), 32 strands are considered by concentric design resulting in an ultimate stress of 0.5 ksi. In Example 2(b), performance is improved by introducing an eccentricity of 1.71 inch (above N.A) which reduces the number of strands to 28, resulting in an ultimate stress of 0.38 ksi. The solid black marker in Figure 7.2(a) shows the eccentric design. Figure 7.2(b) shows the strand configuration of the eccentric design. Table 7.5 shows that the positive and negative moment capacities in Example 2(b) are greater than the ultimate moment demands.

Table 7.5. Capacity ratio for Example 2(b).

	Positive	Negative
Moment capacity, M_n (k-ft)	1672	1710
Ultimate moment, M_u (k-ft)	672.2	859.1
Overstrength (M_n/M_u)	2.49	1.99

It should be noted that from the design space it may seem possible to satisfy the eccentric design with a lower number of strands. However, in practice the choice of eccentricity depends on achieving a feasible strand configuration, resulting in limited options for selecting the number of strands vs. eccentricity.

7.3. Optimization by change in geometry

An alternate attempt to increase serviceability and performance of the bent cap is made by change in geometry. In Example 2, the bent cap in the box beam bridge has a size of 33 inch width and 36 inch depth. An increase in the bent cap geometry is expected to

have the potential for improvement in performance. Table 7.6 presents details of the different iterations in bent cap size that are performed to determine a suitable model for optimization. A reiteration of the details in Example 2 is also presented for reference.

Table 7.6. Example bridges for optimization by change in geometry.

Bridge name	Width (ft) W	Girder type	Span length (ft)	Bent cap size (inch) B x H	No. of columns	Column spacing (ft)	Column edge distance (ft)
Example 2	30	B40 box beam	60	33 x 36	3	13	4.375
Example 2(c)	30	B40 box beam	60	36 x 36	3	13	4.375
Example 2(d)	30	B40 box beam	60	36 x 42	3	13	4.375
Example 2(e)	30	B40 box beam	60	42 x 42	3	13	4.375

Example 2(c), 2(d) and 2(e) are the variations of Example 2 achieved by increasing the bent cap size to a 36 inch square, 36 inch width and 42 inch depth, and a 42 inch square respectively. Table 7.7 summarizes the design results in each bent cap size. In Example 2(c), 22 strands are required for concentric prestressing. The service and ultimate stresses are 0.28 ksi and 0.68 ksi respectively, indicating cracking expected at ultimate. In Example 2(d), 20 strands are required for concentric prestressing. The service and ultimate stresses are 0.22 ksi and 0.52 ksi respectively, indicating no cracking expected at ultimate. In Example 2(e), 20 strands are required for concentric prestressing. The service and ultimate stresses are 0.20 ksi and 0.45 ksi respectively, indicating no cracking is expected at ultimate.

Table 7.7. Summary of results for optimization by change in geometry

Bridge name	Bent cap size (inch) B x H	No. of strands	Service stress (ksi)	Ultimate stress (ksi)	Cracking at ultimate?
Example 2	33 x 36	22	0.36	0.80	Yes
Example 2(c)	36 x 36	22	0.33	0.73	Yes
Example 2(d)	36 x 42	20	0.22	0.52	No
Example 2(e)	42 x 42	20	0.20	0.45	No

In comparison, Example 2 requires 22 strands by concentric prestressing. The service and ultimate stresses are 0.36 ksi and 0.80 ksi respectively, indicating cracking is expected at ultimate. Thus, the increase in size of the bent cap resulted in reduction of tensile stresses and in mitigating cracking expected at ultimate. Example 2(d) and Example 2(e) are preferable options of bent cap size that results in less strands and at the same time are not expected to crack under ultimate loads.

The increase in size of the bent caps necessitates evaluation of its impact on column geometry. In Example 2, 30 inch diameter columns are used. The same column size could be used for Example 2(c) and Example 2(d). A larger column size of 36 inch diameter is preferable in Example 2(e) primarily to maintain the bent cap width 6 inches wider than the column diameter. By design, 10-#9 bars are provided in the 36 inch diameter columns.

7.4. Optimization by change in column configuration

In the bridges with bent caps that have significant reserve capacity, it may be economical to reduce the number of columns. This in turn may require change in overhang length, increase in size, and/or eccentric prestressing. Example 2 and Example 3 are selected as these represent bridges with and without expected cracking respectively; in addition,

both represent two different girder bridges. Several iterations performed in these bridges to determine suitable models for optimization are shown in Table 7.8. To alleviate the high stresses expected from elimination of a column, a concrete strength of 8.5 ksi is used for design.

Table 7.8. Example bridge for optimization by change in column configuration.

Bridge name	Girder type	Bent cap size (inch) B x H	No. of columns	Column spacing (ft)	Column edge distance (ft)
Example 2	B40 box beam	33 x 36	3	13	4.375
Example 2(f)	B40 box beam	42 x 42	2	26	4.375
Example 2(g)	B40 box beam	42 x 42	2	19	7.875
Example 2(h)	B40 box beam	42 x 48	2	19	7.875
Example 3	Tx-54 I-girder	42 x 42	3	8	4
Example 3(a)	Tx-54 I-girder	42 x 42	2	16	4
Example 3(b)	Tx-54 I-girder	42 x 48	2	16	4

Preliminary efforts for optimization were made by eliminating a column in each bent cap. Elimination of the interior column increased the column spacing in the two bridges to 26 ft and 16 ft, resulting in Example 2(f) and Example 3(a) respectively. The optimization in these bridges is discussed in Section 7.4.1 and 7.4.2 respectively.

7.4.1. *Example 2 configuration optimization*

Table 7.4 shows details of Example 2(f) achieved with the removal of a column in Example 2. In addition, the geometry of the bent cap is increased to a 42 inch square to alleviate the high positive stresses expected from elimination of column. Figure 7.3(a)

shows the original bent configuration in Example 2 and Figure 7.3(b) shows the bent configuration in Example 2(f) after elimination of a column. The maximum positive and negative moment demands under dead load are 1892 k-ft and 109 k-ft respectively, indicating a high positive moment in comparison to the negative moment. The design requires 62 strands with an eccentricity of 5.81 inch. The service and ultimate tensile stresses are 0.52 ksi and 1.69 ksi respectively and the minimum concrete strength required is 7.5 ksi. Due to the high positive moment demands, number of strands and tensile stresses, Example 2(f) is not a preferred bridge optimization model.

To reduce the positive moment, columns were moved in, creating a larger overhang and smaller column spacing. The distance by which the columns were moved was based on the attempt to get similar positive and negative moments. Consequently, a move of 3.5 ft was considered on both sides, resulting in Example 2(g) with column spacing of 19 ft. Figure 7.3(c) shows the bent configuration.

In Example 2(g), the maximum positive and negative moment demands under dead load are 636 k-ft and 477 k-ft respectively. Figure 7.4(a) shows the design space; 32 strands are required for concentric prestressing (shown by solid green marker). The ultimate stress is 1.06 ksi, 75 percent higher than the expected cracking stress. By introducing an eccentricity of 2.4 inch (below N.A.) for 40 strands, the ultimate stress is 0.63 ksi indicating no cracking under ultimate loads. The solid black marker in Figure 7.4(a) shows the eccentric design. Figure 7.4(b) shows the strand configuration of the eccentric design. Table 7.9 shows that the positive and negative moment capacities in Example 2(g) are greater than the ultimate moment demands.

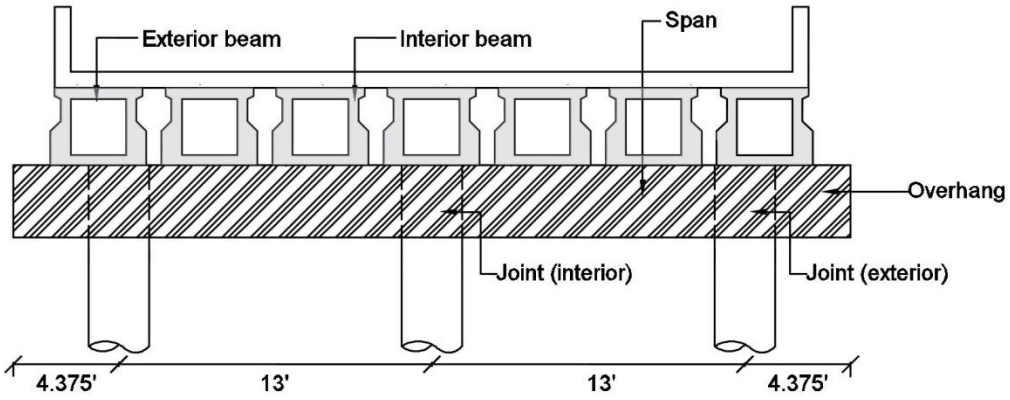

(a) Example 2 with three columns

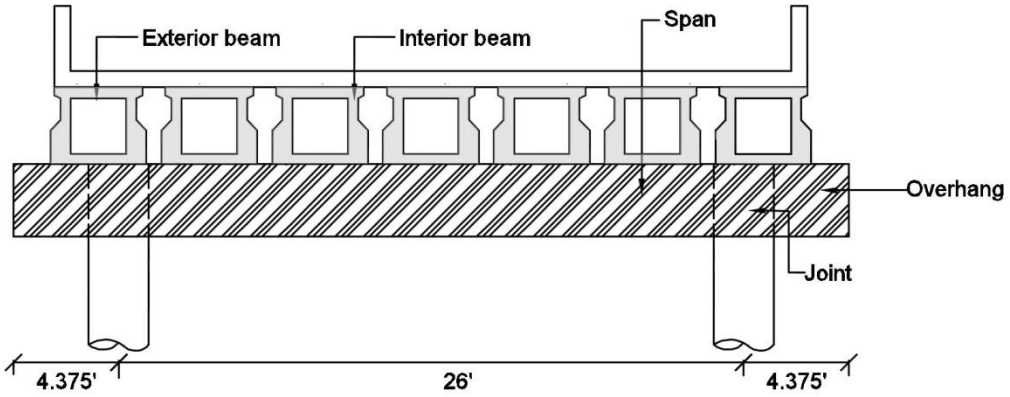

(b) Example 2(f) with two columns

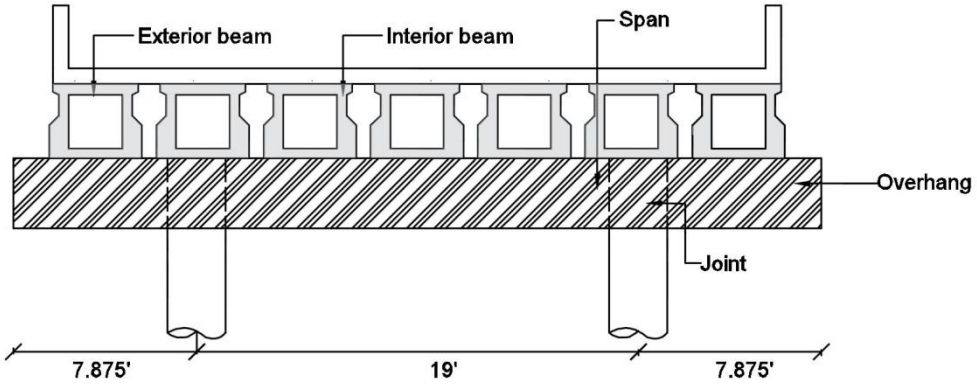

(c) Example 2(g) with two columns

Figure 7.3. Bent configurations in Example 2 before and after a column elimination.

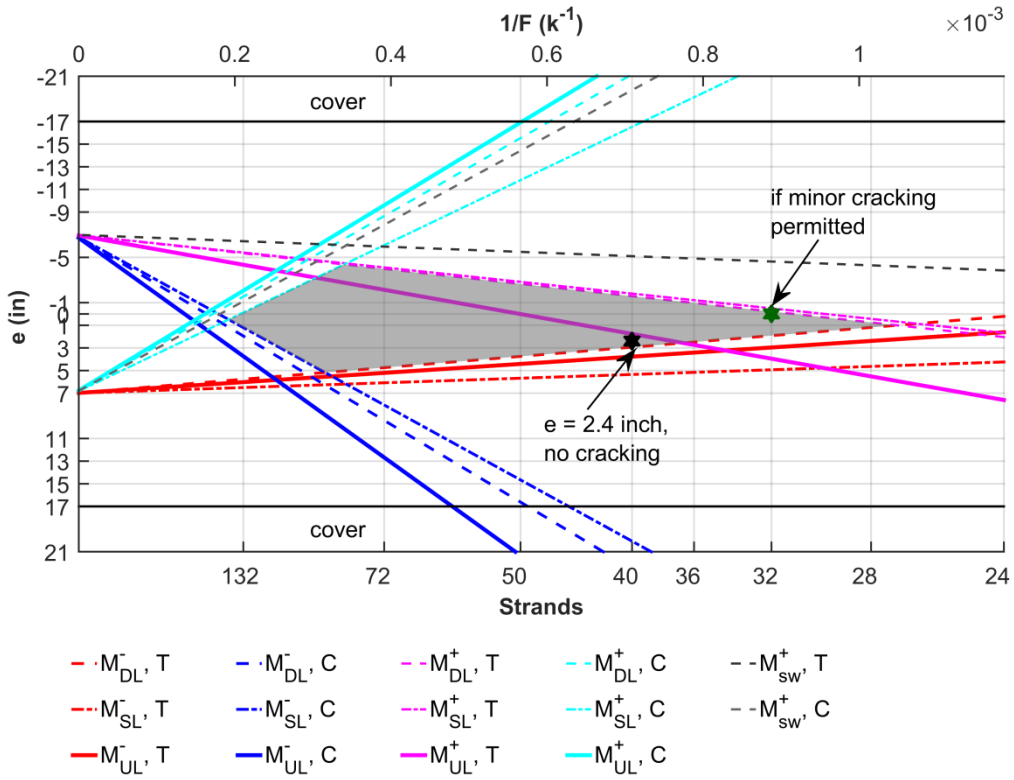

(a) Magnel diagram

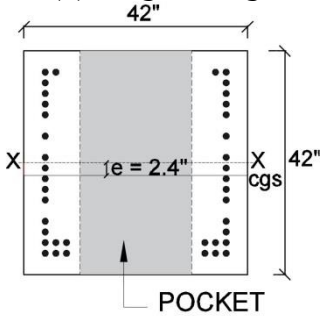

(b) Solution: 40 strands with 2.4 inch eccentricity

Figure 7.4. Optimal design for Example 2(g).

Table 7.9. Capacity ratio for Example 2(g).

	Positive	Negative
Moment capacity, M_n (k-ft)	3128	3051
Ultimate moment, M_u (k-ft)	1746	1099
Overstrength (M_n/M_u)	1.79	2.78

If the size of the bent cap is increased, further increase in performance is expected. Table 7.2 shows Example 2(h) achieved from Example 2(g) by increasing the bent cap height from 42 inch to 48 inch. The maximum positive and negative moment demands under dead load are 640 k-ft and 485 k-ft. Figure 7.5(a) shows the design space; 28 strands are required for concentric prestressing (shown by solid green marker). The ultimate stress is 0.81 ksi, 16 percent higher than the expected cracking stress. By introducing an eccentricity of 1.6 inch (below N.A.) for 30 strands (shown by solid black marker), the ultimate stress is 0.68 ksi indicating no cracking under ultimate loads. Figure 7.5(b) shows the strand configuration of the eccentric design. Table 7.10 shows that the positive and negative moment capacities in Example 2(h) are greater than the ultimate moment demands.

Table 7.11 gives a summary of this section showing the number of strands and if cracking is expected under ultimate loads for Examples 2, 2(f), 2(g) and 2(h). No cracking is expected under ultimate loads in the eccentric designs.

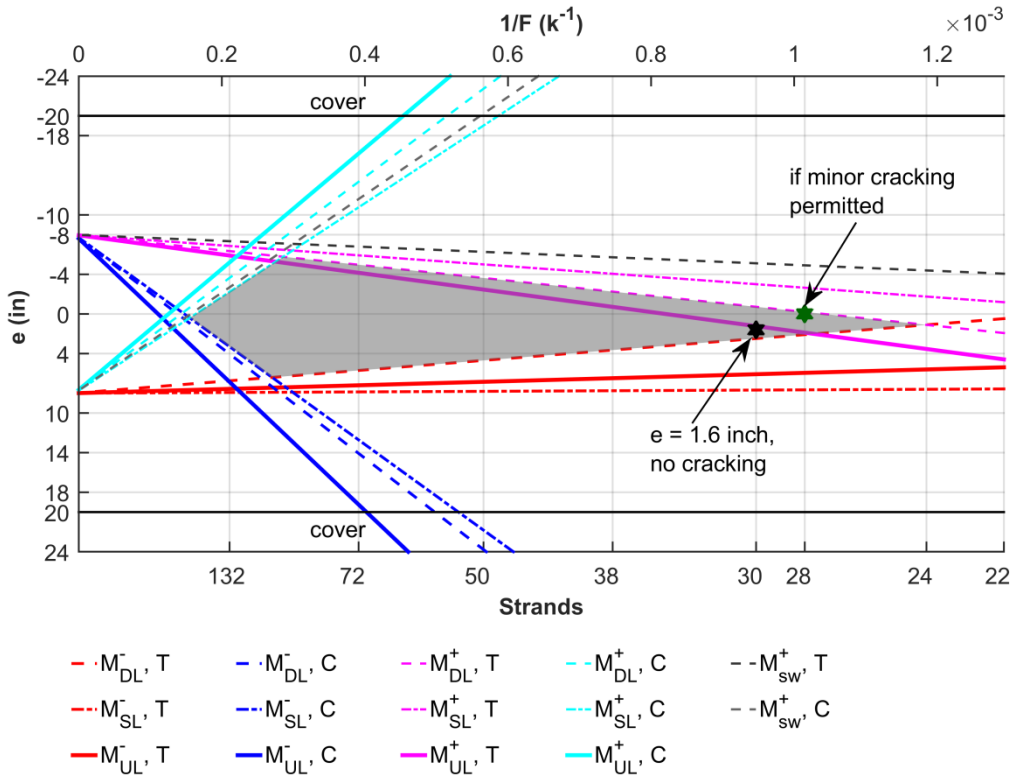

(a) Magnel diagram

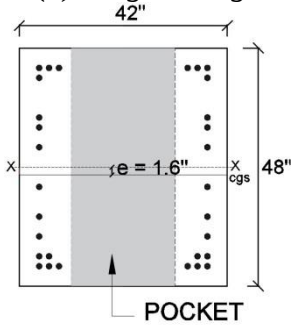

(b) Solution: 30 strands with 1.6 inch eccentricity

Figure 7.5. Optimal solution for Example 2(h).

Table 7.10. Capacity ratio for Example 2(h).

	Positive	Negative
Moment capacity, M_n (k-ft)	3113	2673
Ultimate moment, M_u (k-ft)	1751	1109
Overstrength (M_n/M_u)	1.78	2.41

Table 7.11. Summary of results for optimization in Example 2 by change in column configuration.

Bridge name	Strand design			Cracking at ultimate?
	Concentric N	Eccentric N	Eccentricity (e)	
Example 2	22		0	Yes
Example 2(f)	62		0	Yes
Example 2(g)	32		0	Yes
		40	**2.4**	**No**
Example 2(h)	28		0	Yes
		30	**1.6**	**No**

The base Example 2 has 3 columns of 30 inch diameter each designed with 8-#9 bars. The bridges Example 2(f), 2(g) and 2(h) optimized with elimination of a column and increased bent cap width of 42 inch are evaluated for column design. The two columns in each of these bridges are provided with a size of 36 inch diameter and 10-#9 bars.

The maximum deflection in the span region of the optimized bridges is calculated. For Example 2(g), a maximum deflection of 0.032 inch is determined under vehicular live loads, less than the *span/800* limit (0.3 inches) specified in AASHTO.

Comparison to RC bent cap

While optimization in bridges with pretensioned bent caps could be achieved with elimination of column, a satisfactory performance from such optimization may not be expected in bridges with reinforced concrete bent caps. This section compares the performance of the pretensioned bent cap in Example 2(h) with its companion reinforced concrete bent cap. The RC bent cap is designed with 6-#11 bars at the top and 9-#11 bars at the bottom. Skin reinforcement is provided as 5-#5 bars on each side face of the bent

cap. The eccentric design for the pretensioned bent cap is considered i.e., 30 strands at 1.6 inch eccentricity. Table 7.12 shows a comparison of the overstrength of the two bent caps.

Table 7.12. Comparison of overstrength between RC and PSC bent cap for Example 2(h).

	RC		PSC	
	Positive	Negative	Positive	Negative
Moment capacity, M_n (k-ft)	2644	1787	3113	2673
Ultimate moment, M_u (k-ft)	1751	1109	1751	1109
Overstrength (*Mn/Mu)*	1.51	1.61	1.78	2.41

The cracking moment (M_{cr}) for the reinforced concrete bent cap with 3.6 ksi concrete compressive strength is 612 k-ft. For the prestressed concrete bent cap, M_{cr} is 1783 k-ft.

A comparison of the expected regions of cracking in the pretensioned and RC bent caps is made. For Example 2(h), Figure 7.6(a) shows the regions of cracking of the bent cap at dead and service. The reinforced concrete bent cap cracks at the region of maximum positive moment (at girder in span) under dead load. At service, the cracking spreads to the regions of maximum negative moments (above the columns); the prestressed concrete bent cap is uncracked. Figure 7.6(b) shows the regions of cracking of the bent cap at ultimate. The cracking in the reinforced concrete caps spreads further; the prestressed bent cap does not crack even under ultimate load.

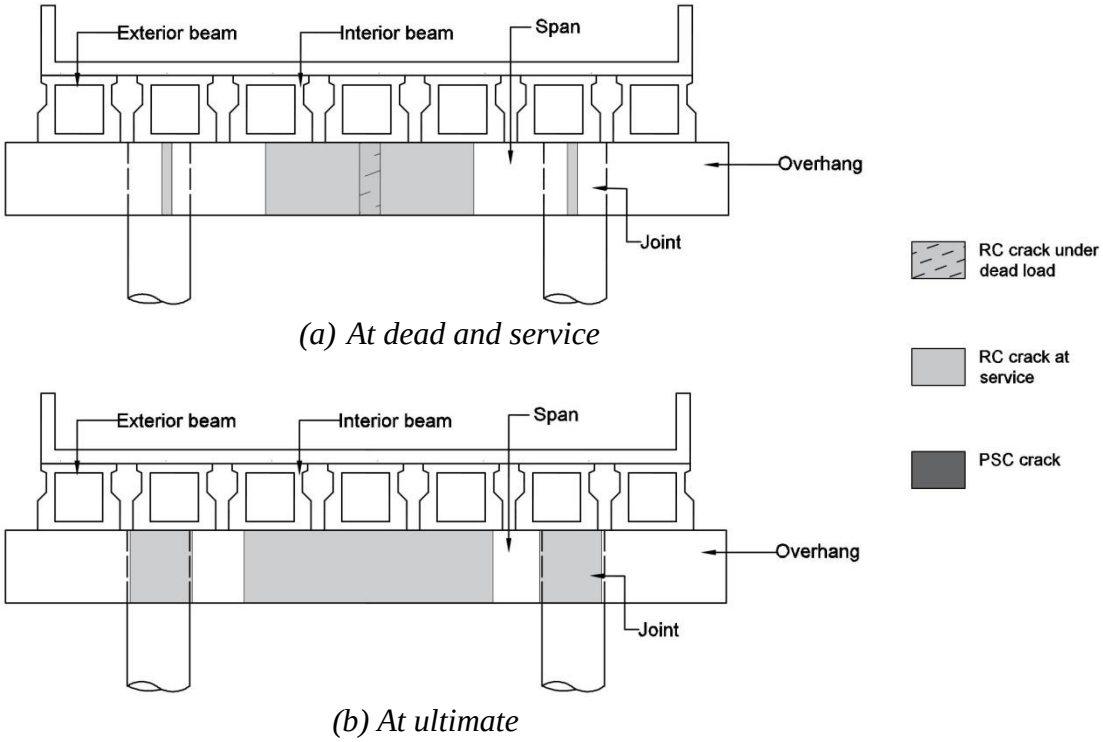

(a) At dead and service

(b) At ultimate

Figure 7.6. Cracking in bent cap for Example 2(h).

7.4.2. *Example 3 configuration optimization*

Table 7.4 shows details of Example 3(a) achieved with the removal of a column in Example 3. Figure 7.7(a) and Figure 7.7(b) shows the bent configurations in Example 3 and Example 3(a) respectively. The maximum positive and negative moment demands under dead load are 677 k-ft and 489 k-ft, respectively. The design space in Figure 7.8(a) shows 34 strands are required for concentric prestressing (shown by solid green marker). The ultimate stress is 0.90 ksi, 29 percent higher than the expected cracking stress. By introducing an eccentricity of 1.9 inch (below N.A) for 38 strands, the ultimate stress is 0.62 ksi indicating no cracking is expected under ultimate loads. The solid black marker in Figure 7.8(a) shows the eccentric design. The strand configuration of the eccentric

design is shown in Figure 7.8(b). Table 7.13 shows that the positive and negative moment capacities in Example 3(a) are greater than the ultimate moment demands.

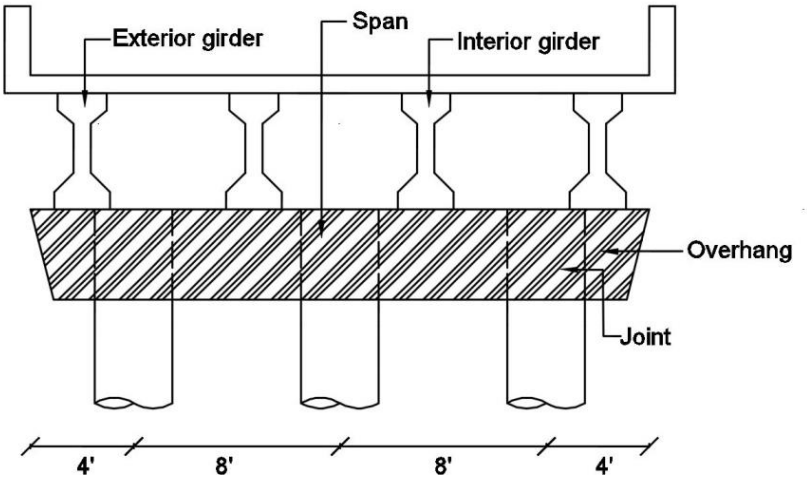

(a) Example 3 with three columns

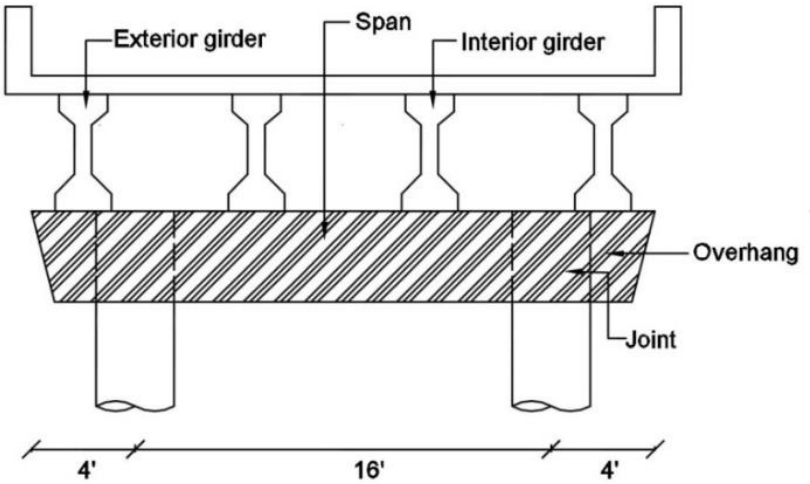

(b) Example 3(a) with two columns

Figure 7.7. Bent configurations in Example 3 before and after a column elimination.

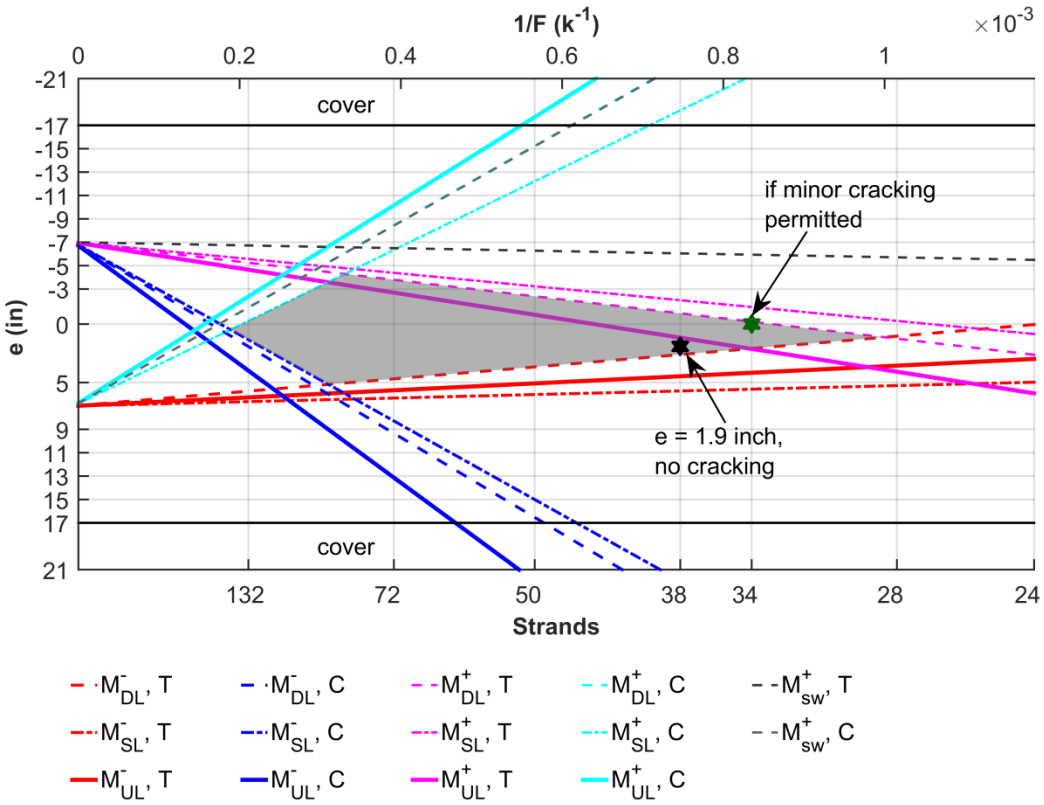

(a) Magnel diagram

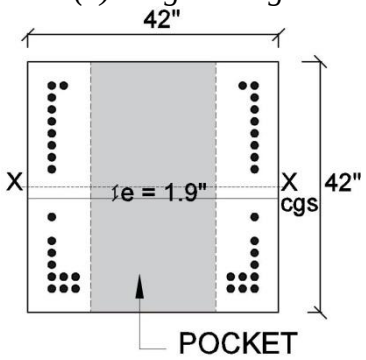

(b) Solution: 38 strands with 1.9 inch eccentricity

Figure 7.8. Optimal solution for Example 3(a).

Table 7.13. Capacity ratio for Example 3(a).

	Positive	Negative
Moment capacity, M_n (k-ft)	2987	2932
Ultimate moment, M_u (k-ft)	1628	1003
Overstrength (M_n/M_u)	1.83	2.92

The depth of the bent cap in Example 3(a) is increased from 42 inch to 48 inch, resulting in Example 3(b). The maximum positive and negative moment demands under dead load are 683 k-ft and 492 k-ft respectively. By concentric design, 30 strands need to be provided. The ultimate stress is 0.693 ksi, indicating no expected cracking. The ultimate strength is greater than the ultimate moment demands.

Table 7.14 gives a summary of this section showing the number of strands and if cracking is expected under ultimate loads for Examples 3(a) and 3(b). No cracking is expected under ultimate loads in the eccentric design for Example 3(a) and for Example 3(b).

Table 7.14. Summary of results for optimization in Example 2 by change in column configuration.

Bridge name	Strand design			Cracking at ultimate?
	Concentric N	Eccentric N	Eccentricity (e)	
Example 3(a)	34		0	Yes
		38	**1.9**	**No**
Example 3(b)	**30**		**0**	**No**

The base Example 3 has 3 columns of 36 inch diameter each designed with 10-#9 bars. The bridges Example 3(a) and Example 3(b) optimized with elimination of a column are evaluated for column design. By design, no change in the size and reinforcement of the 36 inch diameter columns are required.

The maximum deflection in the span region of the optimized bridges is calculated. For Example 3(a), a maximum deflection of 0.02 inch is determined under vehicular live loads, less than the *span/800* limit (0.24 inches) specified in AASHTO.

Comparison to RC bent cap

This section compares the performance of the pretensioned bent cap in Example 3(a) with its companion reinforced concrete bent cap. The RC bent cap for Example 3(a) is designed with 6-#11 bars at the top and 10-#11 bars at the bottom. Skin reinforcement is provided as 5-#5 bars on each side face of the bent cap. The eccentric design for the pretensioned bent cap is considered i.e., 38 strands at 1.9 inch eccentricity. Table 7.15 shows a comparison of the overstrength of the two bent caps.

Table 7.15. Comparison of overstrength between RC and PSC bent cap for Example 3(a).

	RC		PSC	
	Positive	Negative	Positive	Negative
Moment capacity, M_n (k-ft)	1765	1287	2987	2932
Ultimate moment, M_u (k-ft)	1628	1003	1628	1003
Overstrength (M_n/M_u)	1.08	1.28	1.83	2.92

The cracking moment (M_{cr}) for the reinforced concrete bent cap with 3.6 ksi concrete compressive strength is 469 k-ft. For the prestressed concrete bent cap, M_{cr} is 1711 k-ft.

A comparison of the expected regions of cracking in the pretensioned and RC bent caps is made. The regions of cracking under dead and service, and at ultimate are shown in Figure 7.9(a) and (b) respectively. The RC bent cap starts to crack under dead load at the regions of maximum positive moment (at girder in span). At service and ultimate, the cracking spreads further to the regions of maximum negative moment (above the columns). The prestressed concrete bent cap does not crack even at ultimate.

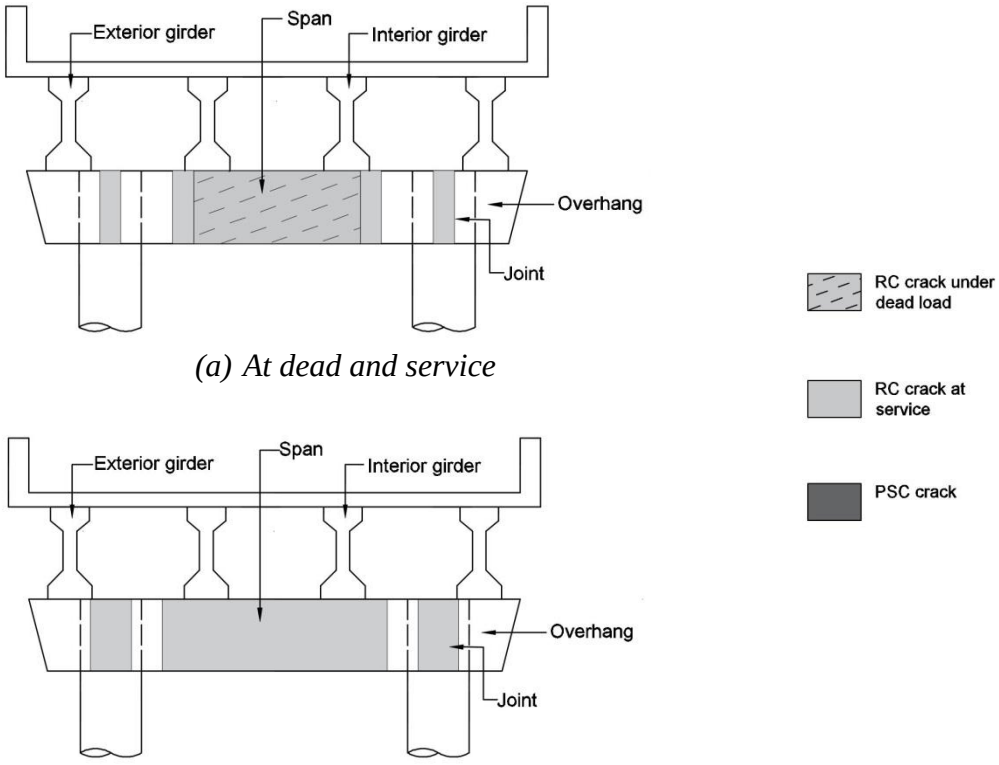

(a) At dead and service

(b) At ultimate

Figure 7.9 Cracking in bent cap for Example 3(a).

7.5. Findings

Efforts have been made to introduce optimization and improve the flexural design performance of pretensioned bent caps. Three example bridges were selected from the bridge inventory for demonstration of the optimization procedure. Optimization has been achieved with change in design eccentricity, cross-section geometry and bent configuration. Increase in the number of strands in concentric or eccentric design of pretensioned bent caps helps in mitigating expected cracking at ultimate. Increase in cross-section geometry is favorable if improvement in overall design and performance is desired. Economic benefits can be achieved with optimization by elimination of

columns. Consequently, the high positive moments can be reduced by moving the columns thereby increasing overhang and reducing column spacing.

Design and analysis shows that even when columns are entirely removed an economical solution remains achievable. A comparison of performance between RC and pretensioned bent caps in optimized bridges showed that the RC bent caps inevitably cracked under dead, service and ultimate loads while the pretensioned bent caps are not expected to crack even under ultimate loads. Column design in the optimized bridge is necessary and may also require slight increase in column diameter for a corresponding increase in bent cap dimensions.

8. SUMMARY, CONCLUSIONS AND RECOMMENDATIONS

8.1. Summary

This research has focused on the development of a flexural design procedure for pretensioned bent caps. The proposed design procedure was based on the objective to achieve zero tension under dead loads. The procedure is expected to allow closure of cracks under ultimate loads following removal of full live loads. The design procedure requires a minimum reinforcement to ensure a ductile failure. In addition, the tensile and compressive service stresses due to applied loads are limited to the allowable service stresses specified in AASHTO LRFD provisions.

For assessment of the design procedure, a wide variety of standard TxDOT bridges, with I-girders, box beams, X-beams were considered. Two nonstandard bridges not conforming to TxDOT limits for girder/column spacing were also evaluated. For each bridge width, three span lengths corresponding to a minimum, intermediate and maximum were respectively considered. The demands in the bent cap of these bridges for dead and vehicular live loads were determined. The proposed flexural design procedure was then applied to the bridge inventory and pretensioned bent caps were designed accordingly. The effect of relocation of the typical top/bottom configuration to a side configuration was assessed. Voided sections, introduced in the interior of pretensioned bent caps for weight reduction, were evaluated using the proposed design procedure.

In order to resist the tensile stresses that occur during transfer, the previous research recommendations on the detailing required for prestressed member ends was

discussed. Based on these previous recommendations, new detailing recommendations have been developed pertinent to prestressed concrete bent caps for standard TxDOT bridges.

A pocket connection has been developed and recommended as an alternative to the grouted vertical duct connection currently used as standard precast connection by TxDOT. The geometry, configuration of dowel bars and demands in this connection were determined. The flexural and shear strength of the connection was calculated and determined to be greater than the demands. In addition, the resistance of column and the associated pocket connection against vehicle collision loads was assessed.

Efforts have been made to optimize bridges with change in strand design, by permitting solutions with eccentric prestress, increase in bent cap cross-section geometry and reduction of number of columns. Eccentric prestressed designs were explored using a design space obtained via the use of Magnel diagrams. The effect of increase in bent cap size on design and performance was determined. To understand the effects of reduced number of columns, two example bridges with pretensioned bent caps were evaluated; one with high over strength suitable for optimization and the other with high tension stresses under service and ultimate loads. A comparison of performance was made in the optimized bridges between RC and PSC bent caps.

8.2. Conclusion

Based on the research conducted herein, the following key findings and conclusions are given:

1. A flexural design procedure is proposed with the objective of achieving zero tension under dead load. This allows expected closure of cracks following removal of full live loads.
2. Application of the proposed design procedure to the bridge inventory confirmed success in achieving the design objectives. In most bridges, the bent caps are not expected to crack even under ultimate loads. For the bridges with large column spacing and longer span lengths, the bent caps are expected to crack at ultimate in the span region under maximum positive moment. Cracking is not expected under ultimate loads in the larger cross section bent cap of skewed bridges, indicating the potential of a larger bent cap size in controlling cracking.
3. In only a few of the bridges examined, there was the potential for cracking at ultimate load demand where the ultimate stress in the bent cap for box beam bridges exceeds the $0.38\sqrt{f'_c}$ stress limit. For such bridges there remains the possibility of optimizing the tendon layout by providing a few additional tendons with overall eccentricity to mitigate potential tensile cracking.
4. The adequate performance of the nonstandard bridges assured that the proposed flexural design procedure could be implemented in all bridges. However, for some of these bridges with large service stresses, additional prestressing is necessary if the minimum concrete strength is limited to 8.5 ksi. This is a variation from the proposed design procedure. For these bridges, a design procedure limiting the service stresses may be more appropriate.

5. The side configuration has limited effect on the strength of a pretensioned bent cap, with a decrease less than 5 percent from the top/bottom configuration.
6. In comparison to solid sections, a voided pretensioned bent cap may require a lower number of strands. However, higher tensile stresses may occur and higher concrete strength may be necessary. For voided sections the overstrength factor may be lower than the solid section counterpart.
7. Pocket connections are recommended as a favorable connection option. Pockets permit the use of concrete instead of grout. Pocket connections also facilitate considerable accidental misalignment of column during construction. Medium diameter pockets with reinforcing bars concentrated about the center has the potential to provide adequate strength for flexural and shear demands that include the effects of vehicle collision loads.
8. Economic benefits can be achieved with the elimination of columns in each bent cap. The increase in positive moment demands can be controlled by reducing the column spacing, and/or providing an eccentric rather than concentric prestressing.

8.3. Recommendations for future research

The following recommendations for future research are given:

1. Experimental verification: The flexural design procedure proposed herein should be verified by experimental testing to demonstrate and validate the successful performance of pretensioned bent caps.

2. Seismic loading: For the implementation of pretensioned bent caps in seismic regions, analysis of seismic loading and additional design and detailing requirements should be considered.
3. Effects of shear: The effect of shear in the design of pretensioned bent caps and possible adverse effects in the optimized bridges should be determined.

REFERENCES

AASHTO LRFD bridge design specifications, U.S. customary units. 7th edition (2014). Washington, DC: American Association of State Highway and Transportation Officials, 2014; 7th edition.

ACI Committee 318. (2014). *Building code requirements for structural concrete (ACI 318-14) and commentary (ACI 318R-14)*, Farmington Hills, MI.

Avendano, A., Hovell, C., Moore, A., Dunkman, D., Nakamura, E., Bayrak, O., Jirsa, J. (2013). "Pretensioned Box Beams: Prestress Transfer and Shear Behavior," Rep.No. FHWA/TX-13/0-5831-3, Center for Transportation Research, Research Project 0-5831, University of Texas, Austin.

Billington, S. L., Barnes, R. W., and Breen, J. E. (1999). "A Precast Substructure Design for Standard Bridge Systems," Report No. FHWA/TX-98/1410-2F, Center for Transportation Research, the University of Texas, Austin.

Bracci, J.M., Keating, P.B., and Hueste, M.B.D. (2001). "Cracking in RC Bent Caps," Rep. No. FHWA/TX-01/1851, Texas Transportation Institute, Texas A & M University, College Station.

Brenes, F. J., Wood, S. L., and Kreger, M. E. (2006). "Anchorage Requirements for Grouted Vertical-Duct Connectors in Precast Bent Cap Systems," Report No. FHWA/TX-06/0-4176-1, Center for Transportation Research, the University of Texas, Austin.

CAP18 Version 6.2.2. [Computer Software]. Texas Department of Transportation.

Cheok, G. S.; Stone, W. C.; and Kunnath, S. K. (1998). "Seismic Response of Precast Concrete Frames with Hybrid Connections," *ACI Structural Journal*, 95(5), 527-538.

Collins, M. P., & Mitchell, D. (1991). Prestressed concrete structures. Englewood Cliffs, NJ: Prentice Hall.

Culmo, M. P. (2009). "Connection Details for Prefabricated Bridge Elements and Systems," Report FHWA-IF-09-010, Federal Highway Administration.

Dunkman, D.A. (2009). "Bursting and Spalling in Pretensioned U-beams," M.S. Thesis, University of Texas, Austin.

Dutta, A., and Mander, J. B. (2001). "Energy Based Methodology for Ductile Design of Concrete Columns". *Journal of Structural Engineering*, 127(12), 1374.

Dutta, A., Mander, J.B., Eeri, M., and Kokorina, T. (1999). "Retrofit for Control and Repairability of Damage". *Earthquake Spectra*, V. 15(4), pp. 657-679.

Ehsani, M. R., and Blewitt, J. R. (1986). "Design Curves for Tendon Profile in Prestressed Concrete Beams," *PCI Journal*, 115.

Emulative Precast Bent Cap Connections for Seismic Regions: Component Tests-Cap Pocket Full Ductility Specimen (Unit 3). Sacramento, CA: California State University, 2009. p. 126, ECSCSUS- 2009-03.

Ferguson, P.M. (1964). "Design Criteria for Overhanging Ends of Bent Caps – Bond and Shear," Research Report 3-5-63-52. Center for Highway Research, University of Texas, Austin.

Fonseca, F., and Rowe, M.D. (2003). "Flexural Performance of Deteriorated Reinforced Concrete Cantilevered Bent Caps – Part 1," Technical Report UT-03.33, Utah Department of Transportation.

Frantz, G.C., and Breen, J.E. (1978). "Control of Cracking on the Side faces of Large Reinforced Concrete Beams," Research Report 198-1F,. Center for Highway Research, University of Texas, Austin.

Freeby, G., Hyzak, M., Medlock, R., Ozuna, K., Vogel, J., & Wolf, L. (2003). "Design and Construction of Precast Bent Caps at TxDOT," Paper presented at the *Proceedings of the Transportation Research Board Annual Meeting.*

Garber, D., Gallardo, J., Deschenes, D., Dunkman, D., Bayrak, O. (2013). "Effect of New Prestress Loss Estimates on Pretensioned Concrete Bridge Girder Design," Center for Transportation Research, Research Project 0-6374-2, University of Texas, Austin.

Haber, Z. B., Saiidi, M. S., & Sanders, D. H. (2014). "Seismic Performance of Precast Columns with Mechanically Spliced Column-Footing Connections" *ACI Structural Journal,* 111 (3), pp. 639-650.

Hewes, J. T. (2013). "Analysis of the state of the art of precast concrete bridge substructure systems," Report No. FHWA-AZ-13-687, AZTrans: The Arizona Laboratory for Applied Transportation Research, Northern Arizona University.

Hieber, D. G., Wacker, J. M., Eberhard, M. O., & Stanton, J. F. (2005). "State-of-the-Art Report on Precast Concrete Systems for Rapid Construction of Bridges," Washington State Transportation Center, Washington State Department of Transportation, University of Washington, Seattle, Washington.

Kapur, J., Yen, W.P., Dekelbab, W., Bardow, A., Keever, M., Sletten, J., Tobias, D., and Saiidi, M.S. (2012). "Best Practices Regarding Performance of ABC Connections in Bridges Subjected to Multihazard and Extreme Events," *NCHRP Project 20-68A Scan 11-02*, Arora and Associates P.C., American Association of State Highway and Transportation Officials, Lawrenceville, New Jersey.

Khaleghi, B., Schultz, E., Seguirant, S., Marsh, L., Haraldsson, O., Eberhard, M., & Stanton, J. (2012). "Accelerated Bridge Construction in Washington State: From Research to Practice," *PCI Journal*, 57(4), 34-49.

Krishnamurthy, N. (1983). "Magnel Diagrams for Prestressed Concrete Beams." *Journal of Structural Engineering*, 109(12), 2761-2769.

Li, L., Mander, J.B., and Dhakal, R.P., (2008). "Bidirectional Cyclic Loading Experiment on a 3D Beam-Column Joint Designed for Damage Avoidance," *ASCE Library, Journal of Structural Engineering*. V. 134 (11), pp. 1733-1742.

Mander, J. B., Ligozio, C., & Kim, J. (1996). "Seismic Performance of a Model Reinforced Concrete Bridge Pier Before and After Retrofit," *Technical Report* NCEER-96-0009, National Center for Earthquake Engineering Research, University at Buffalo SUNY, Federal Highway Administration, Buffalo, New York.

Mander, J.B., (2004). "Beyond Ductility: The Quest Goes On," Department of Civil Engineering, University of Canterbury, Christchurch, *Bulletin of the New Zealand Society for Earthquake Engineering*, V. 37 (1), pp. 35-44.

Mander, J.B., and Cheng, C-T. (1997). "Seismic Resistance of Bridge Piers Based on Damage Avoidance Design," *Technical Report* NCEER-97-0014, National Center for Earthquake Engineering Research, University at Buffalo SUNY, Federal Highway Administration, Buffalo, New York.

Mander, J.B., and Cheng, C-T. (1999). "Replaceable Hinge Detailing for Bridge Columns", *American Concrete Institute, Special Publication SP* – 187, 185-204, Seismic Response of Concrete Bridges.

Marsh, M.L., Wernli, M., Garrett, B.E., Stanton, J.F., Eberhard, M.O., and Weinert, M.D. (2011). "Application of Accelerated Bridge Construction Connections in Moderate-to-High Seismic Regions," *Report 698*, National Cooperative Highway Research Program, Transportation Research Board, Washington, D.C.

Matlock, H., Ingram, W.B. (1996). "A computer program to analyze bending of bent caps," *Summary Report* 56-2 (S). Center for Highway Research, Project 3-5-63-56, University of Texas, Austin.

Matsumoto, E. E. Emulative Precast Bent Cap Connections for Seismic Regions: Component Test Report-Cap Pocket Limited Ductility Specimen (Unit 4). Sacramento, CA: California State University, Sacramento, 2009. p. 149.

Matsumoto, E. E., Waggoner, M. C., Kreger, M. E., Vogel, J., and Wolf, L. (2008). "Development of a Precast Bent Cap System," *PCI Journal*, 53(3), 74-99.

Matsumoto, E. E., Waggoner, M. C., Sumen, G., Kreger, M. E., Wood, S. L., and Breen, J. E. (2001). "Development of a Precast Bent Cap System," Report No. FHWA/TX-0-1748-2, Center for Transportation Research, University of Texas, Austin.

Miller, C., Holt, J., and McCammon, V. (2014). "Precast, Pretensioned, Bent Caps," Bridge Division, Texas Department of Transportation.

Naaman, A. E. (1982). Prestressed concrete analysis and design: Fundamentals (3rd ed.). New York: McGraw-Hill.

O'Callaghan, M. R., & Bayrak, O. (2007). "Tensile stresses in the End Regions of Pretensioned I-beams at Release," *Technical report*: IAC-88-5DD1A003-1, University of Texas, Austin.

Olivia, B. (2014). "Precast Pier Cap and Column Details" Structures Development Section, State of Wisconsin Department of Transportation.

Pang, J. B. K., Steuck, K. P., Cohagen, L., Stanton, J. F., and Eberhard M. O. (2008). "Rapidly Constructible Large-Bar Precast Bridge-Bent Seismic Connection." Report No. WA-RD 684.2, Washington State Transportation Center, Washington State Transportation Commission, University of Washington, Seattle, Washington

Pang, J., B. K., Eberhard, M. O., and Stanton, J. F. (2009). “Large-Bar Connection for Precast Bridge Bents in Seismic Regions.” *Journal of Bridge Engineering*, V. 15 (3), pp. 231–239.

Park, R. (1995). “A Perspective on the Seismic Design of Precast Concrete Structures in New Zealand,” University of Canterbury Christchurch, New Zealand, *PCI Journal*, 40 (3), 40-60.

Restrepo, J. I., Tobolski, M. J., and Matsumoto, E. E. (2011). “Development of a Precast Bent Cap System for Seismic Regions,” NCHRP Report 681, Transportation Research Board, Washington, D.C.

Restrepo, J.I., Tobolski, M.J., and Matsumoto, E.E. (2011). “Development of a Precast Bent Cap System for Seismic Regions”, Attachment DE3: SDC A Design Example- Cap Pocket Connection, NCHRP Report 681.

SAP2000 integrated structural analysis & design software (Version 17.1.0) [Computer software]

Sivakumar, B. (2014). Innovative Bridge Designs for Rapid Renewal: SHRP 2 Project Develops and Demonstrates a Toolkit. *TR News*, (290).

Stanton, J., Eberhard, M., Marsh, M. L., Khaleghi, B., Haraldsson, O. S., Janes, T. M., Tran, H. Viet and Davis. P. (2012). “Accelerated Bridge Construction: Bent on Safety. New Design Toughens ABC During Seismic Events.” *Roads and Bridges*.

Stanton, J., Eberhard, M., Sanders, D., Thonstad, T., Schaefer, J., Kennedy, B., Haraldsson, O., and Mantawy, I. (2014). “A Pre-Tensioned, Rocking Bridge Bent for ABC in Seismic Regions,” *Proceedings of the 10th National Conference in Earthquake Engineering*, Earthquake Engineering Research Institute, Anchorage, Alaska.

Steuck, K., Pang, J.B.K, Stanton, J.F. and Eberhard, M.O. (2007). “Anchorage of Large-Diameter Reinforcing Bars Grouted into Ducts,” WA-RD 684.1, Department of

Environmental and Civil Engineering University of Washington, Washington State Transportation Commission, Seattle, Washington.

Stone, W. C., Cheok, G. S., and Stanton. J. F., (1995). "Performance of Hybrid Moment Resisting Precast Beam-Column Concrete Connections Subjected to Cyclic Loading," *ACI Structural Journal*, V.92,No.2, pp. 229-249

Tadros, M.K., Badie, S.S., Tuan, C.Y. (2010). "Evaluation and Repair Procedure for Precast/ Prestressed Concrete Girders with Longitudinal Cracking in the Web," NCHRP (National Cooperative Highway Research Program) Report 654, Transportation Research Board, Washington, D.C.

Texas Department of Transportation (TxDOT). (2010). "Rectangular Bent Cap Design Example," Bridge Division, Texas Department of Transportation.

Texas Department of Transportation (TxDOT). (2015). "Precast Concrete Bent Cap Option for Round Columns," Bridge Division, Texas Department of Transportation.

Texas Department of Transportation (TxDOT). (Revised 2015). Bridge Division (English) Standards.

Tobolski, M. J. (2010). "Improving the Design and Performance of Concrete Bridges in Seismic Regions," Ph.D. Dissertation, University of California, San Diego.

Tobolski, M. J., Ralls, M. L., Matsumoto, E. E., and Restrepo, J. I. (2006). "State-of-Practice of Precast Bent Cap Systems," Structures Congress 2006 *: Structural Engineering and Public Safety* (pp. 1-10). ASCE.

Tuan, C.Y., Yehia, S.A., Jongpitaksseel, A., Tadros, M.K. (2004). "End Zone Reinforcement for Pretensioned Concrete Girders," *PCI Journal*, 49(3), 68.

Waggoner, M.C. (1999). "Reinforcement Anchorage in Grouted Connections for Precast Bridge Bent Cap Systems," M.S. Thesis, University of Texas, Austin.

Willis, L.K. (1975). Bent cap program user manual. Bridge Division Texas Highway Department.

Wisconsin Department of Transportation (WisDOT). (2014). "Precast Pier Cap and Column Details," Standard Detail Drawings Structures Development Section.

Wisconsin Department of Transportation (WisDOT). (2015). "WisDOT Bridge Manual Chapter 5 - Economic and Costs".

Zhenqiang, L., & Leiva, J. D. (2010). "Pretensioned, Precast Concrete Hollow-Core Units Used for Interchange Bridge Project in Honduras." *PCI journal* 55(2), 71-81.

Ziehl, P. H., Caicedo, J. M., Rizos, D., Mays, T., Larosche, A., ElBatanouny, M., & Mustain, B. (2011). "Testing of Connections between Prestressed Concrete Piles and Precast Concrete Bent Caps," Department of Civil and Environmental Engineering, University of South Carolina, South Carolina Department of Transportation.

APPENDIX A

Pretensioned Bent Cap Design Example

This example provides the procedure followed to design a pretensioned bent cap. A 32 ft roadway width bridge is selected from the TxDOT bridge inventory. The bridge has four numbers of Tx-54 girders and an average span length of 80ft. The bent cap cross-section is a 42 inch square and has a length of 32 ft. The provisions in AASHTO LRFD Bridge design Specifications, Seventh Edition (2014) have been considered. Analysis results are based on TxDOT in-house program CAP18.

Geometry and Design Parameters

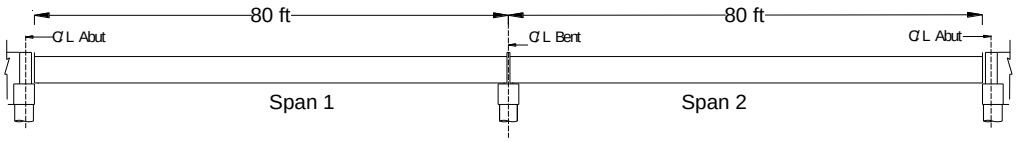

Figure A-1. Plan view of bridge.

Span 1 = Span 2

80 ft Type Tx54 Girders (0.851 k/ft)

4 Girders Spaced @ 9.33 ft with 2 ft overhangs

All Spans

Deck is 34ft wide

Type T551 rail (0.382 k/ft)

8.5 inch Thick slab (0.106 ksf)

Assume 2 inch Overlay @ 140 pcf (0.023 ksf)

Assume

42" x 42" Cap

3 – 36" Columns Spaced @ 12 ft

Cap will be modelled as a continuous beam with simple supports using TxDOT's CAP18 program.

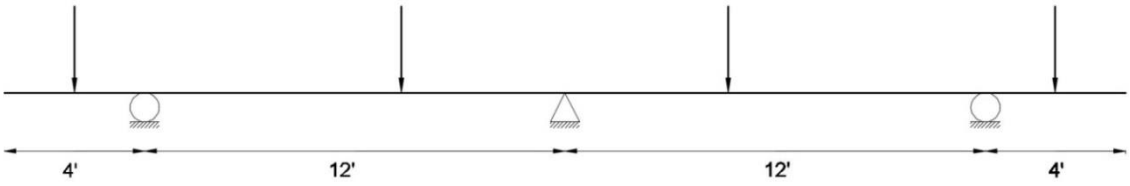

Figure A-2. Postion of columns.

Define Variables

The back span and forward span have the same geometry.

Span = 80 ft	*Span Length*
GdrSpa = 9.33 ft	*Girder Spacing*
GdrNo = 4	*Number of Girders in Span*
GdrWt = 0.851 klf	*Weight of Girder*
Bridge	
RailWt = 0.382 klf	*Weight of Rail*
SlabThk = 8.5 inch	*Thickness of Bridge Slab*
OverlayThk = 2 inch	*Thickness of Overlay*
w_c = 0.150 kcf	*Unit Weight of Concrete for loads*
w_{cE} = 0.145 kcf	*Unit Weight of Concrete for calculation of modulus of elasticity*

w_{Olay} = 0.140 kcf — *Unit Weight of Overlay*

Other Variables

station = 0.5 ft — *Station increment for CAP18*

IM = 33% — *Dynamic load allowance, (AASHTO LRFD Table3.6.2.1-1)*

Cap Dimensions

CapWidth = 3ft + 6inch = 42.00 inch

CapDepth = 3ft + 6inch = 42.00 inch

cover = 4.0 inch — *Measured from Center of prestressing strand*

Material Properties

$f_c^{'}$ = 6.0 ksi — *Concrete Strength*

$E_c = 33{,}000.\, w_{CE}^{1.5}.\sqrt{f_c^{'}(ksi)}$

$= 33{,}000 \text{ x } (0.145)^{1.5} \text{ x } \sqrt{6} = 4463$ ksi — *Modulus of Elasticity of Concrete (AASHTO LRFD Eq. 5.4.2.4-1)*

E_p = 28,500 ksi — *Modulus of Elasticity of strand (AASHTO LRFD 5.4.4.2)*

f_{pu} = 270 ksi — *Tensile strength of strand (AASHTO LRFD Table 5.4.4.1-1)*

A_{PS} = 0.217 in^2 — *Area of 0.6 inch diameter strand*

Loss = 20 % — *Prestress loss conservatively assumed as 20%*

Cap Analysis

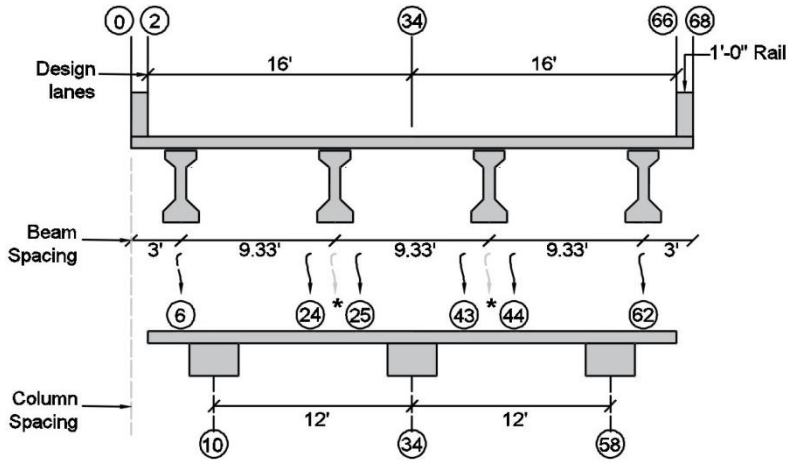

Figure A-3. Cap model.

* indicates the position of actual girder, which has been rounded to the nearest station in CAP18. The circled numbers are the position of stations in CAP18. Each station is assumed as 0.5 ft in the transverse direction of the bridge.

Dead Load

Since Span1 is equal to Span2, the total loads from both the spans is calculated,

$$\text{Rail} = \frac{2\,\text{RailWt.Span}}{\min(\text{GdrNo}, 6)} = \frac{2 \text{ x } 0.382 \text{ x } 80}{\min(4, 6)} = 15.28 \text{ k/girder}$$

$$\text{Slab} = w_c.\text{GdrSpa.SlabThk.Span.}(1.10)$$

$$= 0.150 \text{ x } 9.33 \text{ x } (8.5/12) \text{ x } 80 \text{ x } 1.10 = 87.24 \text{ k/girder}$$

$$\text{Girder} = \text{GdrWt.Span} = 0.851 \text{ x } 80 = 68.08 \text{ k/girder}$$

$$\text{DLRxn} = \text{Rail} + \text{Slab} + \text{Girder} = 15.28 + 87.24 + 68.08 = 170.60 \text{ k/girder}$$

$$\text{Overlay} = w_{\text{Olay}}.\text{GdrSpa.OverlayThk.Span}$$

$$= 0.140 \text{ x } 9.33 \text{ x } (2/12) \text{ x } 80 = 17.42 \text{ k/girder}$$

CAP

$A = \text{CapWidth}.\text{CapDepth}$ *Gross area of cap*

= 42 inch x 42 inch = 1764 in^2 = 12.25 ft^2

$\text{Cap} = w_c A_g$ = 0.150 kcf x 12.25 ft^2 *Dead load of cap*

$= 1.838 \text{ kip/ft} \cdot \frac{0.5 \text{ ft}}{\text{station}} = 0.919 \text{ k/station}$

$I_g = \frac{\text{CapWidth}.\text{CapDepth}^3}{12}$ *Gross moment of inertia*

$= \frac{42 \text{ x } 42^3}{12} = 2.59 \text{ x } 10^5 \text{ in}^4$

$S_x = \frac{\text{CapWidth}.\text{CapDepth}^2}{6}$ *Section modulus*

$= \frac{42 \text{ x } 42^2}{6} = 12348 \text{ in}^3$

$E_c I_g = \frac{4463 \text{ ksi x } 2.59 \text{ x } 10^5 \text{ in}^4}{144 \text{ in}^2/\text{ft}^2} =$ 8.03 x 10^6 ft^2 *Bending stiffness of cap*

Live Load (AASHTO LRFD 3.6.1.2.2 and 3.6.1.2.4)

Lane = 0.64 klf. Span = 0.64 x 80 = 51.2 k/lane

$\text{Truck} = 32 \text{ kip} + 32 \text{ kip}\left(\frac{\text{Span} - 14}{\text{Span}}\right) + 8 \text{ kip}\left(\frac{\text{Span} - 14}{\text{Span}}\right)$

$= 32 \text{ kip} + 32 \text{ kip}\left(\frac{80 - 14}{80}\right) + 8 \text{ kip}\left(\frac{80 - 14}{80}\right) = 65 \text{ k /lane}$

LLRxn = Lane + Truck (1+IM) = 51.2 + 65 x (1 + 0.33) = 137.65 k/lane

P = 16.0 (1 + IM) = 16 x (1 + 0.33) = 21.28 k

$$w = \frac{LLRxn - 2.P}{10\,ft} = \frac{137.65 - 2 \times 21.28}{10\,ft} = 9.51 \text{ kip/ft} = 4.75 \text{ k/station}$$

Cap18 Input

Multiple Presence factors, m (AASHTO LRFD Table 3.6.1.1.2-1)

No. of Lanes	Factor "m"
1	1.20
2	1.00
3	0.85
>4	0.65

Limit States (AASHTO LRFD 3.4.1)

Strength 1

Live Load and Dynamic Load Allowance	*LL + IM = 1.75*
Dead Load Components	*DC = 1.25*
Dead Load Wearing Surface (Overlay)	*DW = 1.25*

Service 1

Live Load and Dynamic Load Allowance	*LL + IM = 1.00*
Dead Load and Wearing Surface	*DC & DW = 1.00*

These values are input in CAP18 for analysis.

CAP 18 Output

	Max + M	Max - M
Dead	posDL = 233.6 k-ft	negDL = -390.8 k-ft
Service	posSL = 447.8 k-ft	negSL = -615 k-ft
Ultimate	posUL = 666.8 k-ft	negUL = -880.9 k-ft

Flexural Reinforcement

M_{dl} = max(posDL, |negDL|)	M_{dl} = 390.8 k-ft
M_s = max(posSL, |negSL|)	M_{sl} = 615 k-ft
M_u = max(posDL, |negUL|)	M_{ul} = 880.9 k-ft

Flexural Design

The flexural design of the bent cap is based on the philosophy of zero tension under dead load. The following steps will be followed for the design and checks following the design:

STEP 0: Define the minimum number of strands

AASHTO LRFD 5.7.3.3.2 specifies that the factored flexural resistance M_r should be at least greater than the less of M_{cr} or $1.33M_u$.

Minimum number of strands

$$-\frac{F}{A}+\frac{M_{cr}}{S_x}=f_r$$

f_r = *Modulus of rupture* = $0.24\sqrt{f_c'} = 0.24\sqrt{6} =$ 0.587 ksi *(AASHTO LRFD Eq. 5.4.2.4-1) where B=D*

$$M_{cr}=(f_r D^2+F)\frac{D}{6}$$

$$M_{cr}=0.24\sqrt{f_c'}\,\frac{D^3}{6}+\frac{FD}{6}$$

$\Phi M_n \geq M_{cr}$, where Φ =1 *AASHTO LRFD 5.5.4.2.1*

$$M_n \geq 0.24\sqrt{f_c'}\,\frac{D^3}{6}+\frac{FD}{6}$$ (A-1)

$$F = n\,T_{strand}$$

where $T_{strand} = f_{pbt}A_{PS}(1-prestress\ loss)$;

$f_{pbt} = 0.75 f_{pu} = 0.75 \text{ x } 270 = 202.5$ ksi *Stress limit in low relaxation strand immediately prior to transfer (AASHTO*

LRFD 5.*9.3-1)*

$T_{strand} = 202.5 \text{ x } 0.217 \text{ x } (1 - 0.2) = 35.15 \text{ kips/strand}$

$F = 35.15\, n$

From Eq. (A-1),

$$M_n \geq 0.24\sqrt{f_c'}\,\frac{D^3}{6} + \frac{FD}{6} = 0.04\sqrt{f_c'}\,D^3 + 5.858\ nD$$

(A-2)

$$M_n \geq n\, A_{PS}\, f_y\, j_d \qquad \text{(A-3)}$$

in which, $f_y = 0.9\, f_{pu}$ *(AASHTO LRFD Table 5.4.4.1-1)*

$j_d = 0.45D$

From Eq. (A-3),

$M_n \geq n\, A_{PS}\, f_y\, j_d$

$= n \text{ x } 0.217 \text{ x } 0.9 \text{ x } 270 \text{ x } 0.45 \text{ x } D = 23.72\, nD \qquad \text{(A-4)}$

Equating Eq. (A-2) and (A-4),

$$0.04\sqrt{f_c'}\,D^3 + 5.858\ nD = 23.72\, nD$$

$$n = \frac{0.04}{17.87}\sqrt{f_c'}\,D^2 = \frac{0.04}{17.87}\sqrt{6} \text{ x } 42^2 = 9.67$$

$n_{\min} = 1.33\, n = 1.33 \text{ x } 9.67 = 12.86$ *The factor 1.33 is to account for the factor 1.33 with* M_u

$n_{\min} \approx 14$ *Rounded up to nearest even integer*

Minimum number of strands = 14

STEP 1: Design for zero flexural tension under Dead load

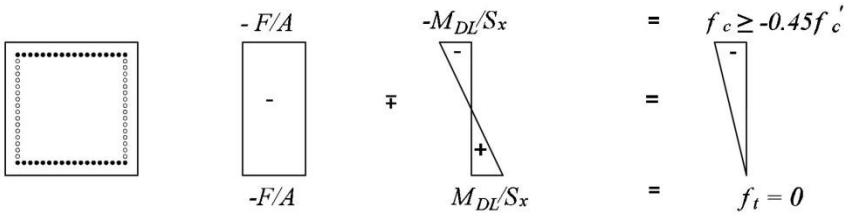

Figure A-4. Stresses under dead load: No tension.

Tension limit,

$$-\frac{F}{A}+\frac{M_{DL}}{S_x}=f_t=0 \qquad \text{(A-5)}$$

Zero tension under dead load

Solve for F from Eq. (A-5),

$$F=\frac{M_{DL}A}{S_x}=\frac{6M_{DL}}{D}$$

$$=\frac{6 \text{ x } 390.8 \text{ x } 12}{42}=669.9 \text{ k}$$

Required prestressing force

$$n=\frac{F}{T_{strand}}=\frac{669.9}{35.15}=19.05\approx 19$$

Number of strands

From *STEP 0*,

$n=19>n_{\min}=14$ *Okay*

Compression limit,

$$-\frac{F}{A}-\frac{M_{DL}}{S_x}\geq f_c=-0.45f_c' \qquad \text{(A-6)}$$

$$-\frac{F}{1764}-\frac{390.8 \text{ x } 12}{12348}\geq -0.45 \text{ x } 6=-2.7$$

Solve for *F*,

F < 4092.86

$$n_{\max} < \frac{F}{T_{strand}} = \frac{4092.86}{35.15} = 116.43 \approx 117$$ *Number of strands*

Solution space $19 < n < 117$

Adopt symmetric solution (requires multiples of 4),

$n = 20$,

Thus $F_{provided} = nT_{strand} = 20 \text{ x } 35.15 = 703 \text{ k}$

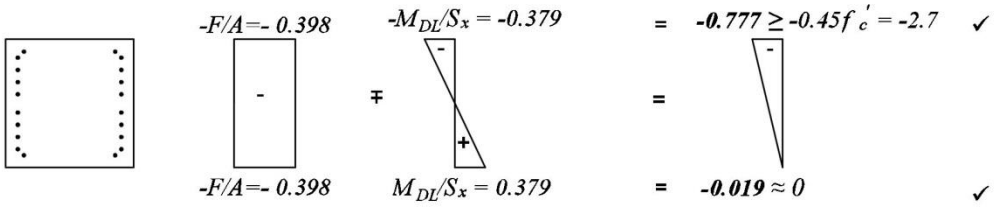

Figure A-5. Solution: Stresses under dead load.

$$-\frac{F}{A} + \frac{M_{cr}}{S_x} = f_r$$

$$-\frac{703}{1764} + \frac{M_{cr}}{12348} = 0.587$$

$$-0.398 + \frac{M_{cr}}{12348} = 0.587$$

M_{cr} = 1014.1 k-ft

Checks

The following checks will be made for the flexural design of the bent cap:

STEP 2: From Service Stress determine required minimum concrete compressive strength

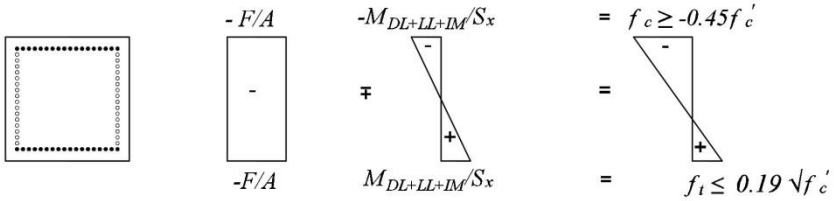

Figure A-6. Stresses under service load.

$$-\frac{F}{A}+\frac{M_{DL+LL+IM}}{S_x} < f_t = 0.19\sqrt{f_c'}$$

$f_t = 0.19\sqrt{f_c'}$ *is the tensile stress limit at service limit state after losses(AASHTO LRFD Table 5.9.4.2.2-1)*

$$-\frac{703}{42^2}+\frac{615 \text{ x } 12}{\left(\frac{42 \text{ x } 42^2}{6}\right)} = 0.199 < f_t = 0.19\sqrt{f_c'}$$

$= 0.19\sqrt{6}$ *Okay*

= 0.465 ksi

Compression

$$-\frac{F}{A}-\frac{M_{DL+LL+IM}}{S_x} > f_c = -0.45 f_c'$$

$f_c = -0.45 f_c'$ *is the compressive stress limit at service limit state after losses(AASHTO LRFD Table5.9.4.2.1-1)*

$$-\frac{703}{42^2}-\frac{615 \text{ x } 12}{\left(\frac{42 \text{ x } 42^2}{6}\right)} = -0.996 > f_c = -0.45 f_c'$$

= -0.45 x 6 *Okay*

= -2.7ksi

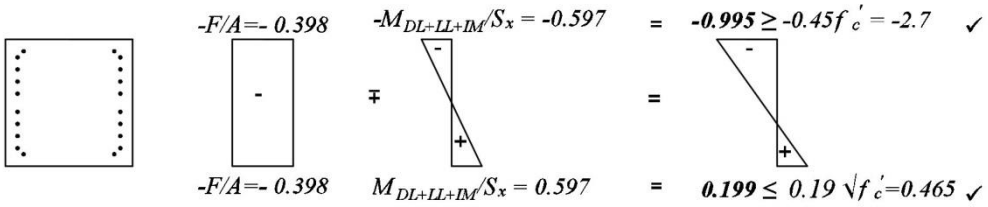

Figure A-7. Solution: Stresses under service load and establish minimum concrete strength.

Based on the stresses determine potential minimum concrete strength:

Tension

$f_t = 0.19\sqrt{f_c'} = 0.199$ ksi

Solving, $f_c' = \left(\frac{0.199}{0.19}\right)^2 = 1.1$ ksi

Compression

$f_c = -0.45 f_c' = -0.996$ ksi

Solving $f_c' = \frac{0.996}{0.45} = 2.2$ ksi

These values are unreasonable low, so use minimum practical concrete strength for prestressed concrete,

Consider $f_c' = 6$ ksi.

STEP 3: Check Ultimate Strength capacity

Determination of nominal moment capacity of prestressed bent cap

The 20 strands can be arranged in the configuration shown in Figure A-8.

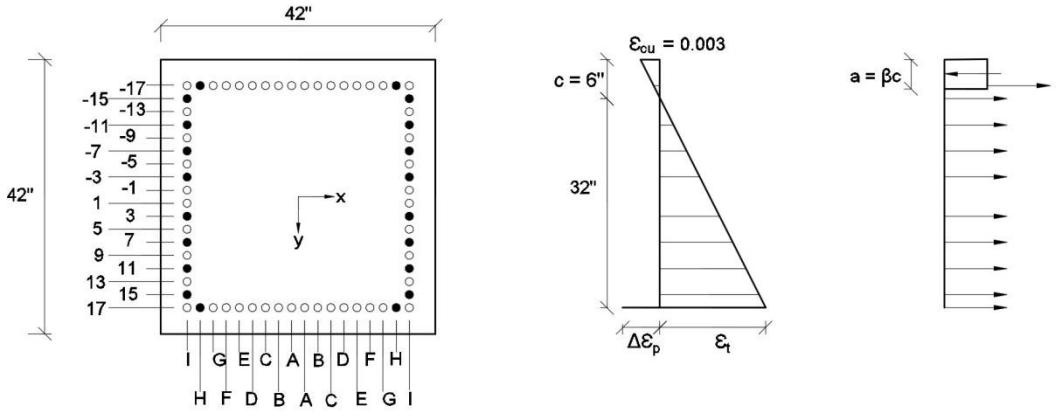

Strand configuration *Strains* *Stresses*

Figure A-8. Ultimate strength capacity.

Define variables

$\Delta\varepsilon_p = \frac{T_{strand}}{E_p A_{PS}} = \frac{35.15}{28500 \text{ x } 0.217} = 0.0056$ — *Prestrain after losses*

$\beta = 0.85 - (f'_c - 4)0.05 = 0.85 - (6-4)0.05 = 0.75$ — For $f_c' > 4.0$ ksi *(AASHTO LRFD 5.7.2.2)*

$B = 42$ inch — *Cap Width*

$\varepsilon_{cu} = 0.003$ — *Maximum strain at extreme compression fiber (AASHTO LRFD 5.7.2.1)*

$Q = 0.03$

$R = 6$ — *Q and R are constants in Menegotta Pinto equation*

Try $c =$ **-15.0 inch** — *Assume c such that tension force equals compression force*

The following equation will be used for each prestressing layer, to determine the moment capacity.

$$\varepsilon_{ti} = \varepsilon_{cu}\left(\frac{-D/2 - d_i}{D/2 - c} - 1\right)$$

Tension strain on concrete in i^{th} layer; d_i is the depth of the prestressing layer shown in Figure A-8

$$f_{psi} = E_p \varepsilon_{si}\left[Q + \frac{1-Q}{\left(1 + \left|\frac{\varepsilon_{si}E_s}{f_y}\right|^R\right)^{\frac{1}{R}}}\right]$$

Menegotta-Pinto equation Stress in i^{th} layer

ε_{si} = total strain on strand in each layer,

where $\varepsilon_{si} = \varepsilon_{ti} + \Delta\varepsilon_p$

$T_i = f_{psi} A_{psi}$ — *Tension force in i^{th} layer; A_{psi} = area of prestressing in each layer*

$jd_i = d_i$ — *Moment arm of i^{th} layer*

$M_i = T_i jd_i$ — *Moment in i^{th} layer*

$C_c = 0.85 f_c' \beta c B$ — *Compression force in the member*

$jd = a$ — *Internal lever arm for concrete*

in which $a = -\frac{D}{2} + \left(-\frac{\beta}{2} \left(-\frac{D}{2} - c \right) \right)$

$= -\frac{42}{2} + \left(-\frac{0.75}{2} \left(-\frac{42}{2} + 15 \right) \right) = -18.75$ inch

Table A-1. Determination of ultimate strength capacity.

Depth of layer (d_i), inch	**No of strands in each layer**	**Strain (ε_{ti})**	**Prestrain ($\Delta\varepsilon_p$)**	**Total Strain (ε_{si})**	**Stress (f_{psi}), ksi**	**Force (T_i), kip**	**Moment arm (jd_i), inch**	**Moment (M_i), kip-in**
-17	2	-0.0010	0.0057	0.0047	132.88	57.67	1.74	100.84
-15	2	0	0.0057	0.0057	159.76	69.34	3.75	259.91
-11	2	0.0020	0.0057	0.0077	204.28	88.66	7.75	686.98
-7	2	0.0040	0.0057	0.0097	229.40	99.56	11.75	1169.69
-3	2	0.0060	0.0057	0.0117	240.22	104.26	15.75	1641.88
3	2	0.0090	0.0057	0.0147	246.78	107.10	21.75	2329.34
7	2	0.0110	0.0057	0.0167	249.27	108.18	25.75	2785.59
11	2	0.0130	0.0057	0.0187	251.32	109.07	29.75	3244.79
15	2	0.0150	0.0057	0.0207	253.19	109.89	33.75	3708.48
17	2	0.0160	0.0057	0.0217	254.09	110.28	35.75	3942.24
					$\sum T_i =$	965 k;	$\sum M_i =$	19869.7 k-inch
$C_c = -0.85 f_c' \beta c B = -0.85$ x 6 x 0.75 x 6 x 42 $\approx$ - 965 k $\quad C_c = \sum T_i$ *Okay*								

$M_n = \sum M_i + C_c j_d$ = 19869.7 + (-965) x (-18.75) = 19870.27 k-inch = 1656 k-ft

$M_n = 1656$ kip-ft > $M_u = 880.9$ k-ft *Okay*

APPENDIX B

Connection Design Example

This example provides the procedure followed to design the bent cap-to-column connection. A 32 ft roadway width bridge is selected from the TxDOT bridge inventory. The bridge has four numbers of Tx-54 girders and an average span length of 80ft. The bent cap cross-section is a 42 inch square and has a length of 32 ft. Design is based on analysis results generated from computer program (SAP2000) for gravity loads, and lateral wind loads acting in the structure and on live loads. The provisions in AASHTO LRFD Bridge design Specifications, Seventh Edition (2014) have been taken into consideration.

1) GEOMETRY AND DESIGN PARAMETERS

Span 1 = Span 2

80 ft Type Tx54 Girders (0.851 k/ft)

4 Girders Spaced @ 9.33 ft with 2 ft overhangs

All Spans

Deck is 34ft wide

Type T551 rail (0.832 k/ft)

8.5 inch thick slab (0.106 ksf)

Assume 2 inch Overlay @ 140 pcf (0.023 ksf)

Use Class C Concrete

f'_{c_cap} = 6 ksi — *Concrete compressive strength of bent cap*

f'_{c_column} = 3.6 ksi — *Concrete compressive strength of column*

w_c = 150 pcf (for weight)

w_{cE} = 145 pcf (for Modulus of Elasticity calculation)

f_y = 60 ksi — *Grade 60 Reinforcing*

Assume

42 inch x 42 inch Cap

3-36 inch Columns Spaced @ 12 ft

Bridge Description

Superstructure

No.Sp = 2 — *Number of Spans*

Span1 = 80 ft

Span2 = 80 ft

$$\text{AvgSp} = \frac{(\text{Span1} + \text{Span2})}{2}$$

$$= \frac{(80 + 80)}{2} = 80 \text{ ft}$$ — *Average span length*

BridgeL = Span1 + Span2 = 160 ft — *Bridge Length*

BridgeW = 34 ft — *Bridge Width*

NoRail = 2 — *Number of T551 Rails*

RailW = 1 ft — *Nominal rail Width (T551)*

RailH = 2 ft + 8 in = 2.67 ft — *Rail Height (T551)*

RailWt = 0.382 klf — *Rail Weight (T551)*

RoadW = BridgeW – NoRail.RailW

= 34 ft – (2 x 1 ft) = 32 ft

Lanes = 2 *Number of lanes*

SlabTh = 8.5 in *Slab Thickness*

OlayTh = 2 in *Overlay Thickness*

w_{Conc} = 0.150 kcf *Unit Weight of Concrete*

w_{Olay} = 0.140 kcf *Unit Weight of Overlay*

NoBm = 4 *Number of Tx-54 Beams*

BmSpac = 9.33 ft *Beam Spacing*

BmH = 54 in *Beam Height*

BmWgt = 0.851 klf *Beam Weight*

Bent Cap

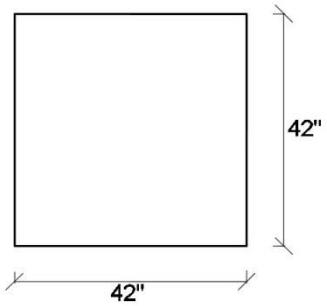

Figure B-1. Bent Cap Section.

L_{Cap} = 32 ft *Cap Length*

b_{Cap} = 3.5 ft *CapWidth*

d_{Cap} = 3.5 ft *CapDepth*

Column

$D_{Col} = 3.0$ ft — *Diameter of Column*

$L_{Col} = 13.75$ ft — *Length of column above ground to centerline of bent cap*

Material Properties

$E_c = 33000 w_{cE}^{1.5} \sqrt{f_c}$ — *Modulus of Elasticity of Concrete, (AASHTO LRFD Eq. 5.4.2.4-1)*

For bent cap:

$E_c = 33000(0.145^{1.5})\sqrt{6} = 4463$ ksi

For column:

$E_c = 33000(0.145^{1.5})\sqrt{3.6} = 3457$ ksi

$E_s = 29000$ ksi — *Modulus of Elasticity of Steel*

2) CALCULATE GRAVITY LOADS

Dead Load from Structural Components and Nonstructural Components (DC)

Rail Loads

$$\text{Rail} = \frac{2.\text{RailWt.}\,\text{AvgSp}}{\text{Min(NoBm,6)}}$$

$$= \frac{2 \text{ x } 0.382 \text{ klf x } 80 \text{ ft}}{4} = 15.29 \ \frac{\text{k}}{\text{girder}}$$

Slab Loads

Slab = wConc. BmSpac. SlabTh. AvgSp. 1.10

$$= 0.15 \frac{k}{ft^3} \text{ x } 9.33 ft \text{ x} \left(\frac{8.5}{12} \right) ft \text{ x } 80 \, ft \text{ x } 1.10$$

$$= 87.24 \ \frac{k}{girder}$$

Beam Loads

Girder = BmWgt. Span = $0.851 \, klf \text{ x } 80 ft$

$$= 68.08 \ \frac{k}{girder}$$

Total Dead Load (DC) = Rail + Slab + Girder

$$= 15.29 \ \frac{k}{girder} + 87.24 \ \frac{k}{girder} + 68.08 \ \frac{k}{girder}$$

$$= 170.61 \ \frac{k}{girder}$$

Bent Cap

$A_g = b_{Cap} d_{cap} = 42 \, inch \text{ x } 42 \, inch$

$= 1764 \, in^2 = 12.25 \, ft^2$ *Gross Area of cap*

$Cap Load = w_{Conc} A_g = 0.15 \text{ kcf x } 12.25 \text{ ft}^2$ *Self weight of Cap*

$= 1.838$ k/ft

$I_g = \frac{1}{12} b_{Cap} d_{Cap}^{\ 3} = \frac{1}{12} \text{ x } 42 \, inch \text{ x } 42^3 inch^3$ *Gross Moment of Inertia*

$= 2.59 \text{ x } 10^5 \, in^4$

$E_c I_g = 4465.15 \text{ ksi x } 2.59 \text{ x } 10^5 \, in^4$

$= 1156.47 \text{ x } 10^6 \text{ k-in}^2 \text{ x } \frac{\text{ft}^2}{144 \text{ in}^2}$ *Bending Stiffness of Cap*

$= 8.03 \text{ x } 10^6 \text{ k - ft}^2$

Dead Load from Wearing Surfaces and Utilities (DW)

Overlay (DW) = w_{Olay}. BmSpac. OlayTh. AvgSp

$= 0.140 \text{ kcf x } 9.33 \text{ ft x } (2/12) \text{ ft x } 80 \text{ ft} = 17.42 \frac{\text{k}}{\text{girder}}$

Live Load (AASHTO LRFD 3.6.1.2 and 3.6.1.2.4)

LongSpan = ShortSpan = AvgSp = 80 ft

IM = 0.33

Lane = 0.64 klf . AvgSp = $0.64 \text{ klf x } 80 \text{ ft} = 51.2 \frac{\text{k}}{\text{lane}}$

Truck = 32 kip + 32 kip. $\frac{(\text{LongSpan - 14 ft})}{\text{LongSpan}}$ + 8 kip. $\frac{(\text{ShortSpan - 14 ft})}{\text{ShortSpan}}$

$= 32 \text{ kip} + 32 \text{ kip}. \frac{(80 \text{ ft} - 14 \text{ ft})}{80 \text{ ft}} + 8 \text{ kip}. \frac{(80 \text{ ft} - 14 \text{ ft})}{80 \text{ ft}} = 65 \frac{\text{k}}{\text{lane}}$

LLRxn = Lane + Truck. (1 + IM) = $51.2 \frac{\text{k}}{\text{lane}} + 65 \frac{\text{k}}{\text{lane}} (1 + 0.33) = 138 \frac{\text{k}}{\text{lane}}$

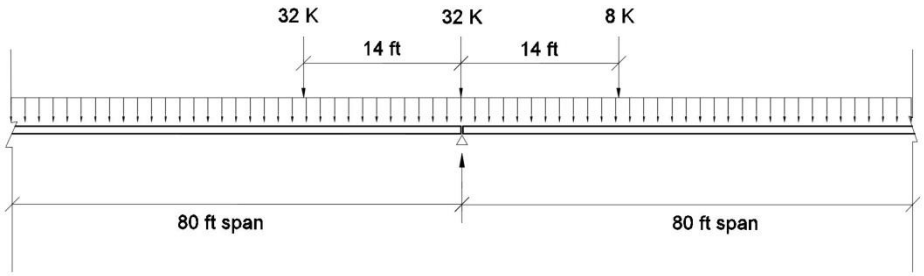

Figure B-2. Live Load on 80 ft span.

DC on each girder = 170.61 k

DW on each girder = 17.42 k

Cap Load = 1.838 k/ ft

Maximum column moment due to live load is obtained when only the exterior girder is loaded.

Assuming full live load on exterior girder,

$LL_{ext,\ girder}$ = 138 k

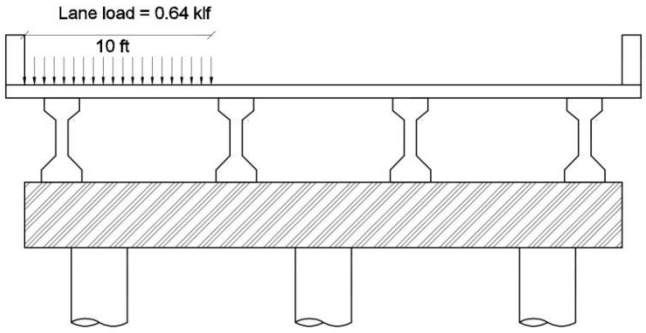

Figure B-3. Live Load on one lane to maximize column moment.

3) CALCULATE WIND LOADS (AASHTO LRFD 3.8)

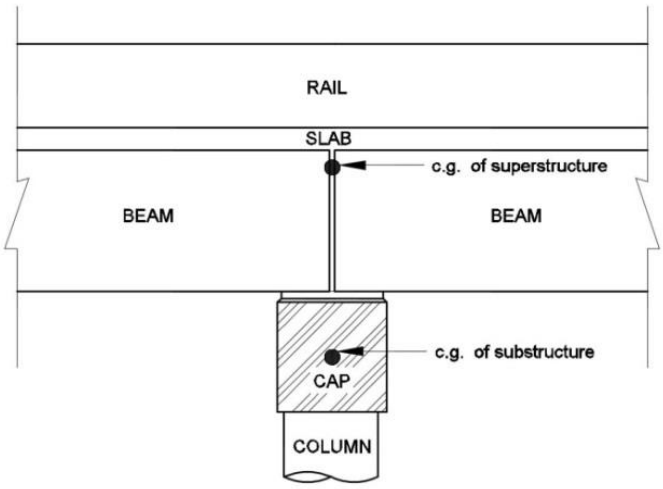

Figure B-4. Wind along X- axis.

(Wind loads acting into page)

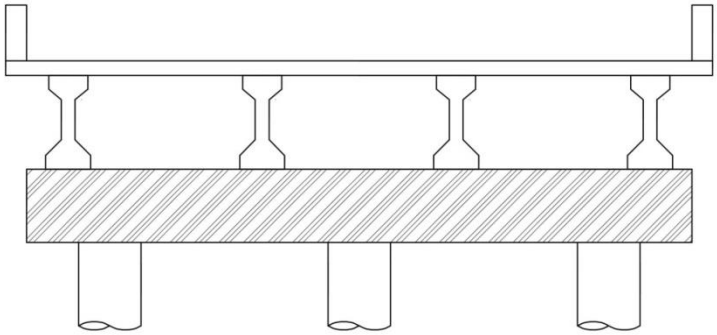

Figure B-5. Wind along Y- axis.

Superstructure

SuperDepth = RailH + SlabTh + BmH *Depth of Superstructure*

= 2.67 ft + (8.5 inch/12) ft + (54 inch/12) ft

= 7.88 ft

A_{Super} = AvgSp x SuperDepth *Area of Superstructure*

= 80 ft x 7.88 ft = 630.4 ft^2

Table B-1 shows the wind loads acting on the superstructure in the lateral and longitudinal directions. q_x_Wsuper and q_y_Wsuper are the wind pressure in the transverse and longitudinal direction of the superstructure, obtained from AASHTO LRFD Table 3.8.1.2.2-1. These are multiplied with the area of the superstructure to determine the wind force in the lateral and longitudinal directions respectively.

Table B-1. Wind loads on superstructure.

Wind Skew(θ)	**Lateral load (ksf) $q_{x\_}W_{super}$**	**$F_{x\_}W_{super}$ (kip) = $q_{x\_}W_{super}$ x A_{super}**	**Longitudinal load (ksf) $q_{y\_}W_{super}$**	**$F_{y\_}W_{super}$ (kip) = $q_{y\_}W_{super}$ x A_{super}**
0	0.050	31.5	0	0
15	0.044	27.7	0.006	3.7
30	0.041	25.8	0.012	7.5
45	0.033	20.8	0.016	10.0
60	0.017	10.7	0.019	11.9

Substructure

SubDepth = Cap Depth = 3.5 ft — *Depth of Substructure*

$Area_{Sub\_X} = b_{Cap} d_{cap} = 12.25\ ft^2$ — *Cap end area that wind acts on in the x- Direction*

$Area_{Sub\_Y} = SubDepth\ L_{Cap} = 112\ ft^2$ — *Cap side area that wind acts on in the y- Direction*

Table B-2 shows the wind loads acting on the substructure. From AASHTO LRFD 3.8.1.2.3, a wind pressure of 0.0040 is assumed to act on the substructure based on a 100 mph base design wind velocity. Wind pressure acting at a skew angle (θ) measured from a perpendicular to the longitudinal axis, is resolved into two components,

a horizontal component $0.0040\cos(\theta)$ and a vertical component $0.0040\sin(\theta)$. These components are multiplied with the area of the bent cap exposed to the winds in those directions to determine the wind loads on the substructure in the lateral and longitudinal directions respectively. Table B-3 summarizes the total wind loads acting on the structure.

Table B-2. Wind loads on substructure.

Wind Skew(θ)	**Lateral load (ksf) $q_{x\_W_{sub}}$ = 0.0040 cosθ**	**$F_{x\_W_{sub}}$ (kip)= $q_{x\_W_{sub}}$ x A_{sub_x}**	**Longitudinal load (ksf) $q_{y\_W_{sub}}$ = 0.0040 sinθ**	**$F_{y\_W_{sub}}$ (kip) = $q_{y\_W_{sub}}$ x A_{sub_y}**
0	0.040	0.49	0	0
15	0.038	0.46	0.010	1.12
30	0.034	0.41	0.020	2.24
45	0.028	0.34	0.028	3.13
60	0.020	0.24	0.034	3.80

Table B-3. Total wind loads on structure.

Wind Skew(θ)	**Superstructure**		**Substructure**		**Total**	
	F_x	**F_y**	**F_x**	**F_y**	**F_x**	**F_y**
0	31.5	0	0.49	0	32	0
15	27.7	3.7	0.46	1.12	28.1	4.8
30	25.8	7.5	0.41	2.24	26.2	9.7
45	20.8	10	0.34	3.13	21.1	13.1
60	10.7	11.9	0.24	3.80	10.9	15.7

Overturning Force (AASHTO LRFD 3.8.2)

Vertical Upward Wind Pressure

q_{OF} = -0.020 ksf

qOF is applied to the entire width of the deck.

Axial Force due to Overturning Force

$P_{OF} = q_{OF}$ BridgeW AvgSp

= -0.020 ksf x 34 ft x 80 ft = - 54.4 k

Wind on Live Load (AASHTO LRFD 3.8.1.3)

AASHTO LRFD 3.8.1.3 specifies the wind pressure on vehicles to be considered as a moving load of 0.10 klf acting normal to and at 6 ft above the roadway. Where the wind load does not act normal to the structure, AASHTO LRFD Table 3.8.1.3-1 specifies the normal and parallel force components applied to the live load. Table B-4 shows the wind loads acting on the live load for different skew angles between the direction of wind and the bent cap axis. The forces acting in the lateral and longitudinal directions are determined by multiplying the lateral and longitudinal loads with the average span length respectively.

Table B-4. Wind loads on live load.

Wind Skew(θ)	**Lateral load (ksf) $q_{x}\_W_L$**	**$F_{x}\_W_L$ (k) = $q_{x}\_W_L$ x AvgSp**	**Longitudinal load (ksf) $q_{y}\_W_L$**	**$F_{y}\_W_L$(k) = $q_{y}\_W_L$ x AvgSp**
0	0.10	8	0	0
15	0.088	7	0.012	0.96
30	0.082	6.5	0.024	1.9
45	0.066	5.2	0.032	2.6
60	0.034	2.7	0.038	3.04

4) LOAD COMBINATIONS (AASHTO LRFD TABLE 3.4.1-1 AND TABLE 3.4.1-2)

The three load cases that are considered for connection design are: Strength I, Strength III, and Strength V. Demands in the bent cap is determined due to gravity loads and forces acting in the lateral direction.

Strength I (max) = 1.25 DC + 1.50 DW + 1.75 LL + 1.0 WA + 1.75 CE + 1.75 BR

Strength I (min) = 0.9 DC + 0.65 DW + 1.75 LL + 1.0 WA + 1.75 CE + 1.75 BR

Strength III (max) = 1.25 DC + 1.50 DW + 1.0 WA + 1.40 WS + 1.40 OF

Strength III (min) = 0.9 DC + 0.65 DW + 1.0 WA + 1.40 WS + 1.40 OF

Strength V (max) = 1.25 DC + 1.50 DW + 1.35 LL + 1.0 WA + 1.35 CE + 0.40 WS + 1.0 WL + 1.35 BR

Strength V (min) = 0.9 DC + 0.65 DW + 1.35 LL + 1.0 WA + 1.35 CE + 0.40 WS + 1.0 WL + 1.35 BR

DC = Dead load of structural components and nonstructural attachments
DW = Dead load of wearing surfaces and utilities
LL = Live Load
WS = Wind Load on Structure
OF = Overturning Force due to wind uplift
WL = Wind Load on Live load
WA = Water Load and steam pressure
BR = Vehicular Braking Force
CE = Vehicular Centrifugal Force

In this example, BR = 0 in the lateral direction of the bridge; CE = 0 for a straight bridge. The loads acting in the three strength limit state load combinations along the lateral direction of the bridge are summarized as follows:

STRENGTH - I

Table B-5. Loads in Strength- I load combination.

	Exterior Column		Interior Column	
	Max	**Min**	**Max**	**Min**
DC	1.25 DC **213.26**	0.9 DC **153.55**	1.25 DC **213.26**	0.9 DC **153.55**
DW	1.5 DW **26.13**	0.65 DW **11.32**	1.5 DW **26.13**	0.65 DW **11.32**
LL	1.75 LL **241.50**	1.75 LL **241.50**	1.75 LL -	1.75 LL -
TOTAL	**480.89**	**406.37**	**239.39**	**164.87**

STRENGTH - III

Table B-6. Loads in Strength- III load combination.

	Exterior Column		Interior Column	
	Max	**Min**	**Max**	**Min**
DC	1.25 DC **213.26**	0.9 DC **153.55**	1.25 DC **213.26**	0.9 DC **153.55**
DW	1.5 DW **26.13**	0.65 DW **11.32**	1.5 DW **26.13**	0.65 DW **11.32**
WS	1.4 WS **44.80**	1.4 WS **44.80**	1.4 WS **44.80**	1.4 WS **44.80**
OF	1.4 OF **-76.16**	1.4 OF **-76.16**	1.4 OF **-76.16**	1.4 OF **-76.16**
TOTAL	**239.39**	**164.87**	**239.39**	**164.87**

STRENGTH - V

Table B-7. Loads in Strength- V load combination.

	Exterior Column	Interior Column

	Max	Min	Max	Min
DC	1.25 DC	0.9 DC	1.25 DC	0.9 DC
	213.26	**153.55**	**213.26**	**153.55**
DW	1.5 DW	0.65 DW	1.5 DW	0.65 DW
	26.13	**11.32**	**26.13**	**11.32**
LL	1.35 LL	1.35 LL	1.35 LL	1.35 LL
	186.30	**186.30**	**-**	**-**
WS	0.4 WS	0.4 WS	0.4 WS	0.4 WS
	(0° skew)		(0° skew)	
	12.80	**12.80**	**12.80**	**12.80**
WL	1.0 WL	1.0 WL	1.0 WL	1.0 WL
	(0° skew)		(0° skew)	
	8.00	**8.00**	**8.00**	**8.00**
TOTAL GRAVITY	**425.69**	**351.17**	**239.39**	**164.87**
TOTAL LATERAL	**20.8**	**20.8**	**20.8**	**20.8**

5) FLEXURAL REINFORCMENT IN THE JOINT

The bridge has been analyzed for the strength limit state load combinations and the highest joint moment is obtained under Strength V load combination. Figure B-6 shows the loading under Strength V load combinations considering the maximum load factors of 1.25 and 1.50 for DC and DW respectively. Figure B-7 shows the bending moment diagrams under this load combination.

Maximum moment = $M_{y\_exterior\ column,\ Strength\text{-}V}$ = 178 k-ft

Moment in the joint is the product of tension reinforcement and the moment arm of the tension reinforcement from the compression force. The dowel bars in the

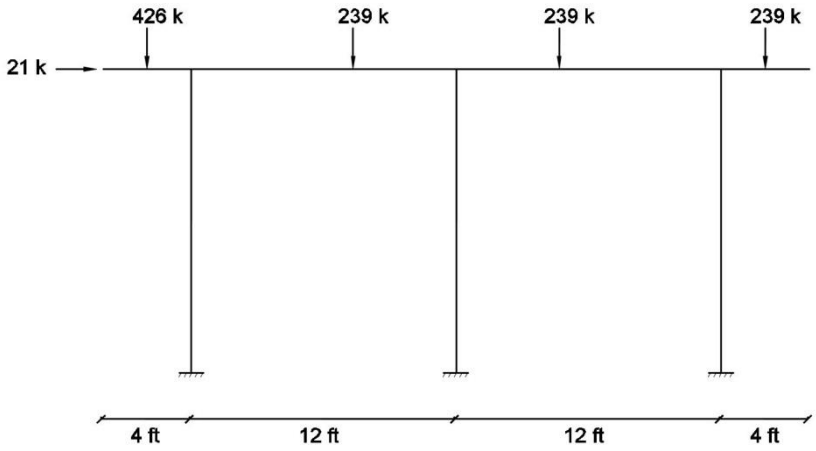

Figure B-6. Strength V loading (1.25 DC + 1.50 DW + 1.35 LL + 0.4 WS + 1.0 WL).

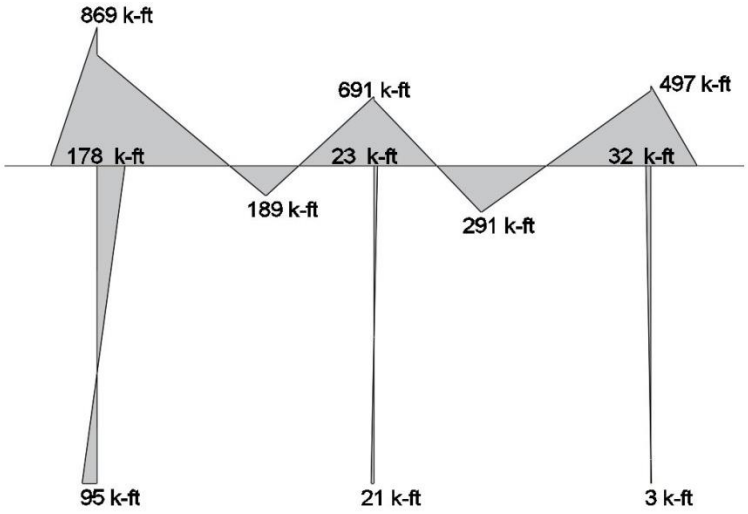

Figure B-7. Bending moment diagram: Strength V loading.

connection can be assumed to be lumped as a single tension reinforcement at the center of the column. Distance between the core tension reinforcement from the compression force is then assumed to be 0.4 times the diameter of the column.

$M_j = Te = T \times 0.4\ D_{col} = 1.2\ T$

$$T = \frac{M_j}{1.2} = \frac{178\ \text{k-ft}}{1.2\ \text{ft}} = 148.3\ \text{k}$$

Provide 6-#11 bars

$$F_y = \frac{T}{6} = \frac{148.3}{6} = 24.7\ \text{k}$$

Tension force in each bar

$f_y = 60$ ksi

Yield strength of mild steel reinforcement

$$A_{b,\ required} = \frac{F_y}{f_y} = 0.41\ \text{in}^2$$

Required area of reinforcement for each bar

Provide 6 # 11 bars

$A_{b,\ provided} = 1.56\ \text{in}^2$

Provided area of reinforcement for each bar

$A_{s,\ provided} = 6 \times 1.56\ \text{in}^2 = 9.36\ \text{in}^2$

Provided area of reinforcement

6) MOMENT CAPACITY OF JOINT

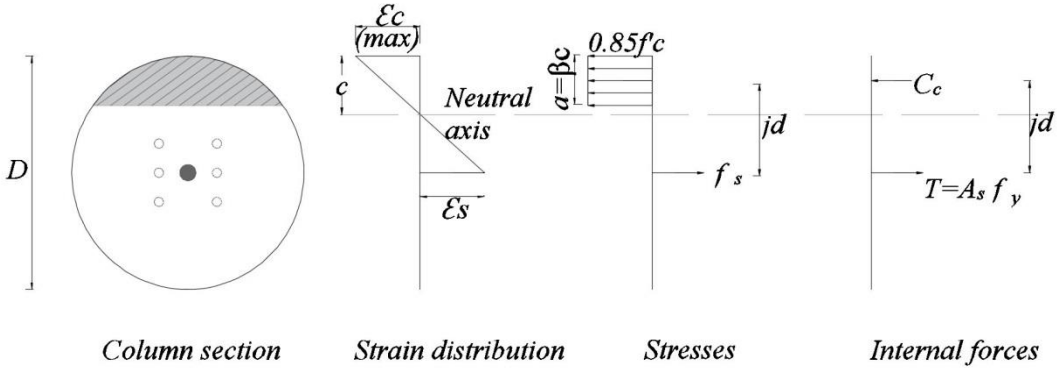

Figure B-8. Calculation of moment capacity.

The compression force in the joint is given by:

$C_c = N + T$ (B-1)

$C_c = N + A_s f_y = 0.85 f'_c ab$

in which f'_c for column = 3.6 ksi; N is the axial load in the joint assumed to result from dead loads. To ensure conservative results, the minimum load factors for the Strength V limit state are used, i.e., 0.9 and 0.65 with DC and DW respectively.

N = 0.9 DC + 0.65 DW = 165 k

For an axial load N = 165 k and T = $A_s f_y$ = 6 x 1.56 x 60 = 561.6 k

From Eq. (B-1), C_c = 165 k + 561.6 k = 726.6 k

From Dutta & Mander (2001),

$$\frac{C_c}{f'_c A_g} = 1.32\alpha\left(\beta\frac{c}{D}\right)^{1.38} \quad \text{(B-2)}$$

For $f_c' \leq 4$ ksi, $\beta_c = 0.85$ and α_c is assumed as 0.85.

$$C_c = 1.122 f'_c A_g \left(\frac{a}{D}\right)^{1.38}$$

$$\frac{a}{D} = 0.92\left(\frac{C_c}{f'_c A_g}\right)^{0.725}$$

$$\frac{a}{D} = 0.92\left(\frac{726.6}{3.6 \text{ x } \frac{\pi}{4} \text{ x } 36^2}\right)^{0.725} = 0.284$$

For a column of diameter D = 3.0 ft,

$$\frac{a}{D} = 0.284$$

a = 0.284 x 3.0 ft = 0.852 ft.

From Dutta & Mander (2001), C_c acts at *0.6a* from the outermost edge,

$$\text{jd} = \frac{\text{D}}{2} - 0.6\text{a} = \frac{3.0\text{ ft}}{2} - 0.6 \text{ x } 0.852 \text{ ft} = 0.988 \text{ ft}$$

$M_j = C_c . jd$ = 726.6 k x 0.988 ft = **718 k-ft > 178 k-ft**

7) VEHICLE COLLISION LOAD (AASHTO LRFD 3.6.5)

For bridges designed to resist vehicle collision loads, the column and connection shall be examined for resistance against such demands. Columns located within a distance of 30 ft from the edge of roadway need to be investigated for vehicle collision. An equivalent static force of 600 kip shall be assumed to be acting at a direction of zero to 15 degrees with the edge of the pavement in a horizontal plane, at a distance of 5.0 ft above ground (AASHTO LRFD 3.6.5.1).

From Section 6.2.2, a pocket size of 21 inch diameter is considered for 36 inch diameter column. The moment capacity of the column with 10-#9 bars is found by P-M interaction diagram to be 727 k-ft. The crash load of 600 kip is assumed to be acting at an angle of 15 degrees with the edge of the pavement at 5.0 ft above the ground. The 600 k force is resolved into two components; 600 cos15 and 600 sin15 along the x and y directions respectively.

F_x = 600 x cos θ = 600 x cos 15 = 579.55 k ≈ 580 k

F_y = 600 x sin θ = 600 x sin 15 = 155.3 k ≈ 155 k

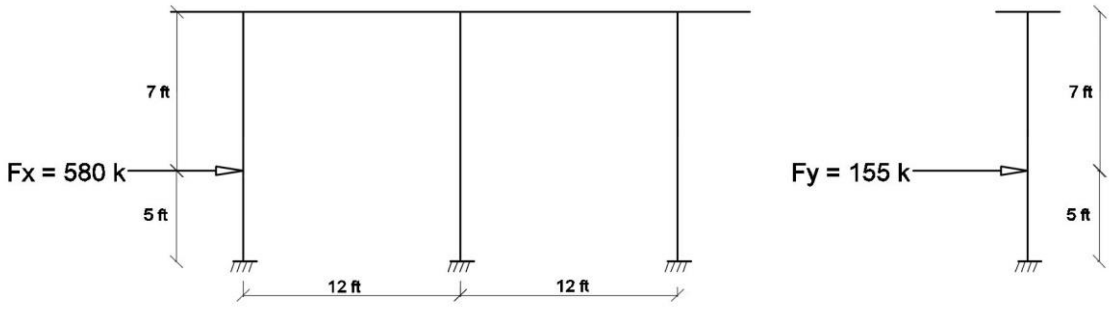

Figure B-9. Vehicle collision load along x and y directions.

The failure mechanisms due to vehicle collision loads are discussed here. A column height (H) of 12 ft from the ground to bottom of bent cap, and column spacing (L) of 12 ft is considered.

The allowable loads in each mechanism are found by equating the external work done to the internal work done as follows:

Mechanism 1: Sidesway (transverse direction)

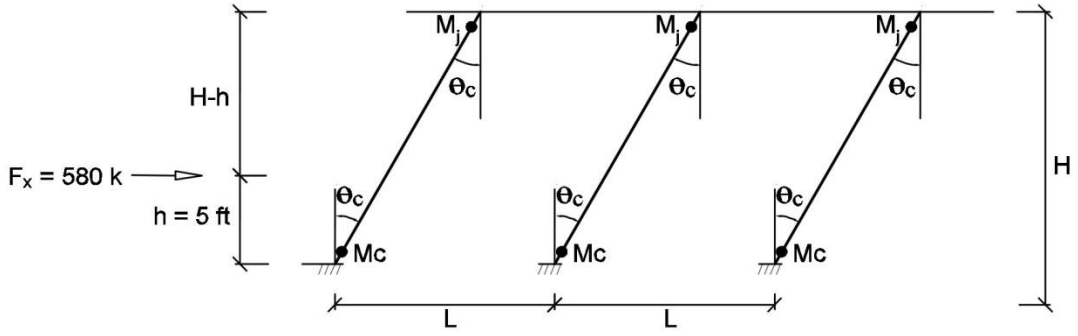

Figure B-10. Mechanism 1.

$$P_a \frac{h}{H}\Delta = 3M_c \frac{\Delta}{H} + 3M_j \frac{\Delta}{H}$$

$$P_a \frac{h}{H} = 3\left(\frac{M_c + M_j}{H}\right)$$

$$P_a = \frac{3}{h}\left(M_c + M_j\right) \tag{B-3}$$

Plugging the values of h = 5 ft, M_c = 727 k-ft, and M_j = 718 k-ft,

$$P_a = \frac{3}{5}\left(727 + 718\right) = 867 \text{ k} > F_x$$

Mechanism 2: Local column (transverse direction)

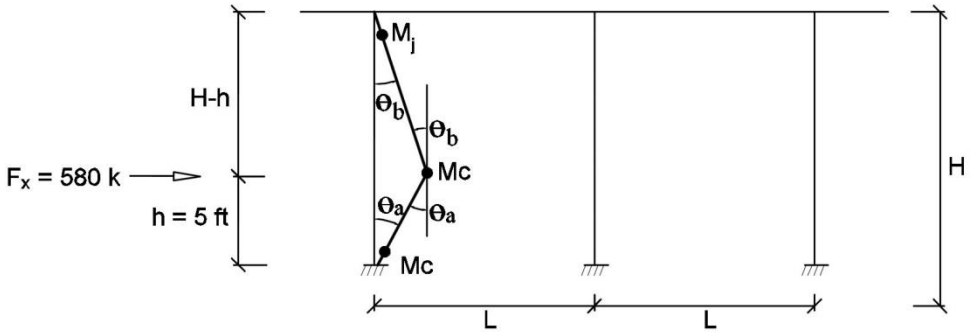

Figure B-11. Mechanism 2.

$$P_a\Delta = M_c\theta_a + M_c\left(\theta_a + \theta_b\right) + M_j\theta_b$$

where $\theta_a = \frac{\Delta}{h}$, and $\theta_b = \frac{\Delta}{H - h}$

$$P_a = \frac{2M_c}{h} + \frac{M_c}{H - h} + \frac{M_j}{H - h} \tag{B-4}$$

$$P_a = \frac{2 \text{ x } 727}{5} + \frac{727}{7} + \frac{718}{7} = 497 \text{ k} < F_x$$

Mechanism 3: Mixed column and sidesway (transverse direction)

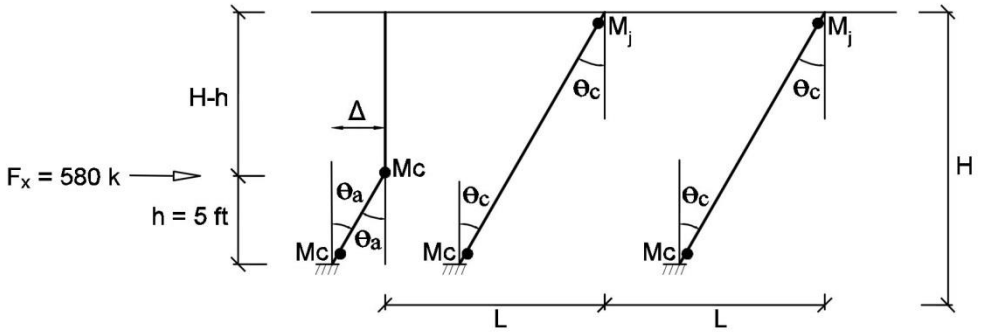

Figure B-11. Mechanism 3.

$$P_a\Delta = M_c(2\theta_a + 2\theta_c) + M_j(2\theta_c)$$

where $\theta_a = \dfrac{\Delta}{h}$, and $\theta_c = \dfrac{\Delta}{H}$

$$P_a = M_c\left(\frac{2}{H} + \frac{2}{h}\right) + M_j\frac{2}{H} \qquad \text{(B-5)}$$

Plugging values in Eq. (B-5),

$$P_a = 727\left(\frac{2}{12} + \frac{2}{5}\right) + 718\left(\frac{2}{12}\right) = 531.6 < \ F_x$$

Mechanism 4: Local column (longitudinal direction

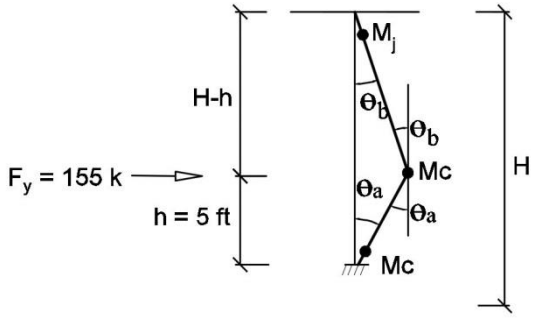

Figure B-12. Mechanism 4.

$$P_a\Delta = M_c\theta_a + M_c(\theta_a + \theta_b) + M_j\theta_b$$

where $\theta_a = \frac{\Delta}{h}$, and $\theta_b = \frac{\Delta}{H-h}$

$$P_a = \frac{2M_c}{h} + \frac{M_c}{H-h} + \frac{M_j}{H-h} \qquad \text{(B-6)}$$

$$P_a = \frac{2 \text{ x } 727}{5} + \frac{727}{7} + \frac{718}{7} = 497 \text{ k} > F_y$$

Mechanism 2 has the least allowable load and is the governing mechanism. The allowable loads in both Mechanism 2 and 3 are less than F_x. The following derivation shows that Mechanism 2 will always be critical for the condition $2h < H$.

Evaluation of condition when Mechanism 2 will be more critical than Mechanism 3

Assume Mechanism 2 < Mechanism 3

$$\frac{2M_c}{h} + \frac{M_c}{H-h} + \frac{M_j}{H-h} < M_c\left(\frac{2}{H} + \frac{2}{h}\right) + M_j\frac{2}{H}$$

$$\frac{M_j + M_c}{H-h} < \frac{2}{H}(M_j + M_c)$$

$$H < 2(H-h)$$

$$2h < H \qquad \text{(B-7)}$$

To make the column resistant to vehicle collision load under Mechanism 2, the number of column bars is increased from 10-#9 to 14-#9 bars. The moment capacity of column with 14-#9 bars is found by P-M interaction diagram to be 921 kip-ft. Then the allowable load under Mechanism 2 is determined from Eq. (B-4) as follows:

$$P_a = \frac{2M_c}{h} + \frac{M_c}{H-h} + \frac{M_j}{H-h} = \frac{2 \text{ x } 921}{5} + \frac{921}{7} + \frac{718}{7} = 602.5 < F_x$$

Okay

8) CAP POCKET JOINT DESIGN

Calculation of joint shear

Figure B-13 shows the joint moments and reactions due to the loads under strength V combination including self-weight of the bent cap and columns. From the reactions, the shear force for the cap beam and beam-column joints is computed. Section 6.2.4 has been followed to determine the joint shear force. The shaded areas in Figure B-14 show the shear force demands in the joint, the highest shear demand is 91 k.

Calculation of joint shear steel

$d_{pocket} = 21$ inch *Diameter of the pocket*

$A_{pocket} = \frac{\pi}{4} d_{pocket}{}^2 = \frac{\pi}{4}(21^2) = 346.36 \text{ in}^2$ *Area of the pocket*

The shear strength V_s is assumed to be provided by spirals around the dowel bars,

$$V_s = \frac{\pi}{2} A_b \frac{d_{pocket}}{s} f_y \quad \text{(B-8)}$$

in which A_b = area of the spirals, s = pitch of spirals assumed as 6 inches.

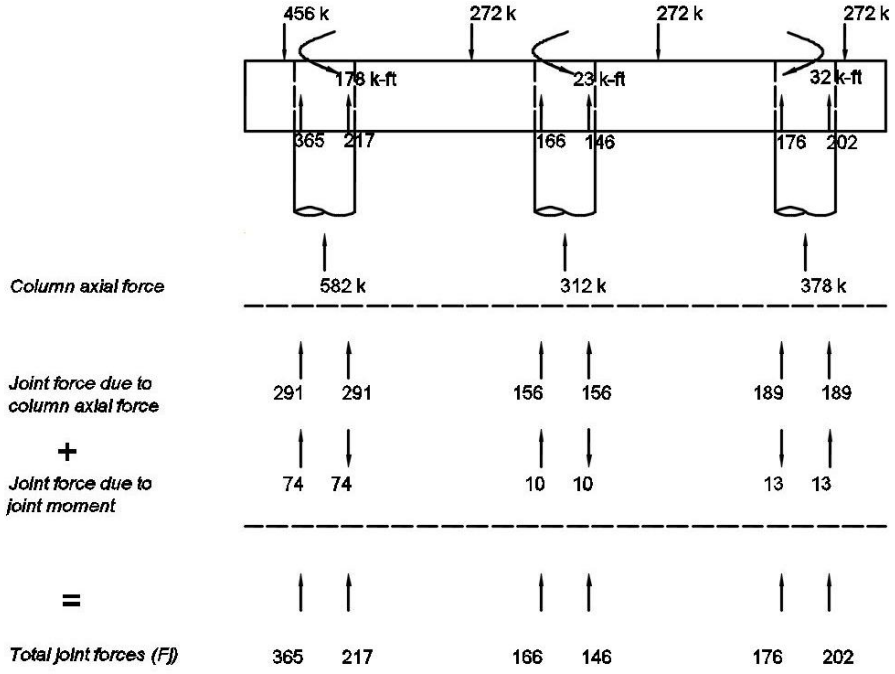

Figure B-13. Distribution of forces in the joint: Strength V loading.

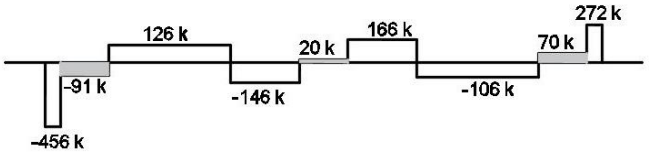

Figure B-14. Shear force diagram: no joint opening.

Reinforcement ratio is given by

$$\rho_s = \frac{\text{volume of steel}}{\text{volume of concrete}} = \frac{\pi\, d_{pocket}\, A_b}{\frac{\pi}{4}(d_{pocket}{}^2)s} = \frac{4\, A_b}{d_{pocket}\, s} \tag{B-9}$$

From Eq. (B-9), (B-10)

$$A_b = \frac{1}{4}\rho_s\, d_{pocket}\, s$$

Putting Eq. (B-10) in Eq. (B-8),

$$V_s = \frac{\pi}{2}\left(\frac{1}{4}\rho_s\, d_{pocket}\, s\right)\frac{d_{pocket}}{s} f_y = \frac{1}{2}\frac{\pi}{4}\rho_s\, d_{pocket}{}^2 f_y \qquad \text{(B-11)}$$

The shear strength is provided by an equivalent corrugated pipe of thickness t_{pocket} and steel tensile strength f_{yp} of 33 ksi,

$$\rho_t = \frac{\text{area of steel}}{\text{area of concrete}} = \frac{\pi\, d_{pocket}\, t_{pocket}}{\frac{\pi}{4}(d_{pocket}{}^2)} = \frac{4\, t_{pocket}}{d_{pocket}} \qquad \text{(B-12)}$$

Equating Eqs. (B-9) and (B-12),

$$\rho_s = \rho_t$$

$$\frac{4\, A_b}{d_{pocket}\, s} = \frac{4\, t_{pocket}}{d_{pocket}}$$

$$\frac{A_b}{s} = t_{pocket}$$

$$t_{pocket} = \frac{A_b}{s} = \frac{0.11}{6} = 0.0183\,\text{inch} \qquad \textit{For \#3 spirals, } A_b = 0.11\,\text{in}^2$$

Considering a minimum corrugated pipe of 16 gage number, $t_{pocket} = 0.060$ inch.

$$\rho_s = \rho_t = \frac{4\, t_{pocket}}{d_{pocket}} = \frac{4 \text{ x } 0.060\,\text{inch}}{21\,\text{inch}} = 0.0114$$

From Eq. (B-11),

$$V_s = \frac{1}{2}\frac{\pi}{4}\rho_s\, d_{pocket}{}^2 f_{yp} = \frac{1}{2}\frac{\pi}{4} \text{x } 0.0114 \text{ x } (21\text{inch})^2 \text{ x } 33\,\text{ksi} = 65.1 \text{ k}$$

$$A_v = 0.8 A_g = 0.8\frac{\pi}{4} \text{x } 36^2 = 814 \text{ in}^2$$

$$V_c = 2\sqrt{\frac{f'_{c\_col}}{1000}} A_v = 2\sqrt{\frac{3.6\,\text{ksi}}{1000}} \text{x } 814\,\text{in}^2 = 97.7\,\text{k}$$

Total strength V_r is the contribution of both concrete and steel,

$V_r = V_c + V_s = 97.7\text{ k} + 65.1\text{ k} = 163\text{ k} > 91\text{ k}$ Okay